Technical Report Documentation Page

1. Report No.	2. Government Accession No.	3. Recipient's Catalog No.
UM-HSRI-78-21		

4. Title and Subtitle	5. Report Date
Mechanisms, Tolerances and Responses Obtained Under Dynamic Superior-Inferior Head Impact, A Pilot Study	May 1978
	6. Performing Organization Code
7. Author(s) R. Culver, M.Bender, J. Melvin	8. Performing Organization Report No. UM-HSRI-78-21
9. Performing Organization Name and Address Highway Safety Research Institute The University of Michigan Ann Arbor, Michigan 48109	10. Work Unit No. (TRAIS) 015628/015631 11. Contract or Grant No. 77-12121 / 77-12123
12. Sponsoring Agency Name and Address National Institute for Occupational Safety and Health 944 Chestnut Ridge Road Morgantown, West Virginia 26505	13. Type of Report and Period Covered Final June 1977 - March 1978
	14. Sponsoring Agency Code

15. Supplementary Notes

16. Abstract

Limited biomechanical data exists concerning S-I head impacts. Eleven S-I head impacts of unembalmed cadavers were performed to study the mechanisms, tolerances, and responses involved. The 9.9 kg padded impactor at 6.8 to 10.2 m/s velocity produced cervical vertebrae fractures with no basal skull fracture. Peak forces over 5.7 kN, peak velocities over 7.5 m/s, and initial pulse work over 380 N·m began fracturing cervical vertebrae in anatomically normal subjects. The damage mechanism appeared to be compressive arching.

17. Key Words	18. Distribution Statement
Head Impact, S-I, Mechanisms, Tolerances, Responses Cadaver	Unlimited

19. Security Classif. (of this report)	20. Security Classif. (of this page)	21. No. of Pages	22. Price
Unclassified	Unclassified	104	

MECHANISMS, TOLERANCES, AND RESPONSES OBTAINED UNDER DYNAMIC SUPERIOR-INFERIOR HEAD IMPACT

A Pilot Study

Prepared for:

National Institute for Occupational Safety and Health
944 Chestnut Ridge Road
Morgantown, West Virginia 26505

Prepared by:

Roger H. Culver
Max Bender
John W. Melvin

Highway Safety Research Institute
The University of Michigan
Ann Arbor, Michigan 48109

Final Report for Period June 1977 through March 1978

May 1978

TABLE OF CONTENTS

LIST OF FIGURES

LIST OF TABLES

1.0 FOREWORD

Insufficient biomechanical data exists concerning tolerance of the skull and cervical spine to dynamic loading in the superior-inferior direction for establishment of industrial protective helmet performance specifications. Therefore, this research study was undertaken to generate new data about the mechanisms and tolerances of the basal skull and upper spine under dynamic superior-inferior (S-I) loading. Technical tasks involved developing an appropriate experimental method of impacting unembalmed human cadavers to determine the mechanisms, forces, velocities, energies and skeletal damage related to S-I dynamic impacts. A reference list of appropriate literature was to be included. This study was not meant to be comprehensive and could address only limited variations with limited depth. The purpose of this final report is to describe the test methodology, present the experimental results, discuss what the results mean, make certain conclusions and recommendations, and provide a list of references.

2.0 SUMMARY

Dynamic superior-inferior impacts to eleven cadavers were performed. Basal skull fractures were not produced, but rather spinal fractures. The mechanism of cervical vertebrae fracturing appeared to be the compressive arching of the neck -- placing loads on the spinous processes and connecting arches. Fracture production is not the best criterion for judging the severity of a neck or head injury, but provides a reasonable first step. For the test conditions of this research, it was found that fractures of the cervical vertebrae of normal subjects began to occur for peak forces over 5.7 kilonewtons, peak impactor velocities over 7.5 meters per second, and initial impact pulse work values of 380 joules. Subjects with weak or abnormal structure can be expected to begin fracturing at approximately a peak force of 3.6 kilonewtons, a peak impactor velocity of 6.3 meters per second, and an initial impact pulse work value of 250 joules. Future research in this area should carefully define real world situations, control all confounding variables (particularly initial orientations), consider the role of ligaments and muscles, utilize a comprehensive head-neck injury scale, and investigate mechanisms using high-speed cineradiography.

3.0 BACKGROUND

A brief look at what is available from the literature is helpful to better understand the significance of the research leading to this report. Contract limitations did not permit examination of all available related literature, but it is important that nothing was found thus far describing dynamic impacts in the superior-inferior (S-I) direction to the crowns of intact unembalmed cadavers. The literature to be mentioned below, however, indicates that at least a few aspects of the desired impacts can be studied through previous research.

Numerous papers concerning skull fracture, brain injury, and neck trauma resulting from acceleration of the head relative to the torso from automobile crash conditions abound in the Stapp Car Crash Conference Proceedings. (1, 2, 3) Such work is currently relevant but is not generally applicable to the S-I situation except where areas of the head above the Frankfort plane contact the vehicle interior (windshield, A-pillar) or approximately S-I impact accelerations produce brain injury. This is not to say that properly modified models used in the research are not useful for quite the contrary is true. The investigation of motorcycle and racing helmet performance in accidents offers further worthwhile data sources, however.

Another group of papers is typified by the work of Sonada (4) and concern themselves with modifed structures tests which subject specific body components (often using both human and animal specimens) like the skull, vertebrae, spinal cord, and intervertebral discs to somewhat arbitrary input loadings and note various responses. Some of the relevant results include: the compressive breaking load found by Sonada for a single cervical wet human vertebrae for an age group of 60-79 years is 190 kg ± 6.0 or 1.86 kN; the compressive breaking load of a wet human cervical intervertebral disc (40-59 years) is again according to Sonada 320 kg or 3.14 kN; and the static load required to cause basal skull fracture when the skull and 3 or 4 vertebrae are compressed according to Messerer (5) is approximately 270 kg or 2.65 kN. Messerer (1880) makes two other relevant statements. First, vertebrae were often fractured before the base of the skull was and second, Messerer mentions that repeated examples of spinal penetration into the skull under blunt loading to the crown are "in the literature." This literature has yet to be examined. Here again, structures tests are not generally applicable. Values of load required to break body components must be interpreted carefully to be useful relative to the research of this report.

Further, clinical investigations such as Schneider's (6) and laboratory investigations such as Gosch's (7, 8, 9) and Roaf's (10) propose mechanisms for certain spinal injuries. Results of interest are the important roles rotation and muscle tension play in the severity of the trauma. Gosch and Schneider (7, 8, 9) performed dynamic S-I impacts on monkey animal models and came closest to the conditions of our research. Inadequate instrumentation and animal to human correlations negate their quantitative data's usefulness at this time. A survey of this kind of work through 1970 is that by White and Albin. (11).

Finally, it is quite apparent that the biomechanical data available in the literature is wholly insufficient to be used for protective industrial helmet design specifications. Data concerning the fracture characteristics and mechanisms of the cervical spine and more importantly causes of spinal cord damage are needed.

4.0 METHODOLOGY

4.1 Test Objectives

The overall objective of this study was to learn as much about S-I impacts as possible with ten (10) to twelve (12) cadaver impacts. The research was approached in two (2) phases.

The first phase impacted six (6) unembalmed cadavers and sought to do the following:

4.1.1 develop an effective experimental method

4.1.2 determine if basal skull fracture constitutes the suspected damage response

4.1.3 for whatever damage response is found, formulate some mechanisms and tolerance levels

4.1.4 begin a literature search.

The results of Phase One were reported in an interim letter report to NIOSH in January 1978 with the title Pilot Study of Basal Skull Fracture.

The second phase impacted 5 unembalmed cadavers using the entirely new data obtained during Phase One as a basis and sought to do the following:

4.1.5 refine the experimental method where necessary

4.1.6 determine the fracture tolerance force, velocity, and energy involved for whatever conditions are possible

4.1.7 propose a reasonable damage mechanism

4.1.8 finish an appropriate literature reference list

4.1.9 make recommendations for further research in this area

4.1.10 report all findings.

4.2 Test Procedures (and Developmental Reasoning)

The test procedure which has been developed is as follows:

4.2.1 Obtain the test subject, sanitarily cleanse and seal body openings, take pre-test x-rays of skull and neck in the anterior-posterior and left-right directions, and dress the subject in a vinyl exercise suit. Remove the hair in the area of the impact, mask the subject's face, and trim the vinyl suit to expose the upper thorax and shoulders. The described treatment provides ease of handling and exposed viewing.

4.2.2 Place the subject in a supine position and align the cervical spine as nearly along the impactor axis as possible. Check the alignment with an in-position x-ray and reposition if necessary. Rigidly fix the subject's lower torso and legs to the support system. This positioning takes into account the importance of head and neck orientation. Axial alignment attempts to achieve the maximum load carrying capability of the spine and thereby improve chances for basal skull fractures while reducing the role of orientation initiated fractures. Taking an in-position x-ray assures the best alignment possible and allows one to examine relationships between non-axial orientation and damage location. Rigid fixation of the lower torso and legs more closely simulates the erect human body and minimizes the amount of force lost to moving the subject's entire body so that the force data obtained will be a better representation of the force needed to cause skeletal damage.

4.2.3 Target the subject's head, the subject's shoulder, and the impactor for analysis of the 3000 frame per second high-speed color movies taken of the impact. Targeting in the movies allows qualitative and quantitative analysis of relative motions for investigating possible damage mechanisms and test conditions.

4.2.4 Impact the subject with a padded impactor face varying either cannon pressure or impactor stroke (essentially impact force or force input distance). It is necessary to pad the impactor face to prevent fracturing the crown of the skull yet allow transmission of the force to the basal skull and spine. Further, any experiment attempts to vary only one test parameter while maintaining all others constant. For this research, force and force input distance (stroke) were determined to be the most important parameters which could be varied for so limited a number of tests. Piston impact mass, impact type, face padding, pre-impact impactor travel, head-neck orientation and body fixation were all held as constant as possible. Bone characteristics and general condition of the unembalmed cadaver subject could only be roughly screened.

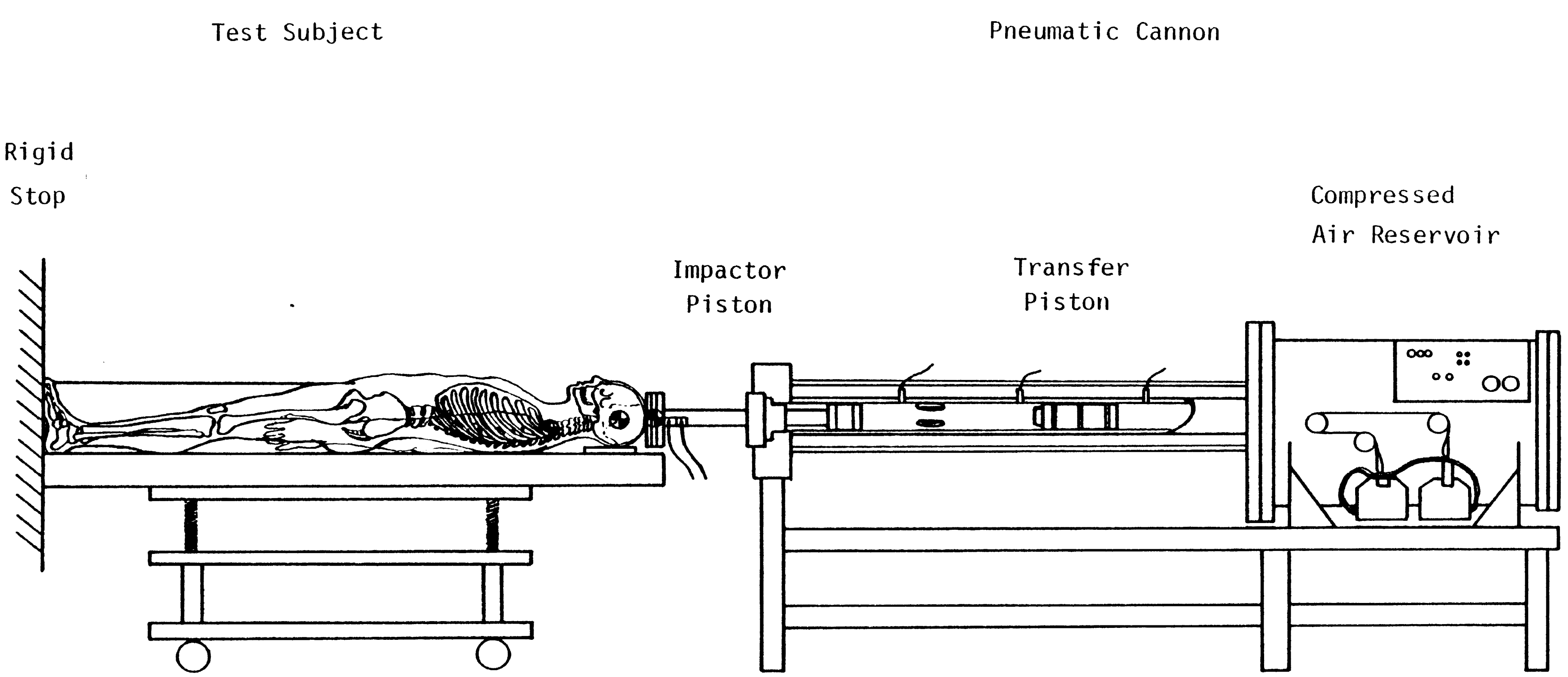

Figure 1 - Experimental Test Set-up

4.2.5 Take post-test A-P and L-R x-rays of the head-neck region.

4.2.6 Pathologically examine the subject's skull and spine for impact damage.

4.3 Facilities

The primary impact device used for this research was the "Impact Cannon," a pneumatically operated testing machine designed and constructed especially to move a striking mass at a specific velocity for impact studies. The machine consists of an air reservoir, and a ground and honed cylinder with two carefully fitted pistons. The transfer piston is propelled by compressed air through the cylinder and transfers its momentum to the impact piston. A striker plate attached to the impact piston travels about ten centimeters, where an inversion tube absorbs the enrgy of the impact piston and halts its movement. The machine may be operated over a velocity range of 2 to 26 meters per second with a 9.9 kilogram impact piston, and 3 to 53 meters per second with a 3 kilogram impact piston, using a maximum of 690 kilopascals. For this study pressures of 131 to 276 kilopascals provided velocities between 6.76 and 10.2 meters per second. An accelerometer and inertia compensated force transducer are mounted directly behind the striker plate. The force, acceleration, and velocity data were recorded on a Honeywell 7600 FM magnetic tape recorder for later playback onto a Clevite 6-channel Brush chart recorder.

The first impact device that was used and found to produce insufficient force levels was the pendulum actuated Linear Impactor. This system uses a loaded pendulum which is released to impart its energy to a bearing race-guided impactor.

4.4 Subjects

The test subjects required for this research were eleven (11) unembalmed human cadavers obtained from the University of Michigan Hospital Anatomy Department under the guidelines of the University's Human Use Committee. All subjects were screened for communicable diseases and anatomical anomalies. General data about each subject appears in Table 5.2.2 along with percent mineral content and mean tensile strength of femoral bone.

5.0 RESULTS

5.1 Raw Data Obtained and Analysis Techniques

5.1.1 Compensated Force vs. Time - A load cell behind the impactor face was associated with an accelerometer similarly located to provide input impactor force compensated for the mass of the impactor head in front of the load cell. The output of the load cell and accelerometer was recorded on a Honeywell 7600 tape recorder and later converted to permanent record with a Clevite 6-channel Brush recorder along with a time base, all effectively filtered at 1600 Hz. The actual traces appear in Appendix 9.2 while the peak input compensated force (kN) and the total impact duration (ms, the time impactor was in contact with subject) appear in columns 2 and 3 of Test Summary Table 5.2.1.

5.1.2 High-Speed Movies - A Hycam high-speed movie camera at right angles to and approximately one and one half meters (1.5 m) from the impactor axis took ~ 3000 frames per second color movies of each impact. The impactor, cadaver head, and cadaver shoulder were generally targeted. The film generally had visible timing lights for frame rate determination. In addition to study of overall surface motion in a qualitative manner, the movies with targeting were analyzed, digitized and then processed using the University of Michigan's central computer, an Amdahl 470V/6, to plot the head responses, horizontal position, (x or P-A) vertical position (z or I-S), angle, resultant position, resultant velocity, and resultant acceleration versus time. Resultant position was calculated using

$$P = \sqrt{x^2 + z^2}$$

where P = resultant position
x = horizontal position
z = vertical position

Resultant velocity was calculated.using

$$v = \sqrt{(\dot{x})^2 + (\dot{z})^2}$$

where V = resultant velocity
$\dot{x}$ = differentiated horizontal position (horizontal velocity)
$\dot{z}$ = differentiated vertical position (vertical velocity)

Resultant acceleration was calculated using

$$A = \sqrt{(\ddot{x})^2 + (\ddot{z})^2}$$

where A = resultant acceleration

$\ddot{x}$ = double differentiated horizontal position (horizontal acceleration)

$\ddot{z}$ = double differentiated vertical position (vertical acceleration)

Impactor plots were similarly determined.

The computer program for this processing was developed at HSRI by Dr. Nabih Alem and the plots for each test that was adequately targeted appear in Appendix 9.2 . Error with film analysis is unfortunately quite high for determining accelerations.

5.1.3 Set-up Conditions - The pertinent data concerning the initial cannon and cadaver set-up (impactor mass, pressure padding, cadaver fixation) along with set-up photographs appear in Appendix 9.2. A series of still x-rays was taken for nearly all the test subjects; pre-test A-P (anterior-posterior) and L-R (left-right), post-test A-P and L-R, and an initial condition L-R to check alignment of the cervical spine and skull with the impactor axis. The pre-test and post-test x-rays were supposed to reveal possible fractures and dislocation but did not do so for these tests. An attempt was made to quantify the initial position of the head and neck for possible use as a normalizing coefficient. These attempts were not successful but the numbers appearing in Appendix 9.2 illustrate a need for better uniformity in initial positioning.

5.1.4 Cadaver Data - Test subject characteristics (sex, age, weight, height, cause of death, mean ultimate tensile strength of femur samples, and percent mineral content of femur samples) appear in Table 5.2.2.

Of special interest here is the mean ultimate tensile strength of femur samples. These values were obtained as part of other ongoing research at HSRI but became important as a method for improving the correlation between the input force and resultant skeletal fracture severity. (See Appendix 9.3 for details of bone tests.) A relative fracture index value was assigned to the skeletal damage of each test subject as follows:

0 ≡ No fractures observed
1 ≡ A few fractures of spinous process tips
2 ≡ Spinous process and transverse process fractures
3 ≡ Moderate vertebral body fracture
4 ≡ Body fracture with spinous or transverse process fractures
5 ≡ Multiple and extensive body and process fracture

One should keep in mind that this scale is an arbitrary design of the author and has no relation to the AAAM AIS whole body scale nor takes into account tissues or conditions other than fractures of the spinal vertebrae. Next, a bone strength coefficient for each test subject was calculated by dividing the mean ultimate tensile strength of femur samples for that test subject by the average mean ultimate tensile strength of femur samples for all the test subjects. These coefficients appear in the last column of Table 5.2.2. Values of the coefficient were estimated for test subjects that did not have the tensile tests performed (20817, 20921, 20941). The bone strength coefficient was then multiplied times the Relative Fracture Index Value to obtain a Bone Strength Corrected Fracture Index Value (C.F.I.). The usefulness of this action was shown by the improvement from the correlation coefficient between fracture index and peak force (~0.4, significance level 0.2) to that between corrected fracture index and peak force (~0.5, significance level 0.1). It was also found that the percent mineral content of femur samples correlated better with fracture index values than ultimate tensile strength of femur samples did. Future correction factors should take this into account.

The percent mineral content of femur samples for each subject was also obtained as part of ongoing research at HSRI. The method of obtaining this data appears in Appendix 9.3. It is presented for general information.

An autopsy was performed on each test subject to determine the location and magnitude of skeletal fractures. A brief Skeletal Damage Description appears in Table 5.2.1 and in Appendix 9.2.

5.2 Data Summaries

The following tables and graphs present data which was found to be especially pertinent or illuminating. Interpretation and conclusions appear in section 6.0. Peak values were read off the data traces in Appendix 9.2 for force and velocity and plotted versus corrected fracture index values. Enveloping lines indicate the values ranges while suspect cases, poor position and swan neck, are noted. Initial pulse work done on cadaver values were calculated by finding the area under the initial pulse of the force vs. displacement curves in Appendix 9.2 with a polar planimeter. Finally, peak input force was plotted versus the initial pulse work done on cadaver with the corrected fracture index value noted by each point.

TABLE 5.2.1 TEST SUMMARY - INPUTS

TEST NUMBER	STROKE LENGTH (cm)	PEAK INPUT FORCE (kN) ± 4%	TOTAL IMPACT DURATION (ms) ± 4%	WORK DONE DURING MAIN INPUT PULSE BY IMPACTOR (N·m)	CALCULATED PEAK IMPACTOR VELOCITY (m/s) ± 5%
77H101	15.2	6.70	31.7	644	7.92
77H102	15.2	6.95	29.0	563	9.55
77H103	15.2	7.2	37.6	470	8.75
77H104	20.3	8.85	45.0	590	10.0
77H105	20.3	7.45	28.4	530	9.6
78H106	20.3	6.62	26.5	390	8.35
78H107	10.2	8.45	13.0	570	10.2
78H108	10.2	8.00	13.6	470	9.85
78H109	10.2	7.03	17.0	400	8.4
78H110	10.2	4.71	18.8	260	6.76
78H111	10.2	6.05	17.7	390	7.64

TABLE 5.2.2 TEST SUMMARY - RESPONSES

TEST NUMBER	CALCULATED PEAK RESULTANT HEAD VELOCITY (m/s) ±5%	CALCULATED PEAK RESULTANT HEAD ACCELERATION (m/s^2) ±15%	SPINAL FRACTURE DESCRIPTION	RELATIVE FRACTURE INDEX VALUE	BONE STRENGTH CORRECTED FRACTURE INDEX VALUE
77H101	NA	NA	No fracture of the skull or spine detected.	0	0
77H102	6.40	1380	No fracture of the skull or spine detected.	0	0
77H103	6.65	1620	Fracture of Rt. clavicle mid-shaft, Lt. clavicle distally, both rt. and lt. 1st rib near spine, and completely through body of 5th cervical vertebra	3.0	2.6
77H104	NA	NA	(Scoliotic), Intervertebral disks C_{3-4}, C_{4-5}, C_{5-6} crushed, transverse processes of C_5 and T_1 fractured, T_2 severely crushed.	4.9	4.6
77H105	5.85	556	Spinous process of C_2 fractured from body at arches, tip of C_6 spinous process fractured, slight crushing of C_{5-6} disk and T_1 left facet.	3.4	3.8
78H106	6.78	696	No fracture of skull or spine.	0	0
78H107	8.25	1040	Complete fracture from body of C_3 and C_4 left transverse processes, chip fracture of spinous process of C_5, C_6, C_7, T_2	3.0	3.7

TABLE 5.2.2 TEST SUMMARY - RESPONSES (Continued)

TEST NUMBER	CALCULATED PEAK RESULTANT HEAD VELOCITY (m/s) ±5%	CALCULATED PEAK RESULTANT HEAD ACCELERATION (m/s^2) ±15%	SPINAL FRACTURE DESCRIPTION	RELATIVE FRACTURE INDEX VALUE	BONE STRENGTH CORRECTED FRACTURE INDEX VALUE
78H108	9.33	1528	Complete fracture of spinous process of C_1, T_1, T_2 through arches, fractured tip of spinous process of C_2, C_4, C_7	4.8	4.4
78H109	7.88	1200	Spinous processes of C_7, T_1 fractured, Rt and lt transverse process of T_1 fractured, rt. transverse process C_7 crushed	4.0	4.4
78H110	4.08	588	(swan neck) spinous process of C_4, C_5, C_6 fractured, transverse process of C_5 fractured, body of C_5 crushed on rt side	3.6	3.0
78H111	6.88	981	Fracture of tips of spinous processes of C_3, C_4, C_5	1.0	0.9

TABLE 5.2.3 TEST SUBJECT CHARACTERISTICS

TEST NUMBER	CADAVER NUMBER	SEX	AGE (years)	WEIGHT (kilograms)	HEIGHT (centimeters)	CAUSE OF DEATH	% MINERAL CONTENT OF FEMUR SAMPLE	MEAN ULTIMATE TENSILE STRENGTH OF FEMUR SAMPLE (N/cm^2)	BONE STRENGTH COEFFICIENT
77H101	20817	Male	45	55.1	169.2	Pneumonia	NA	NA	1.0
77H102	20827	Male	78	89.3	176.5	Cardiac Arrest	83.9	7554	0.90
77H103	20824	Female	85	58.8	150.0	Cardiac Arrest	75.7	7291	0.869
77H104	20869	Female	79	59.7	149.7	Myocardial Infarction	61.7	7929	0.946
77H105	20881	Male	69	75.0	178.5	Myocardial Infarction	61.4	9308	1.11
78H106	20896	Male	58	73.2	NA	Congestive Heart Failure	NA	7584	0.904
78H107	20901	Female	39	53.5	162.3	Cardiovascular Accident	63.8	10370	1.23
78H108	20904	Female	82	64.1	NA	Disecting Thoracic Aneurysm	46.5	7768	0.926
78H109	20922	Female	55	64.0	NA	Carcinoma of Lungs	59.1	9308	1.11
78H110	20921	Male	86	45.6	NA	Respiratory Failure	NA	NA	0.84
78H111	20941	Male	66	72.5	NA	Cerebral Anoxia	NA	NA	0.94
AVERAGE	NA	6M/5F	67.5	64.6				8389	

- Figure 2 -

Peak Input Force
vs.
Corrected Fracture
Index

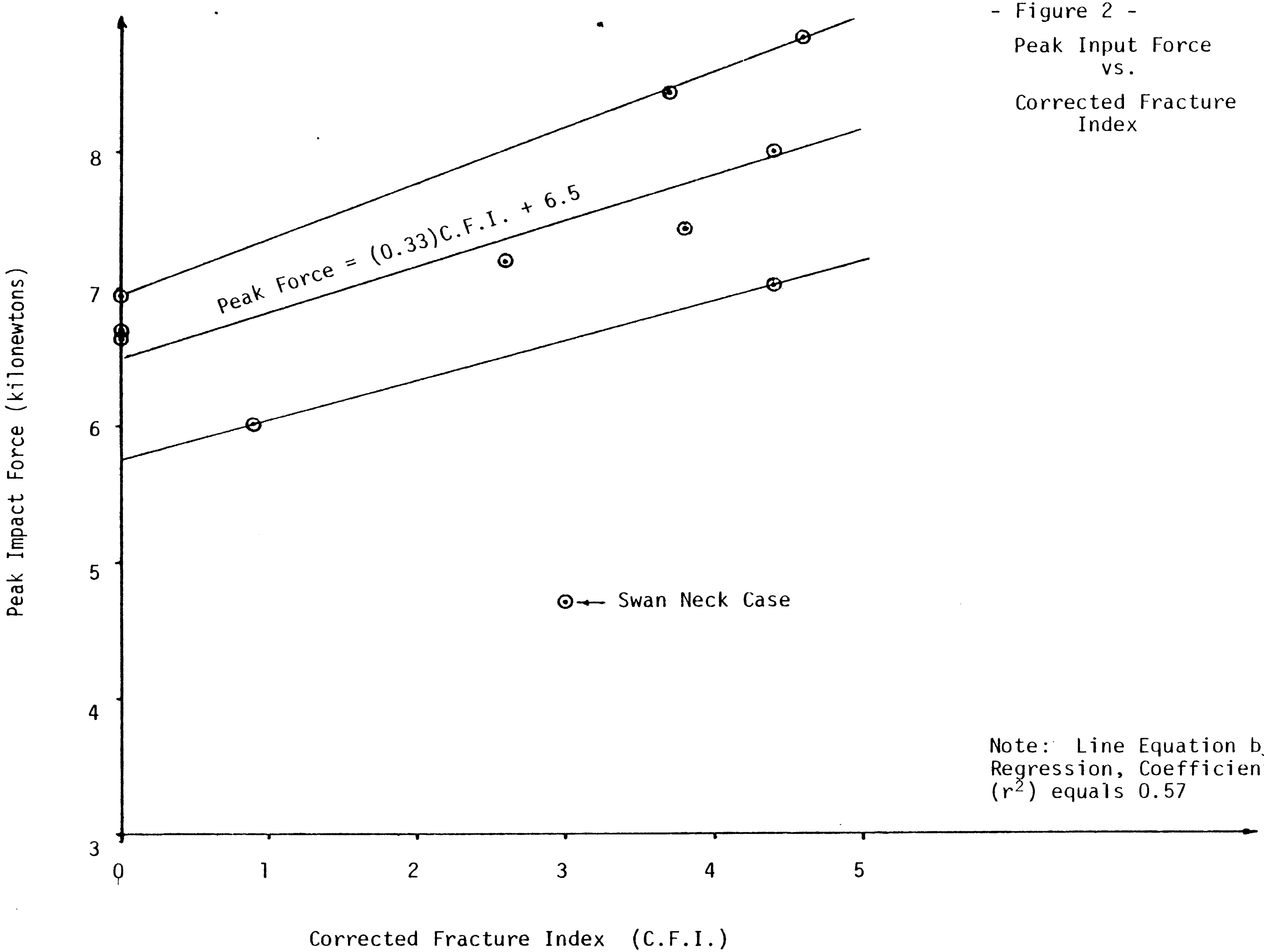

Note: Line Equation by Linear Regression, Coefficient of Determination (r^2) equals 0.57

- Figure 3 -
Peak Impactor Velocity
vs.
Corrected Fracture Index

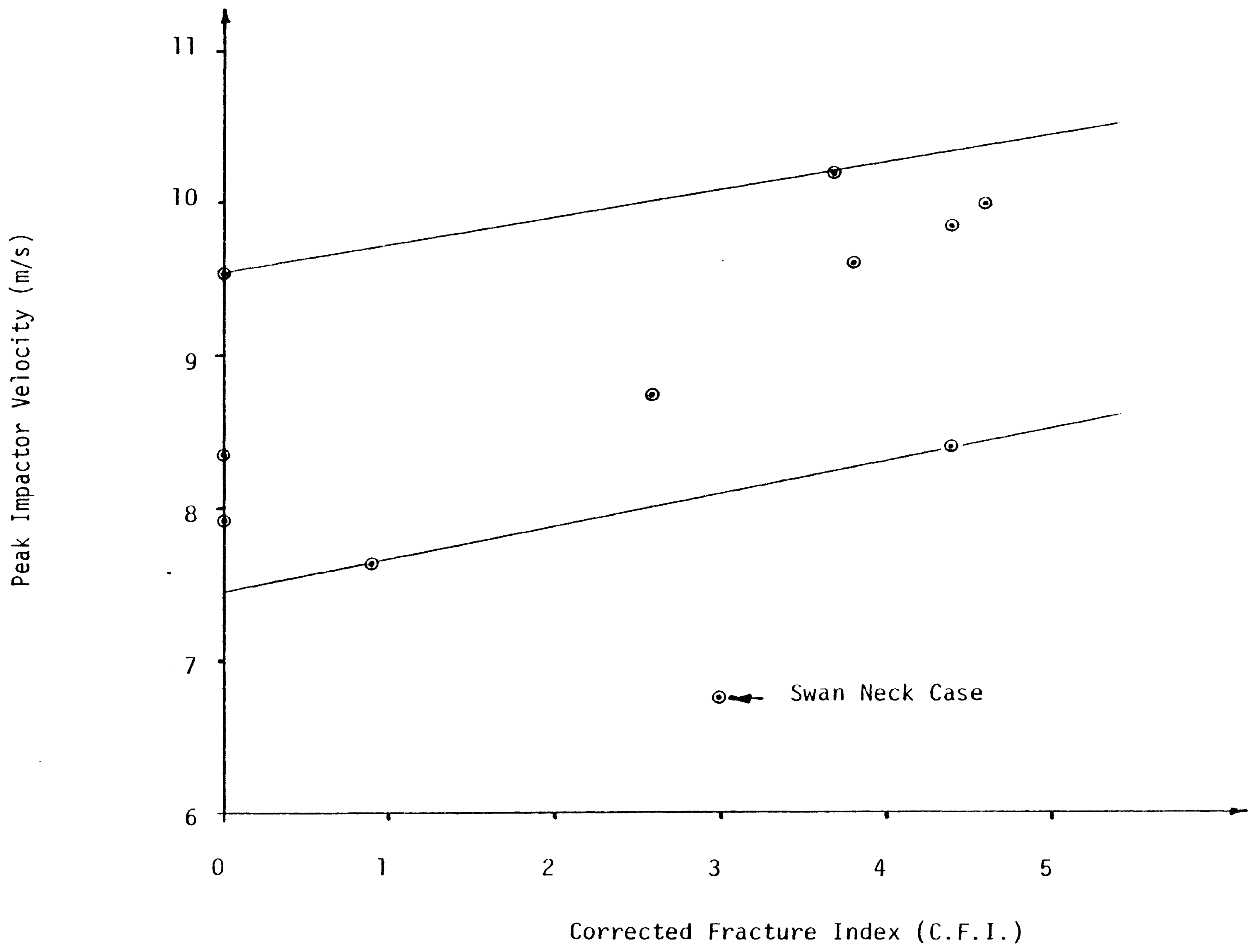

- Figure 4 -
Initial Pulse Work Done on Cadaver
vs.
Corrected Fracture Index

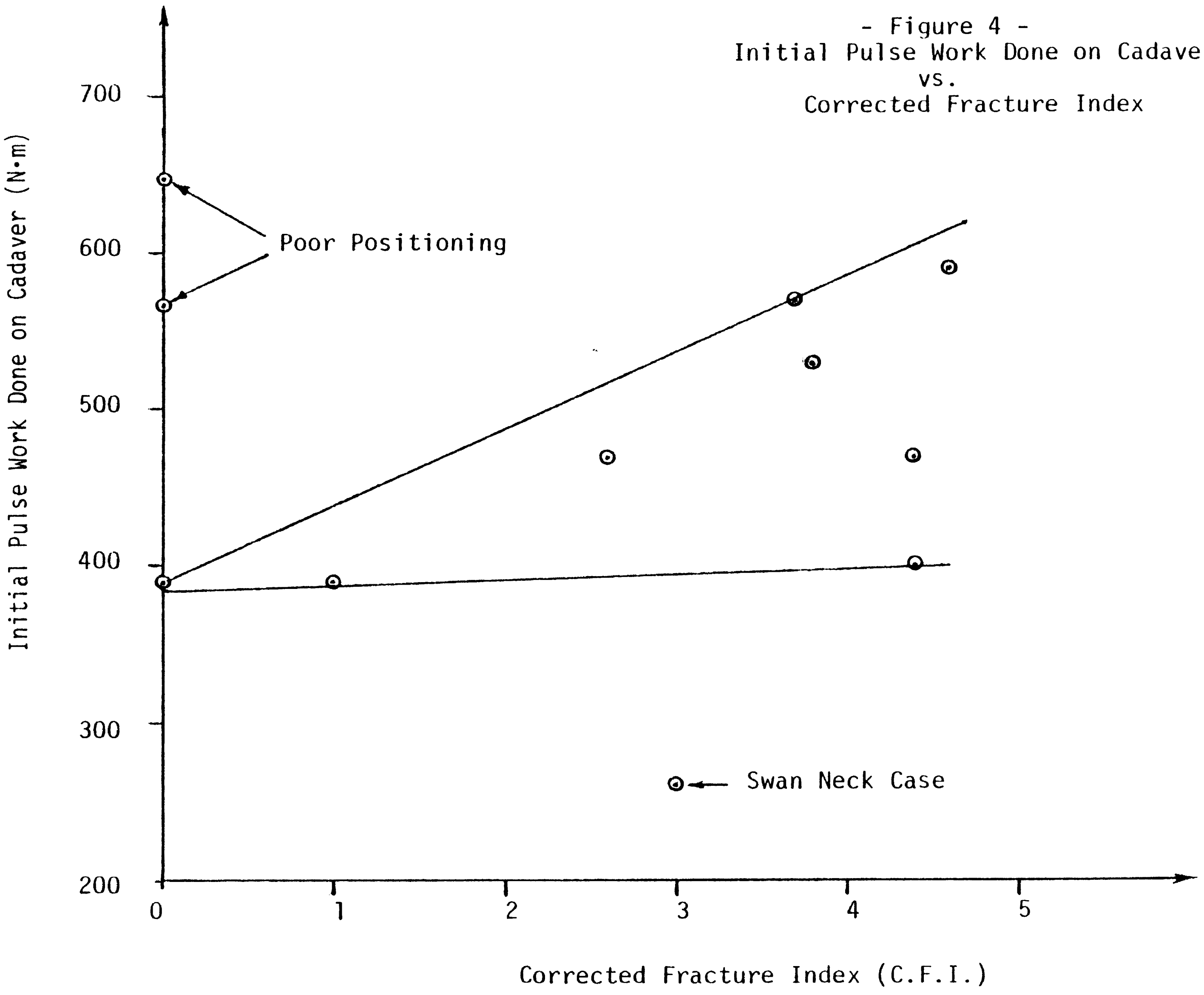

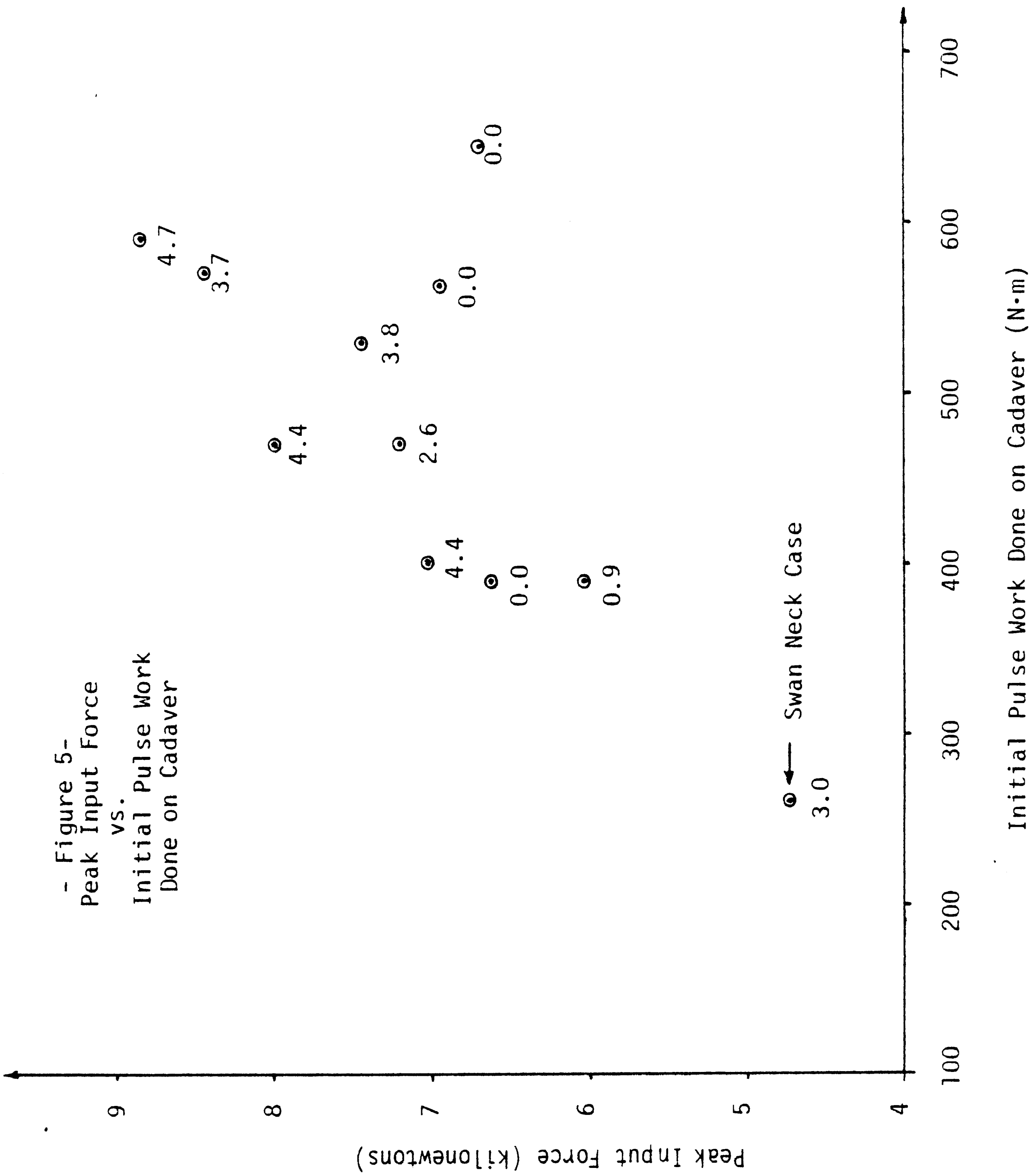

- Figure 5-
Peak Input Force
vs.
Initial Pulse Work
Done on Cadaver

6.0 CONCLUSIONS

6.1 Mechanisms

These experiments are apparently the first of their kind, and previously proposed mechanisms must be considered in light of the new findings. With regard to fracture, the high-speed movies and spinous process fractures both indicate a compressive arching of the cervical spine. The arching follows the normal lordotic curvature of the cervical spine and appears to depend on the initial rotation of the head and axial alignment of the spine. If the head is rotated rearward or the head placed above the axis of the spine, the arching is increased. This increase does not imply more serious fracture because the applied load works to translate the head rather than compress and load vertebrae. Probability of dislocation may be increased but none was found in our impacts. When the neck undergoes compressive arching, the spinous processes are loaded to fracture rather than the bodies. This arching is clearly the case in this series of experiments, perhaps a peculiarity of our test set-up, as opposed to the tear-drop body fractures of Schneider's investigations. The fracture of transverse processes can be considered the result of one or several occurrences. With arching, the articular facets load each other in the form of couples. This places a torsional loading on the transverse processes. Also the compression during impact may be bending the neck sideways slightly. Further, the rotation mentioned as critical by other experimenters may be occurring. See Figure 6. The best way to verify a mechanism for a given loading condition would be with high-speed cineradiographics, a capability HSRI has.

It should be remembered that no muscle tension was present, a factor which other investigators (11) consider important. By looking at this arching concept, it seems possible that if the neck were bent forward slightly the bodies of the vertebrae would be loaded more than the processes, and might offer sufficient resistances to produce basal skull fracture.

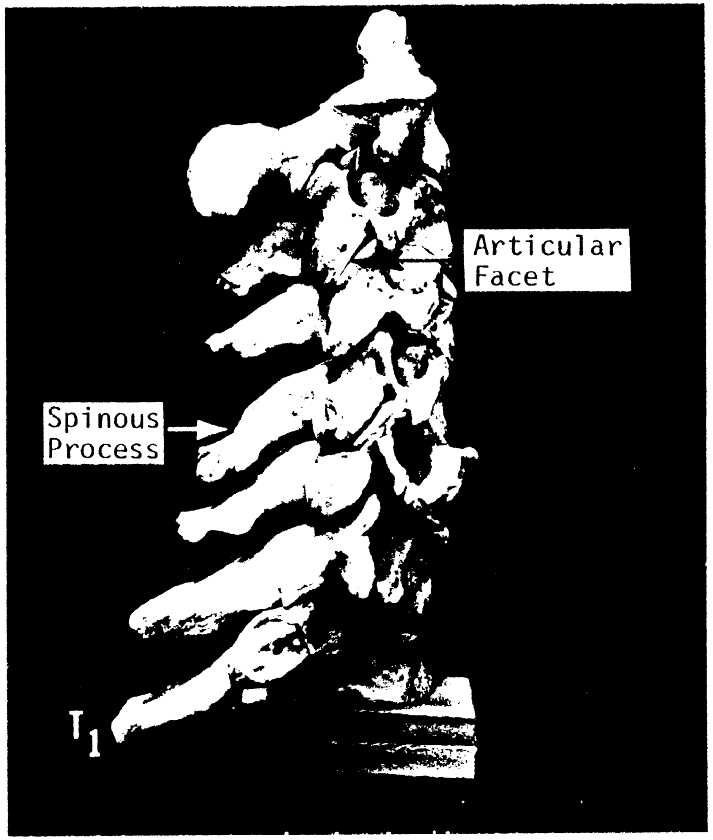

Initial Axial Alignment

Damaging Force Couples from Compressive Arching

Figure 6 - Initial Axial Alignment and Damaging Force Couples from Compressive Arching

6.2 Tolerance Levels

Although only a very limited number of impacts were performed, definite trends for the force, velocity, and energy required to produce skeletal damage under the described test conditions were found in the graphs of Figures 2, 3, 4 and 5. The graphs indicate that peak impact forces of 5.7 kilonewtons, peak impactor velocties of 7.5 meters per second, and initial pulse works done on the cadaver of 380 N·m are levels above which cervical spine fractures will begin to occur for an average cadaver. On the other hand, the levels for abnormal cadavers, such as those with "swan necks," are considerably lower. (A "swan neck" is long, thin, and has little musculature.) A peak impact force of 3.6 kilonewtons, peak impactor velocity of 6.3 meters per second, and initial pulse work done on the cadaver of 250 N·m were found to produce significant cervical spine fractures in the "swan neck" test subject used in test number 78H110. It should also be noted that the first few impact tests did not have the neck axially aligned as well as later tests which accounts for the high values of initial pulse work done on cadaver producing low damage values.

6.3 Recommendations

Future investigations into the damage produced by S-I impacts to the crowns of cadavers can benefit by these experiments.

6.3.1 Strict control and description of confounding variables must be maintained. The initial orientation conditions should be established and recorded with in-position roentgenograms. Attempt to keep cadaver variability to a minimum.

6.3.2 The wide variation of results produced by varied initial test conditions implores definition of the conditions of specific interest, the industrial accident situation for example.

6.3.3 High-speed cineradiography offers perhaps the best method of examining fracture mechanisms and should be funded.

6.3.4 Improved photo-instrumentation of the spine, and skull could assist response determination. Accelerations should also be measured to aid in correlating this data to related research.

6.3.5 The performance of static tests of head and upper spinal column should be pursued to better understand response to loading. As part of this, dynamic tests with load cells placed at intervals in the spinal column would be instructive.

6.3.6 Bone properties can provide valuable insight into the cadaver quality and should be obtained for each test subject whenever possible to assist in normalizing data. In particular, the percent mineral content seems to hold promise over ultimate tensile strength.

6.3.7 The role of muscles and tendons should be researched both in the literature and laboratory as it relates to S-I impacts.

6.3.8 It should be remembered that fractures of the vertebrae are not the most important damage caused by S-I impacts but rather nervous and vascular tissue since these are the most debilitating when injured.

6.3.9 Pre-test and post-test roentgenograms of the skull and neck provided extremely little useful information and removing their time consuming taking should be considered.

6.3.10 Variations in force input distance between 15.2 and 20.3 cm did not alter damage results and a stroke length in keeping with the real situation of interest needs to be determined.

7.0 ACKNOWLEDGMENTS

The authors acknowledge the vital assistance of Dr. Nabih M. Alem Joe Benson, Marv Dunlap, Jean Brindamour, and Jeff Axelrod without whose help these experiments would have been unreasonably difficult.

8.0 TEXT REFERENCES

1. Stalnaker, R. L., et al.: Head Impact Response. Proc. Twenty-first Stapp Car Crash Conf., New Orleans, La. 770921, 1977.

2. Ommaya, A. K., et al.: The role of whiplash in cerebral concussion. Proc. Tenth Stapp Car Crash Conf., Holbman A.F. Base, N.M., 1966, p. 197.

3. Clemens, H. J, Burow, K.: Experimental Investigation on Injury Mechanisms of Cervical Spine at Frontal and Rear-Front Vehicle Impacts. Proc. Sixteenth Stapp Car Crash Conf., Detroit, MI, 720960, 1972, p. 76.

4. Sonada, T.: Studies on the strength for compression, tension and torsion of the human vertebral column. J. Kyoto Pref. Med. Univ., 71: 659-702, 1962.

5. Messerer, O.: Uber Elasticitat und Festigkeit der Menschlichen Knachen. Verlag der J. G. Cottashen Buchhandlung, Stuttgart, 1880.

6. Schneider, R. C.: Head and Neck Injuries in Football. Williams and Wilkins Co., Baltimore, Md., 1973.

7. Gosch, H. H., et al.: Mechanisms and Pathophysiology of Experimentally Induced Cervical Spinal Cord Injuries in Adult Rhesus Monkeys. Surg. Forum, 21: 455, 1970.

8. Gosch, H. H., et al.: Cervical Spinal Cord Hemorrhages in Experimental Head Injuries. J. Neurosurg. 33:640, 1970.

9. Gosch, H. H. et al.: An Experimental Study of Cervical Spine and Cord Injuries. J. Trauma, 12:570, 1972.

10. Roaf, R.: A study of the mechanisms of Spinal Injury. J. Bone Surg. 42B: 810, 1960.

11. White, R. J. and Albin, M. S.: Spine and Spinal Cord Injury. Impact Injury and Crash Protection, edited by E. S. Gurdjian, W. R. Lange, L. M. Patrick et al., pp. 63-85. Charles C. Thomas, Pub. Springfield, Ill. 1970.

9.0 APPENDICES

APPENDIX 9.1

Bibliography

BIBLIOGRAPHY

Breig, A.: Biomechanics of the Central Nervous System. Stokholm, Almqvist and Wiksel, 1960.

Breig, A. and El-Nadi, A. F.: Biomechanics of the cervical spinal cord. Acta Radiol. 4:602, 1964.

Coe, J. E., Calvin, T. H., Rodenberg, R. H. and Yew, C. H.: Concussion-like state following cervical cord injury in the monkey. J. Trauma, 7:512, 1967.

Djindjian, R., Hurth, M. and Houdart, R.: In Angiography of the Spinal Cord. L'angiographie de la Moelle Epiniere. University Press, Baltimore, 1970.

Drake, C. G.: Cervical spinal cord injury. J. Neurosurg. 19:487, 1962.

Evans, F. G.: Studies in human biomechanics. Ann N Y Acad Sci, 63(4): 586-615, 1955.

Evans, F. G., Lissner, H. R. and Lebow, M.: The relation of energy, velocity and acceleration to skull deformation and fracture. Surg Gynecol Obstet, 107:593-601, 1958.

Fielding, J. W.: Cineroentgenography of the Normal Cervical Spine. J. Bone Joint Surg., 39-A: 1280, 1957.

Freytag, E.: Autopsy Findings in Head Injuries from Blunt Forces. Statistical Evaluation of 1,367 Cases. Arch. Pathol. 75: 402, 1963.

Gosch, H. H., Gooding, E. and Schneider, R. C.: Distortion and Displacement of the Brain in Experimental Head Injuries. Surg. Forum, 20:425, 1969.

Gosch, H. H., Gooding, E. and Schneider, R. C.: Mechanism and Pathophysiology of Experimentally Induced Cervical Spinal Cord Injuries in Adult Rhesus Monkeys. Surg. Forum, 21: 455, 1970.

Gosch, H. H., Gooding, E. and Schneider, R. C.: Cervical Spinal Cord Hemorrhages in Experimental Head Injuries. J. Neurosurg., 33: 640, 1970.

Gosch, H. H., Gooding, E. and Schneider, R. C.: An Experimental Study of Cervical Spine and Cord Injuries. J. Trauma, 12:570, 1972.

Gurdjian, E. S., Webster, J. E., Latimer, F. R. and Haddad, B. F.: Studies on Experimental Concussion: Relation of Physiological Pressure Increase at Impact. Neurology, 4:674, 1954.

Gurdjian, E. S., Webster, J. E. and Lissner, H. R.: Observations on the Mechanism of Brain Concussion, Contusion and Laceration. Surg. Gynecol. Obstet., 101:680, 1955.

Gurdjian, E. S., Hodgson, V. R., Thomas, L. M. and Patrick, L. M.: Significance of Relative Movements of Scalp, Skull and Intracranial Contents during Impact Injury of the Head. J. Neurosurg., 29: 70, 1968.

Hirsch, C.: The reaction of intervertebral discs to compression forces. J. Bone Joint Surg. 37A:1188, 1955.

Hodgson, V. R., Gurdgian, E. S. and Thomas, L. M.: Experimental Skull Deformation and Brain Displacement Demonstrated by Flash X-Ray Technique. J. Neurosurg., 25:549, 1966.

Horton, W. G.: Further observations on the elastic mechanism of the intervertebral disc. J. Bone Joint Surg. 40B552, 1958.

Howorth, M.B. and Petrie, J. G.: Injuries of the Spine. The Williams & Wilkins Company, Baltimore, 1964.

Jefferson, G.: Discussion on fractures and dislocations of the cervical vertebrae. Proc. Roy. Soc. Med. 33:657, 1940.

Kahn, E.A. and Rossier, A. B.: Acute Injuries of the Cervical Spine. Postgrad. Med., 39:37, 1966.

LeCount, E. R., Apfelbach, C. W.: Pathologic anatomy of traumatic fractures of cranial bones and concomitant brain injuries. J.A.M.A. 1920, 74:501.

Lindenberg, R. and Freytag, E.: The Mechanisms of Cranial Contusions. A Pathologic-anatomic Study. A.M.A. Arch. Pathol., 69:440, 1960.

Liss, L.: Fatal Cervical Cord Injury in a Swimmer. Neurology, 15: 675, 1965.

Melvin, J. W., Robbins, D. H. and Roberts, V. L.: The mechanical behavior of the diploë layer of the human skull in compression. Proceedings of the Eleventh Midwestern Mechanics Conference, 1969a, vol. 5 pp. 811-816.

Messerer, O: Uber Elasticitat und Festgkeit der Menschlichen Knochen. Verlag der J. G. Cotaschen Buchhandlung, Stuttgart, 1880.

Mixter, S. J. and Osgood, R. B.: Traumatic lesions of the atlas and axis. Ann. Surg. 51:193, 1910.

Ommaya, A. K., Hirsch, A. E., Martinez, J. L.: The role of whiplash in cerebral concussion. Proc. Tenth Stapp Car Crash Conference. Holbman A. F. Base N.M., 1966, p. 197.

Pierson, G. A.: Anatomy of the Spine and Spinal Cord. In Surgery of the Spine and Spinal Cord, edited by C. H. Frazier and A. R. D. Allen, Appleton-Century-Crofts, New York, 1918.

Roaf, R.: A study of the mechanisms of spinal injury. J. Bone Surg. 42B:810, 1960.

Schneider, R. C., Cherry, G., Pantek H.: The syndrome of acute central cervical spinal cord injury: with special ref. to the mechanisms involved in hyperextension injuries to the cerv. spine. J. Neurosurg 11: 546-577, 1954.

Schneider, R. C.: Trauma to the Spine and Spinal Cord. In Correlative Neurosurgery, 2nd ed. edited by E. A. Kahn, E. C. Crosby, R. C. Schneider and J. A. Taren, Chap. 26, Charles C. Thomas, Publisher, Springfield, Ill., 1969.

Selecki, B. R., Williams, H. B. L.: Injuries to the Cervical Spine and Cord in Man. Sydney, N.S.W., Australian Medical Publishing Co., Ltd., 1970.

Sherk, H. H. and Nicholsen, J. T.: Fractures of the Atlas. J. Bone Joint Surg. 52-A:1017, 1970.

Smith, F. P.: Experimental biomechanics of transvertebra disc rupture. J. Neurosurg. 19:594, 1962.

Sonada, T.: Studies on the strength for compression, tension and torsion of the human vertebral column. (Japanese text with English summary.) J. Kyoto Pref. Med. Univ. 71(9):659-702, 1962.

Taylor, A. R.: The mechanism of injury to the spinal cord in the neck without damage to the vertebral column. J. Bone Joint Surg, 33B: 543, 1951.

Taylor, A. R. and Blackwood, W.: Paraplegia in hyperextension injuries with normal radiographic appearances. J. Bone Joint Surg. 30B:245 1951.

Taylor, A. R.: The mechanism of injury to the spinal cord in the neck without damage to the vertebral column. J. Bone Joint Surg., 33-B: 543: 1951.

White, R. J. and Albin, M. S.: Spine and Spinal Cord Injury. In Impact Injury and Crash Protection, edited by E.S. Gurdjian, W. R. Lange, L. M. Patrick et al., pp. 63-85, Charles C. Thomas, Publisher, Springfield, Ill. 1970.

APPENDIX 9.2

TEST DATA

APPENDIX 9.2.1

TEST DATA FOR

77H101

TEST NO. 77H101

Piston Mass 23.36 kg

Stroke 15.2 cm

Drop Angle 99.5°

Padding description 2.54 cm ensolite, 2.54 cm styrofoam

Photographic Coverage 35 mm BW and color slides, 1500 fps color movies

Fixation description crotch block, rope at shoulders

% Skull Area Below Impactor Axis NA

Approximate Cervical Spine Radius of Curvature NA

Damage: No fracture of the skull or spine detected.

77H101 Instrumentation Traces

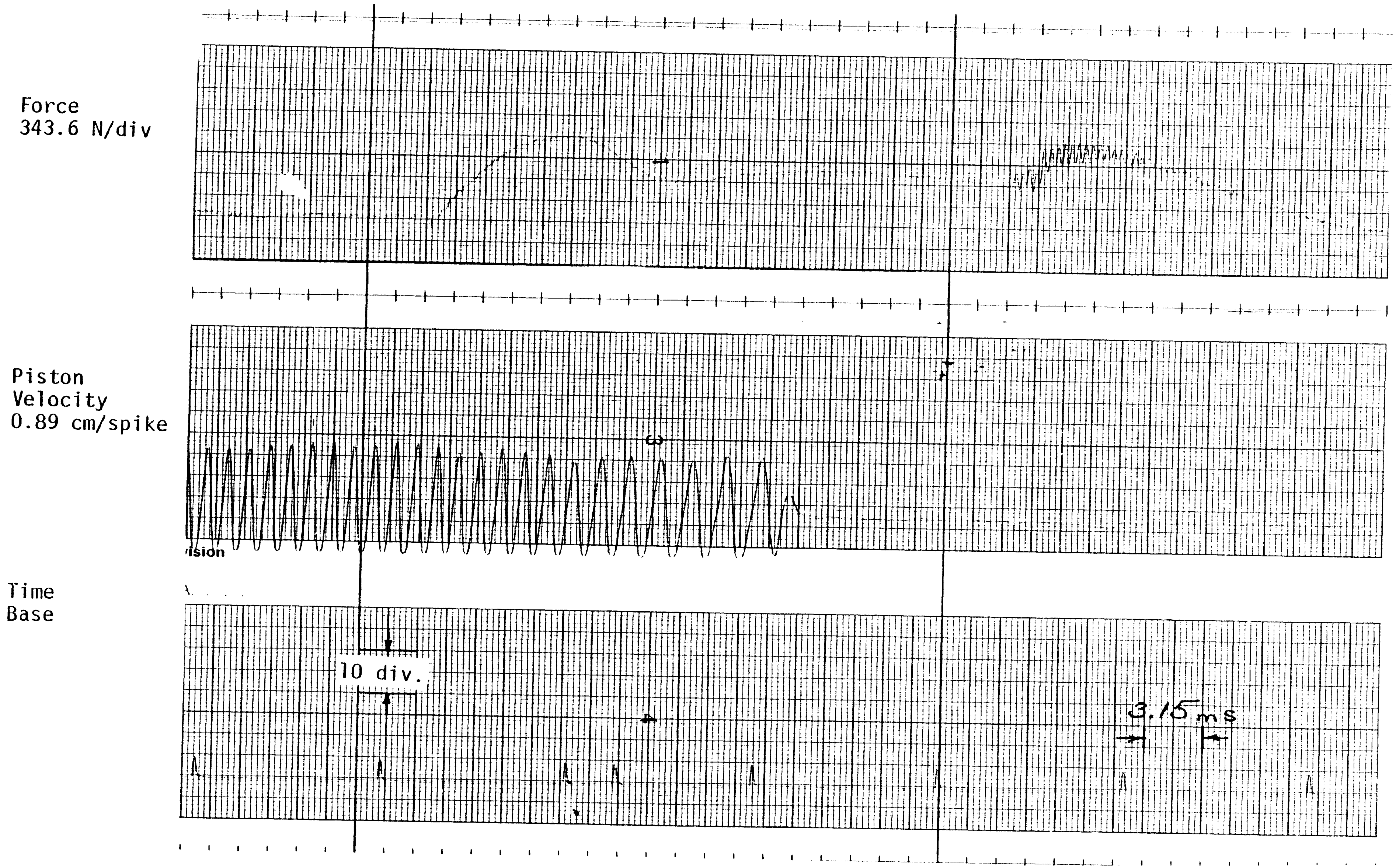

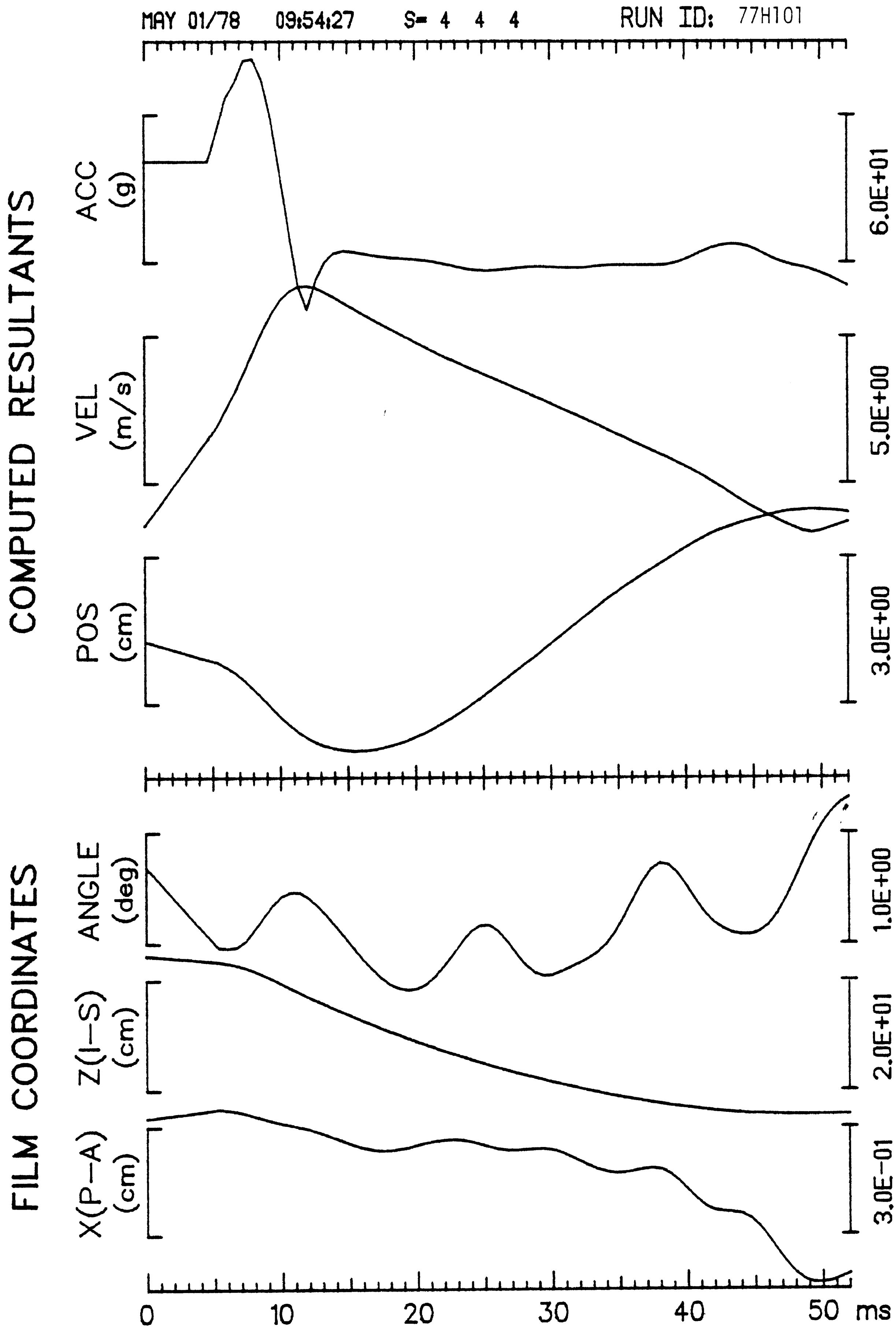

Impactor motion vs. time

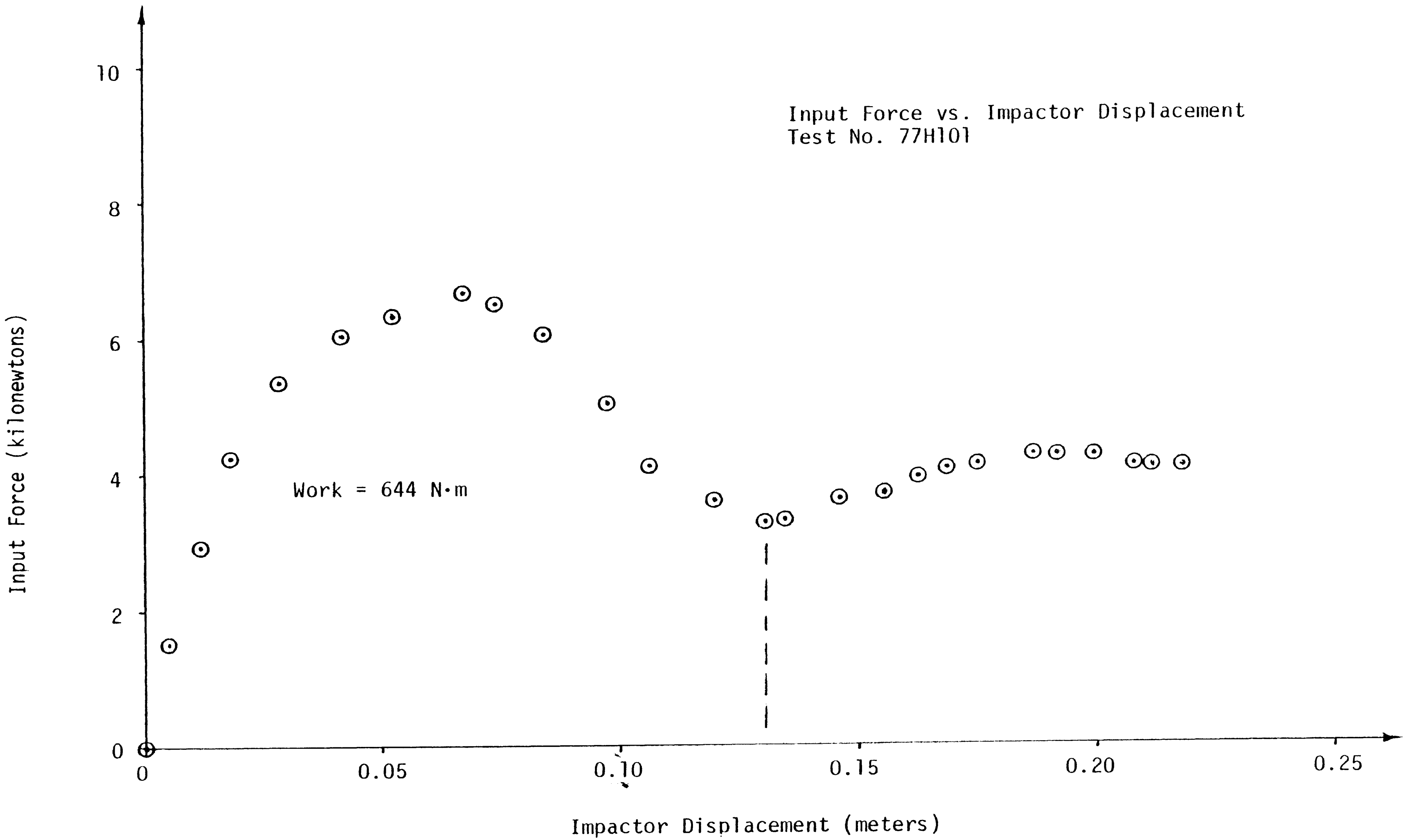

Input Force vs. Impactor Displacement
Test No. 77H101
Work = 644 N·m
Input Force (kilonewtons)
0
2
4
6
8
10
0
0.05
0.10
0.15
0.20
0.25
Impactor Displacement (meters)

APPENDIX 9.2.2

TEST DATA FOR

77H102

TEST NO. 77H102

Piston Mass 9.9 kg

Stroke 15.2 cm

Pressure 276 kPa

Padding description 2.54 cm ensolite, 2.54 cm styrofoam

Photographic Coverage 35 mm BW and color slides, 3000 fps color movies

Fixation description rope at shoulders

% Skull Area Below Impactor Axis NA

Approximate Cervical Spine Radius of Curvature NA

Damage: No fracture of the skull or spine detected.

TEST 77H102 Instrumentation Traces

Compensated Force
177.9 N/div
Effectively Filtered
at 1600 Hz

Force
444.8 N/div
Effectively Filtered
at 1600 Hz

Acceleration
6 g's/div
Effectively filtered.
at 1600 Hz

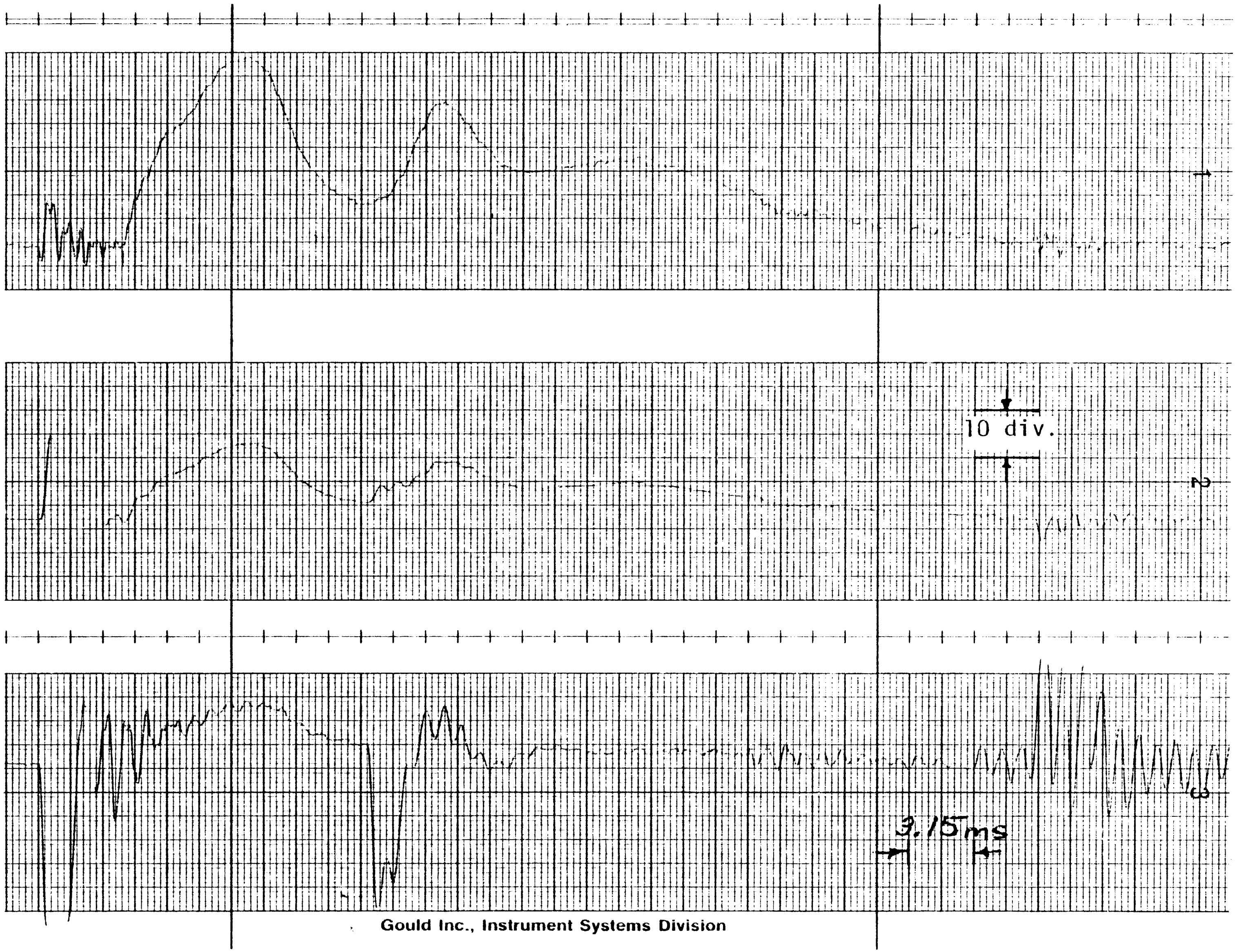

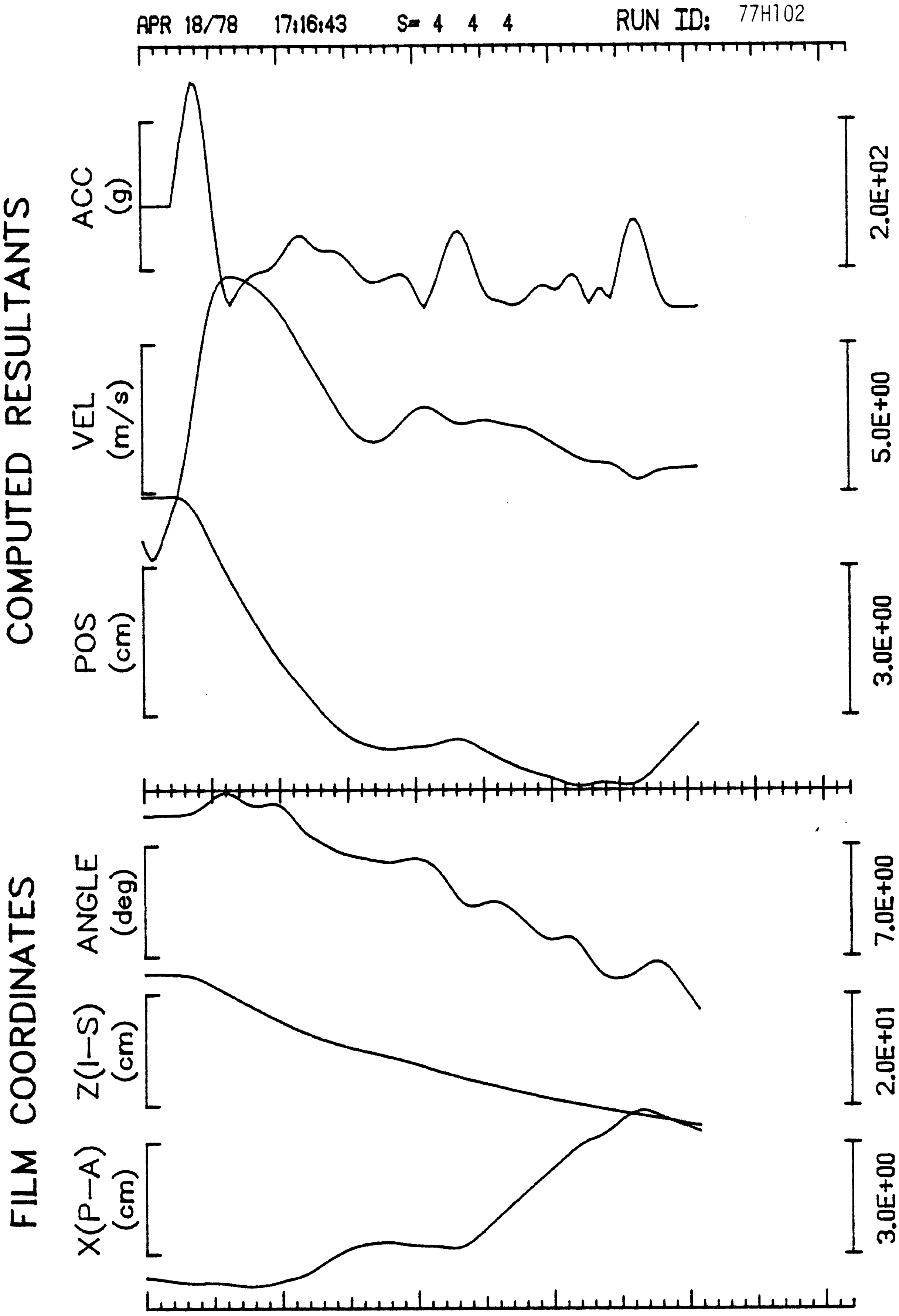

Impactor motion vs. time

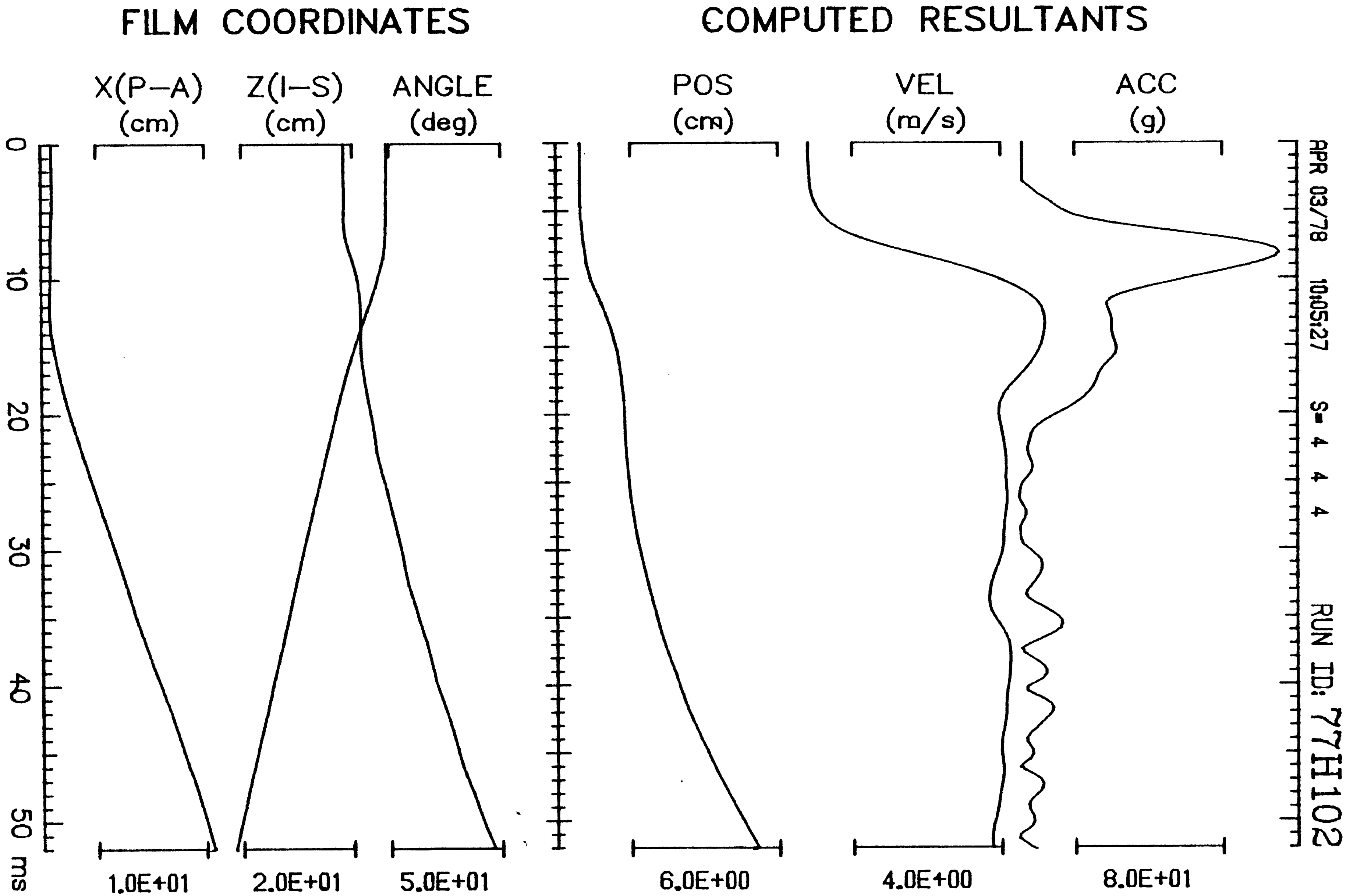

Head Motion vs. Time

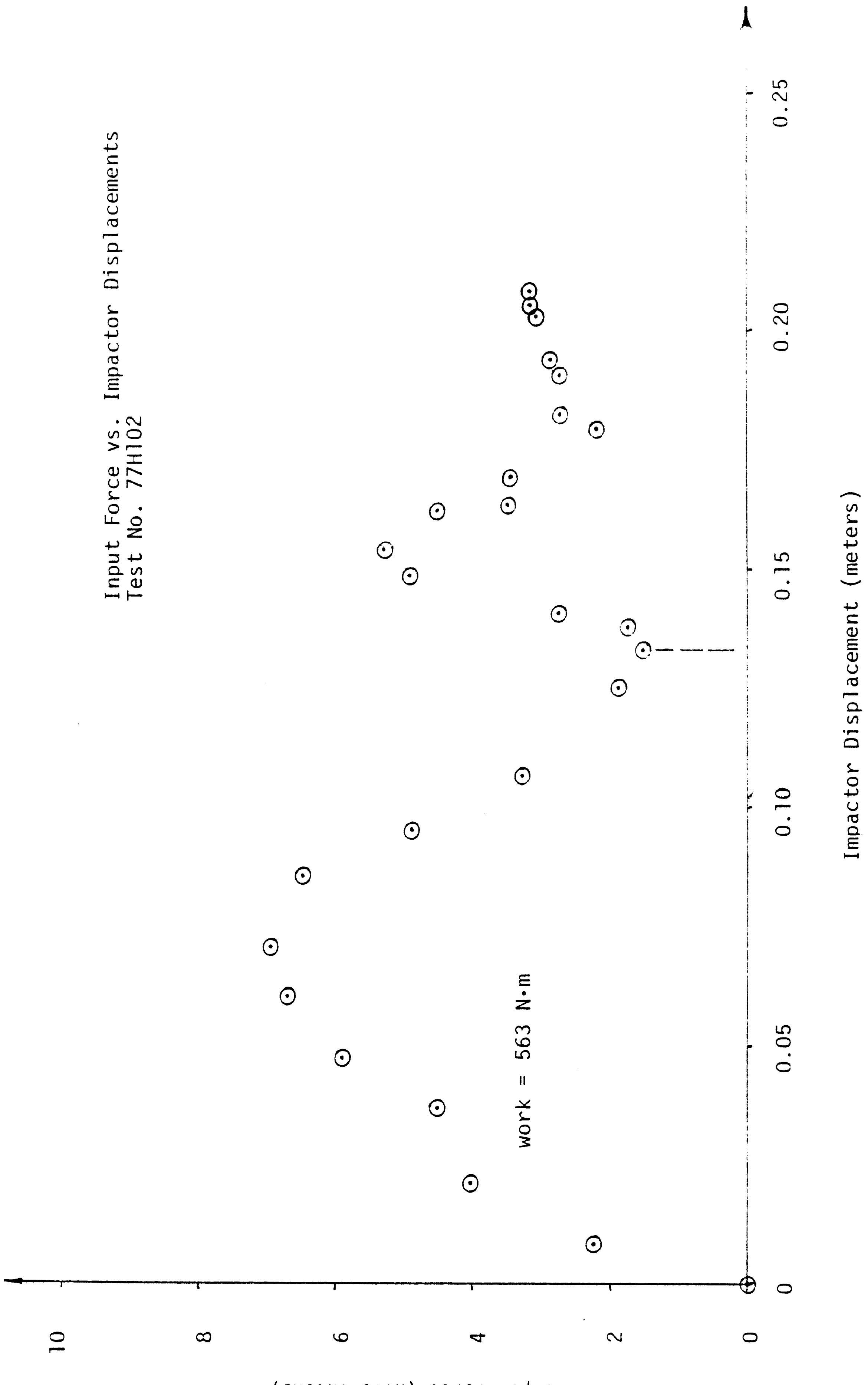
Input Force vs. Impactor Displacements
Test No. 77H102
work = 563 N·m
Input Force (kilonewtons)
0
2
4
6
8
10
Impactor Displacement (meters)
0
0.05
0.10
0.15
0.20
0.25

APPENDIX 9.2.3

TEST DATA FOR

77H103

TEST NO. 77H103

Piston Mass 9.9 kg

Stroke 15.2 cm

Pressure 276 kPa

Padding description 2.54 cm ensolite, 2.54 cm styrofoam

Photographic Coverage 35 mm BW and Color slides, 3000 fps color movies

Fixation description Ropes to shoulders, torso taped down

% Skull Area Below Impactor Axis NA

Approximate Cervical Spine Radius of Curvature NA

Damage: Fracture of Rt. Clavicle midshaft, Lt. Clavicle distally, both Rt. and Lt. 1st rib near spine and completely through body of 5th Cervical vertebra.

TEST 77H103 Instrumentation Traces

Compensated Force
177.9 N/div
Effectively Filtered
at 1600 Hz

Force
444.8 N/div
Effectively Filtered
at 1600 Hz

Acceleration
6 g's/div
Effectively filtered
at 1600 Hz

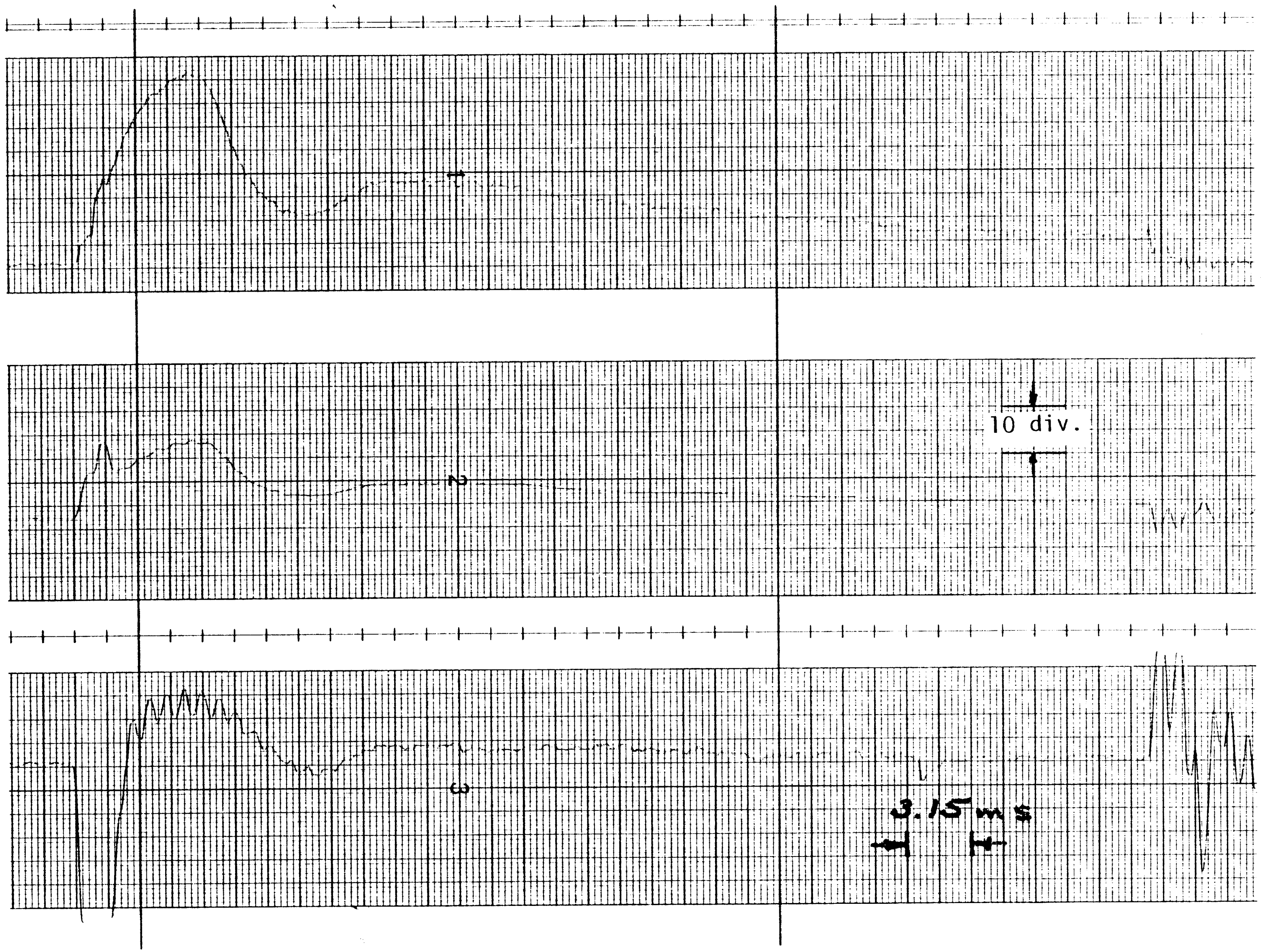

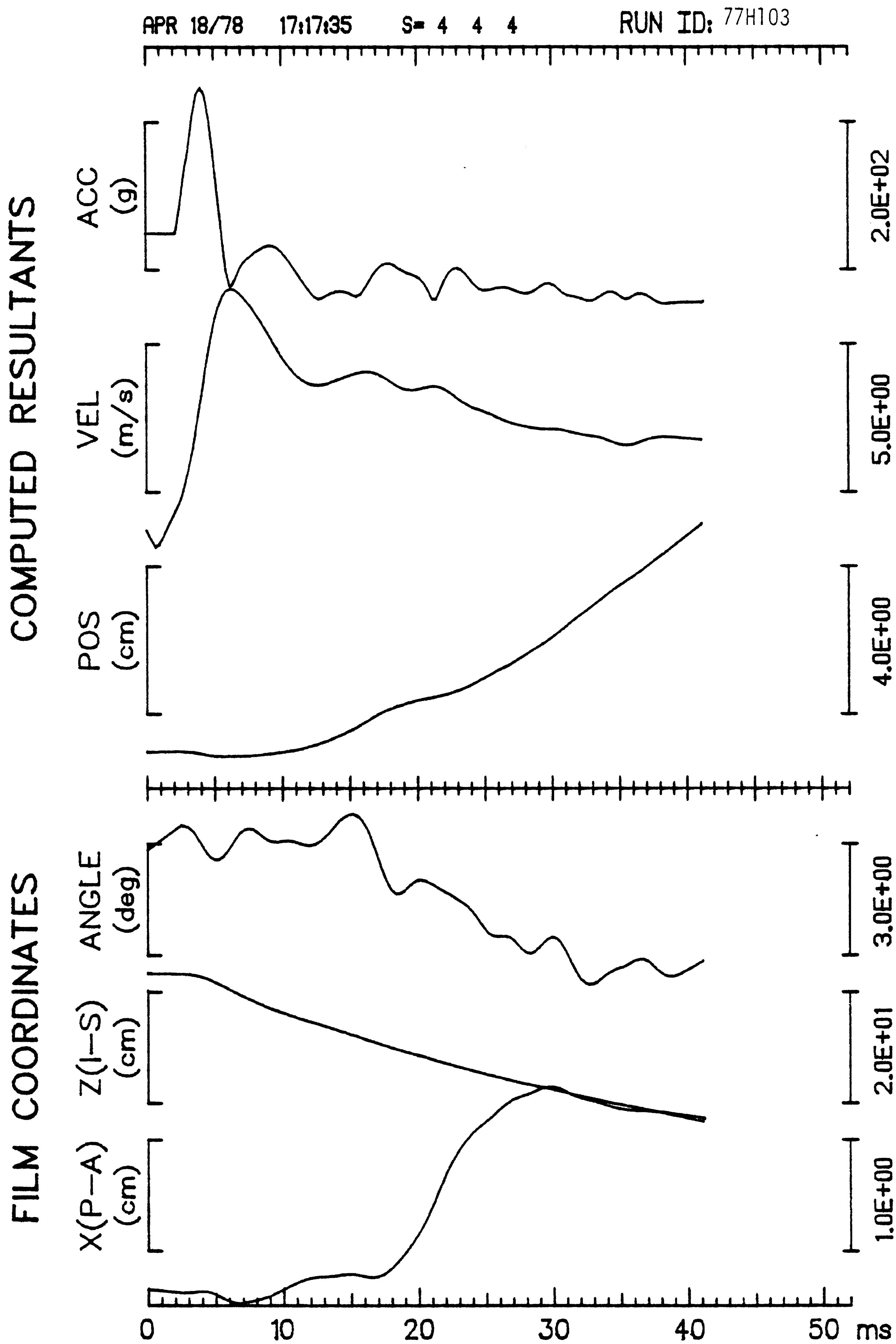

Impactor motion vs. time

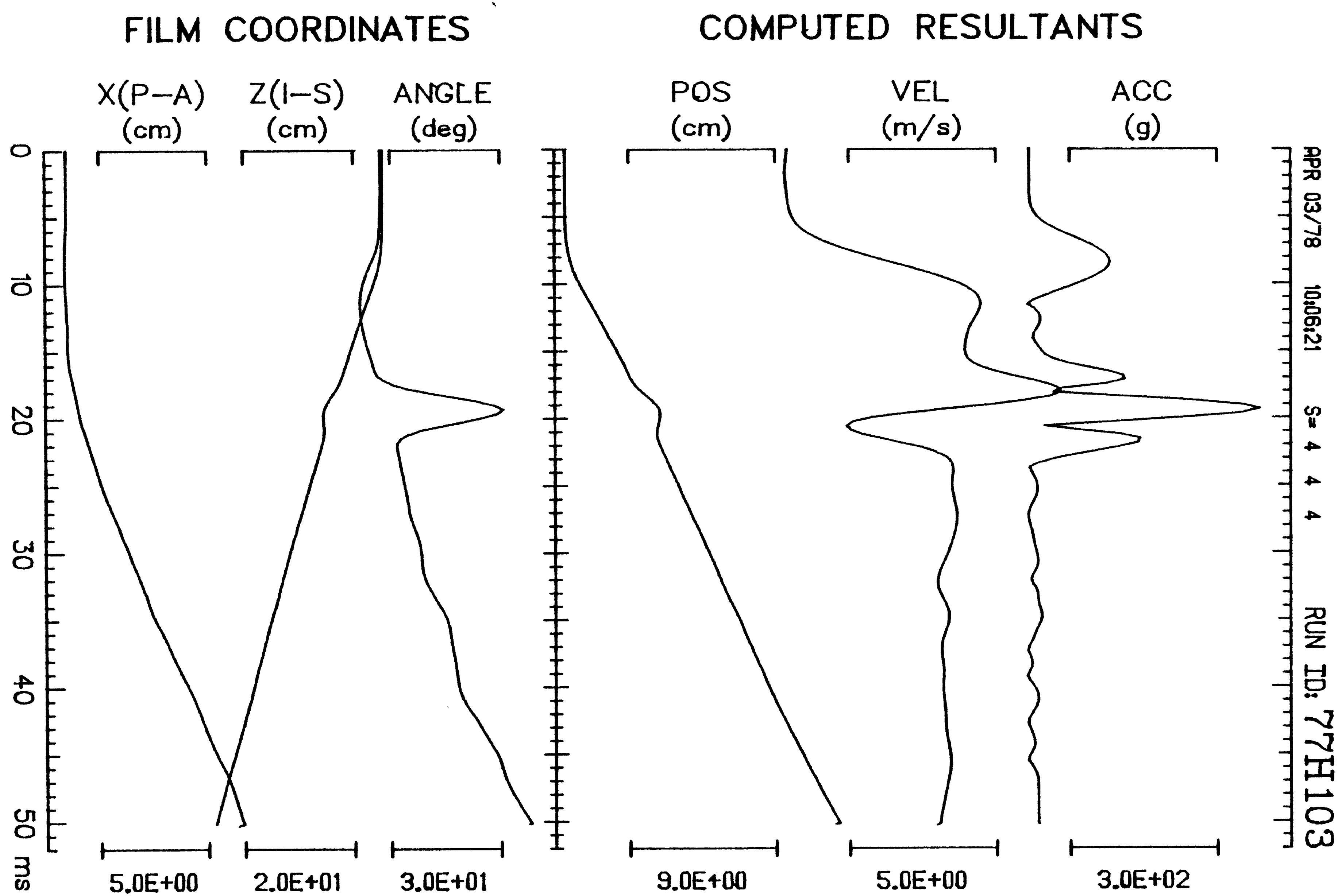

Head Motion vs. Time

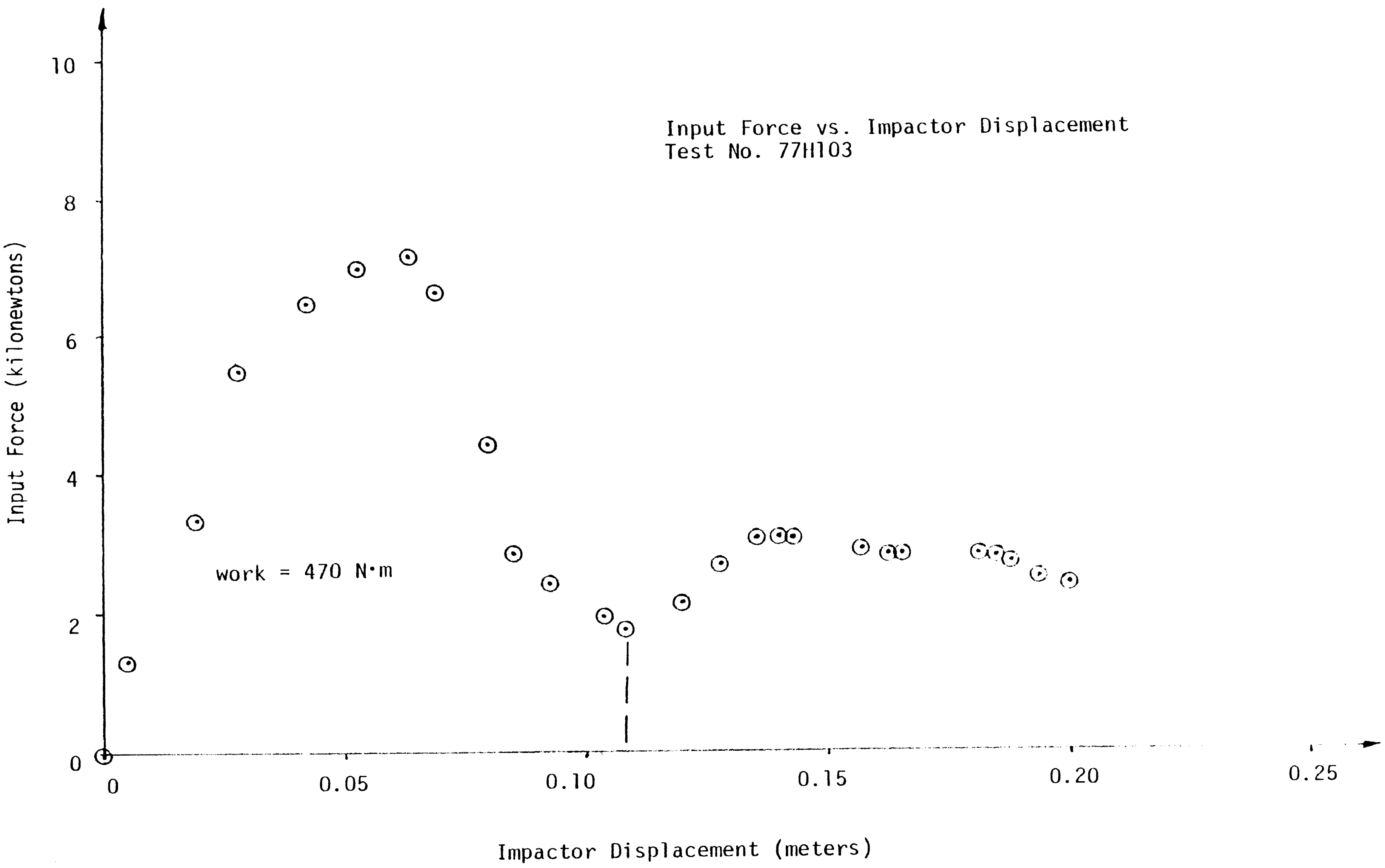

Input Force vs. Impactor Displacement
Test No. 77H103
work = 470 N·m
Input Force (kilonewtons)
Impactor Displacement (meters)
0
2
4
6
8
10
0.05
0.10
0.15
0.20
0.25

APPENDIX 9.2.4

TEST DATA FOR

77H104

TEST NO. 77H104

Piston Mass 9.9 kg.

Stroke 20.3 cm

Pressure 276 k Pa

Padding description 2.54 cm ensolite, 2.54 cm styrofoam

Photographic Coverage 35 mm BW and color slide 3000 fps color movies

Fixation description crotch blocked, torso taped down.

% Skull Area Below Impactor Axis NA

Approximate Cervical Spine Radius of Curvature NA

Damage: (Scoliotic), Intervertebral disks C_{3-4}, C_{4-5}, C_{5-6} crushed, Transverse processes of C_5 and T_1 fractured, T_2 severely crushed.

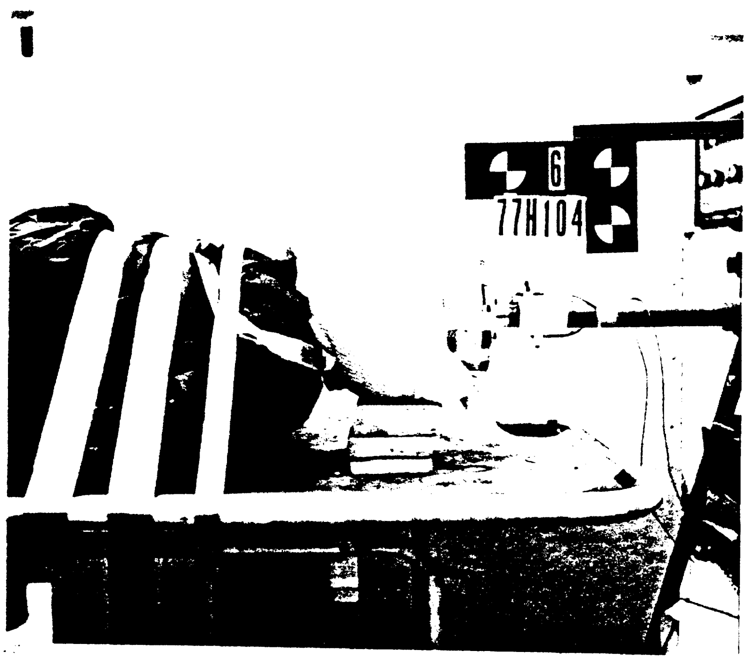

TEST 77H104 Instrumentation Traces

Compensated Force
444.8 N/div
Effectively Filtered
at 1600 Hz

Force
222.4 N/div
Effectively Filtered
at 1600 Hz

Acceleration
25 g's/div
Effectively filtered
at 1600 Hz

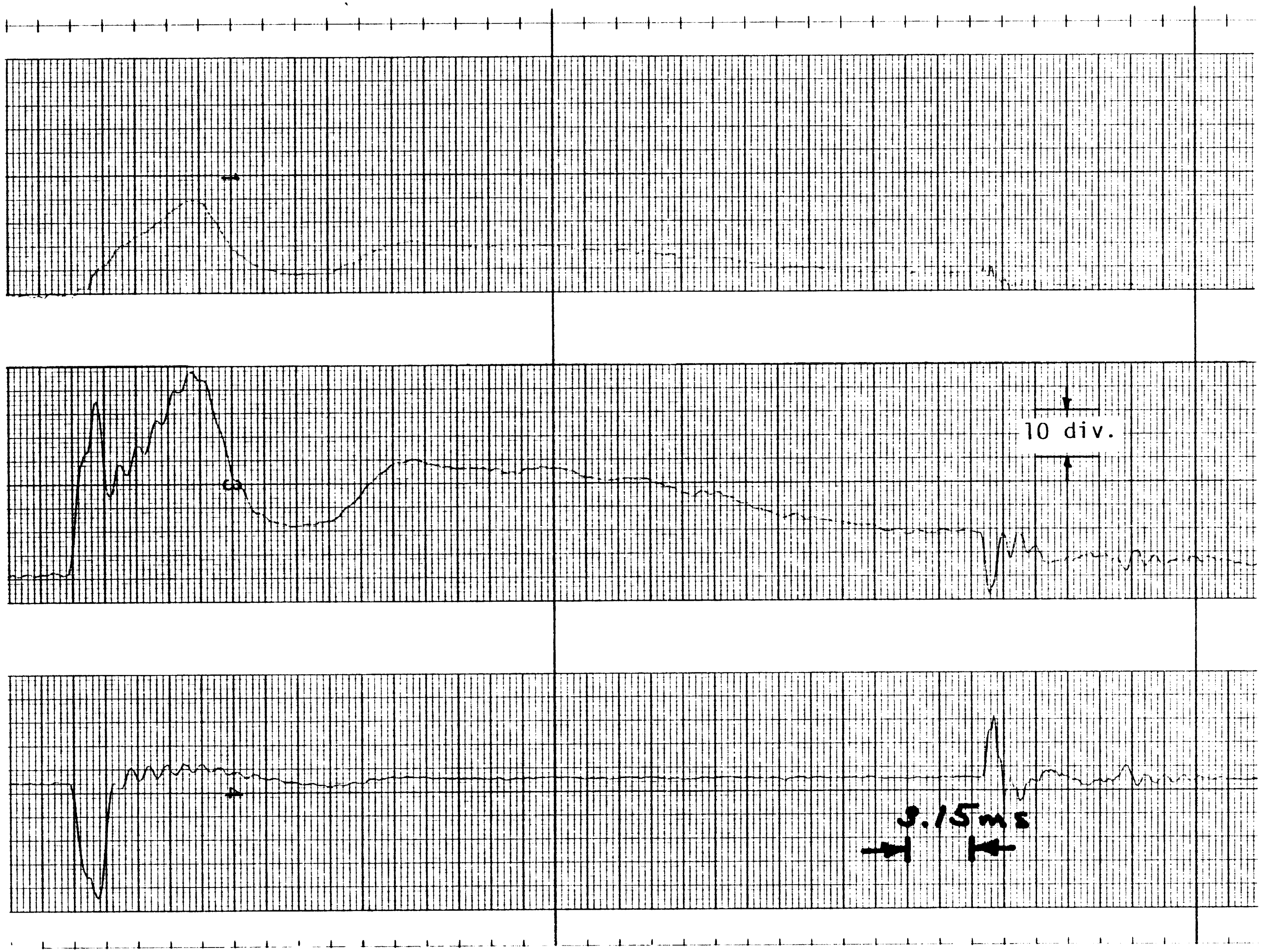

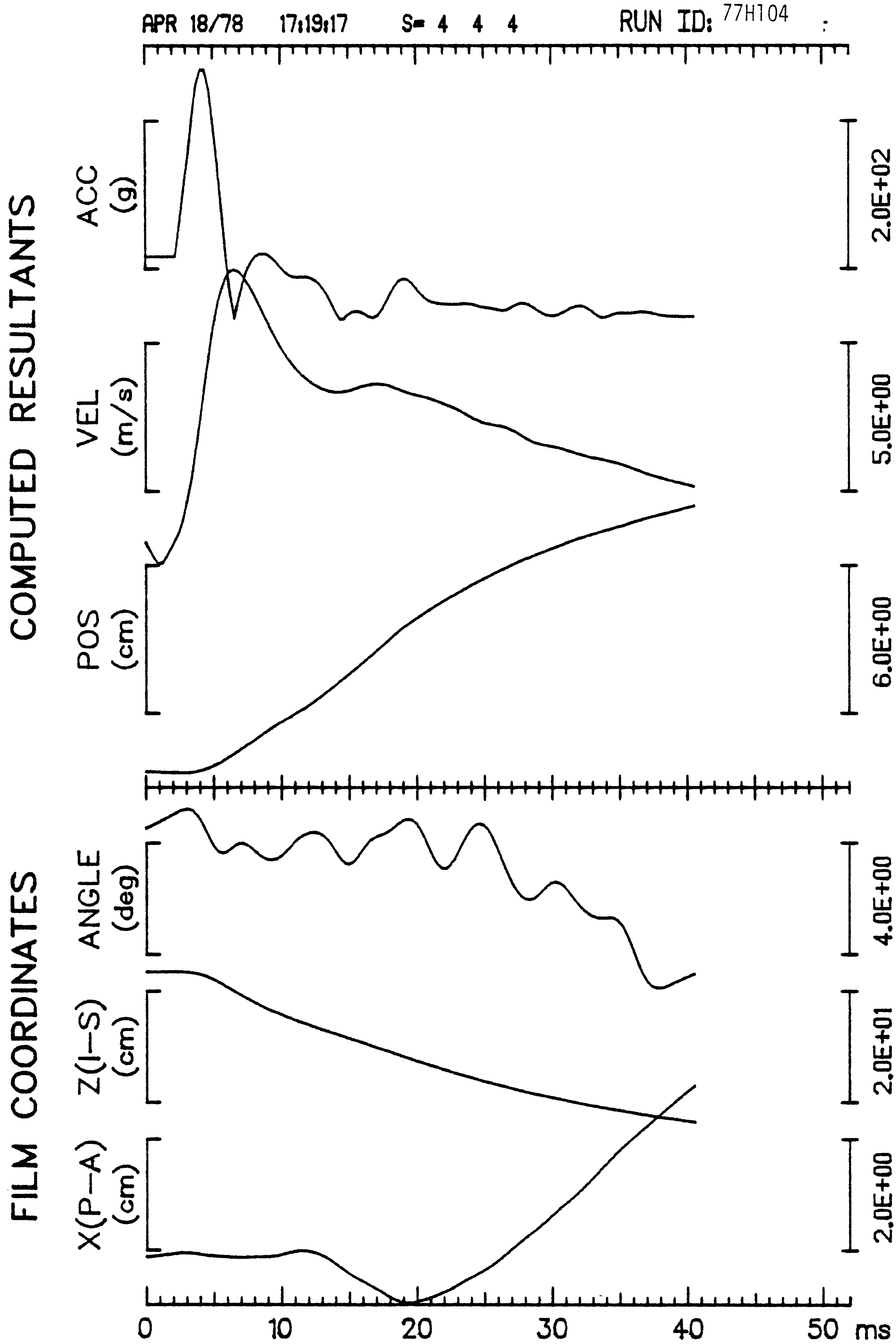

Impactor motion vs. time

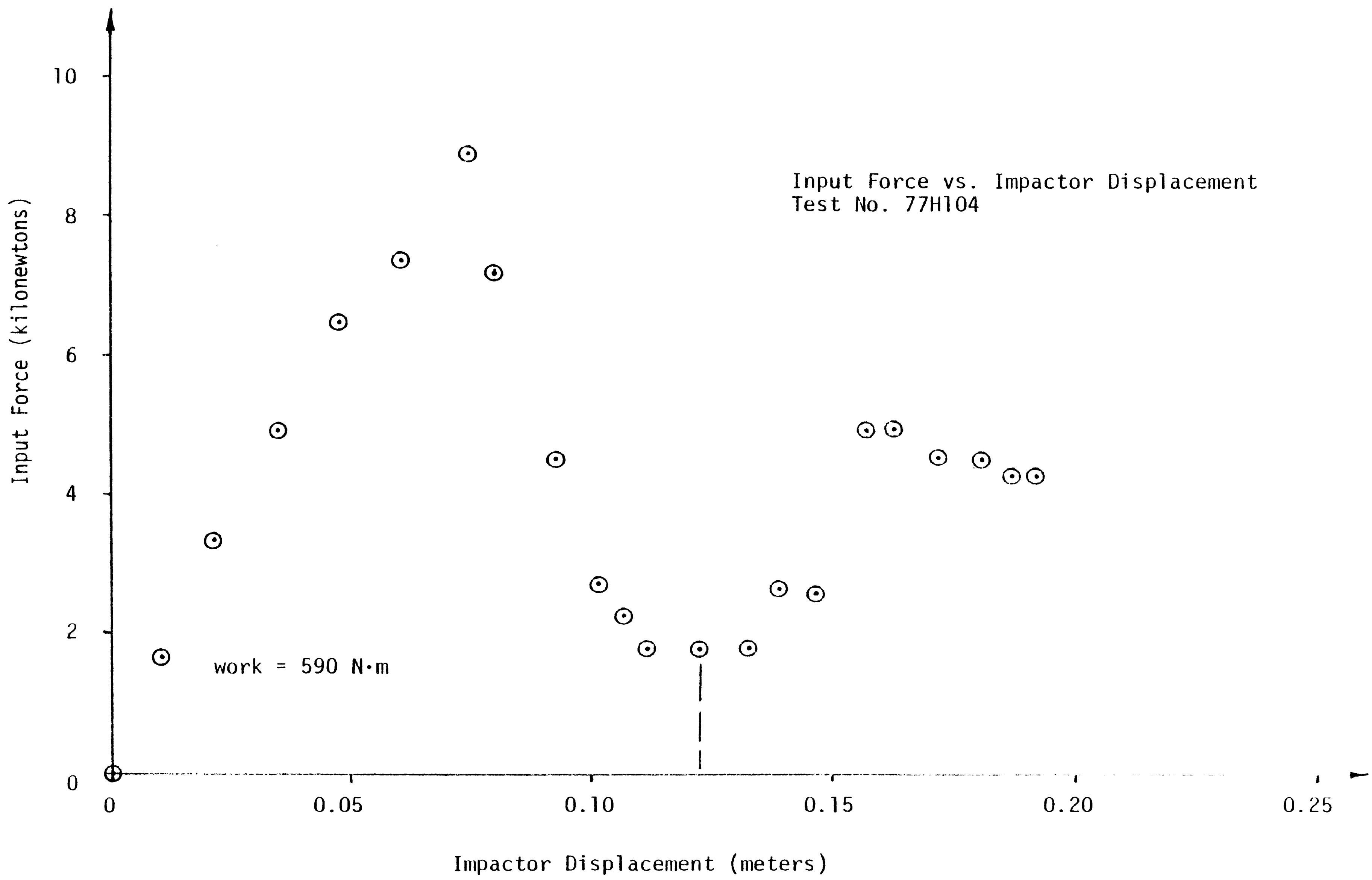
Input Force vs. Impactor Displacement
Test No. 77H104
work = 590 N·m
Input Force (kilonewtons)
Impactor Displacement (meters)
0
2
4
6
8
10
0
0.05
0.10
0.15
0.20
0.25

APPENDIX 9.2.5

TEST DATA FOR

77H105

TEST NO. 77H105

Piston Mass 9.9 kg

Stroke 20.3 cm

Pressure 241 kPa

Padding description 2.54 cm ensolite, 2.54 cm styrofoam

Photographic Coverage Polaroid set-up, 35 mm BW slide, 3000 fps color movies

Fixation description Feet placed against rigid stop, crotch block, torso taped down.

% Skull Area Below Impactor Axis 85%

Approximate Cervical Spine Radius of Curvature 11 cm.

Damage: Spinous process of C_2 fractured from body at arches, tip of C_6 spinous process fractured, slight crushing of C_{5-6} disk and T_1 left facet.

TEST 77H105 Instrumentation Traces

Compensated Force
444.8 N/div
Effectively Filtered
at 1600 Hz

Force
NA N/div
Effectively Filtered
at 1600 Hz

Acceleration
25 g's/div
Effectively filtered
at 1600 Hz

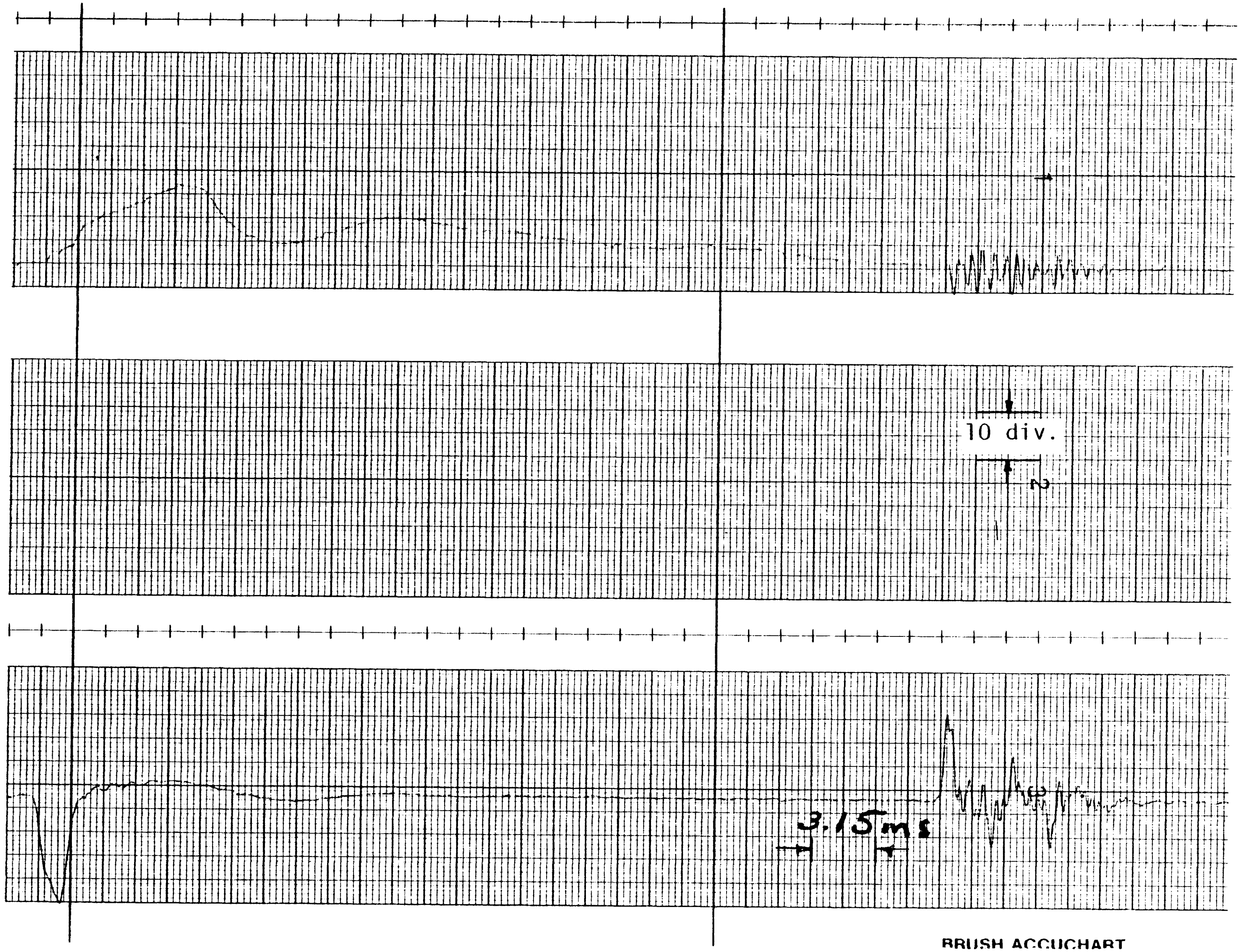

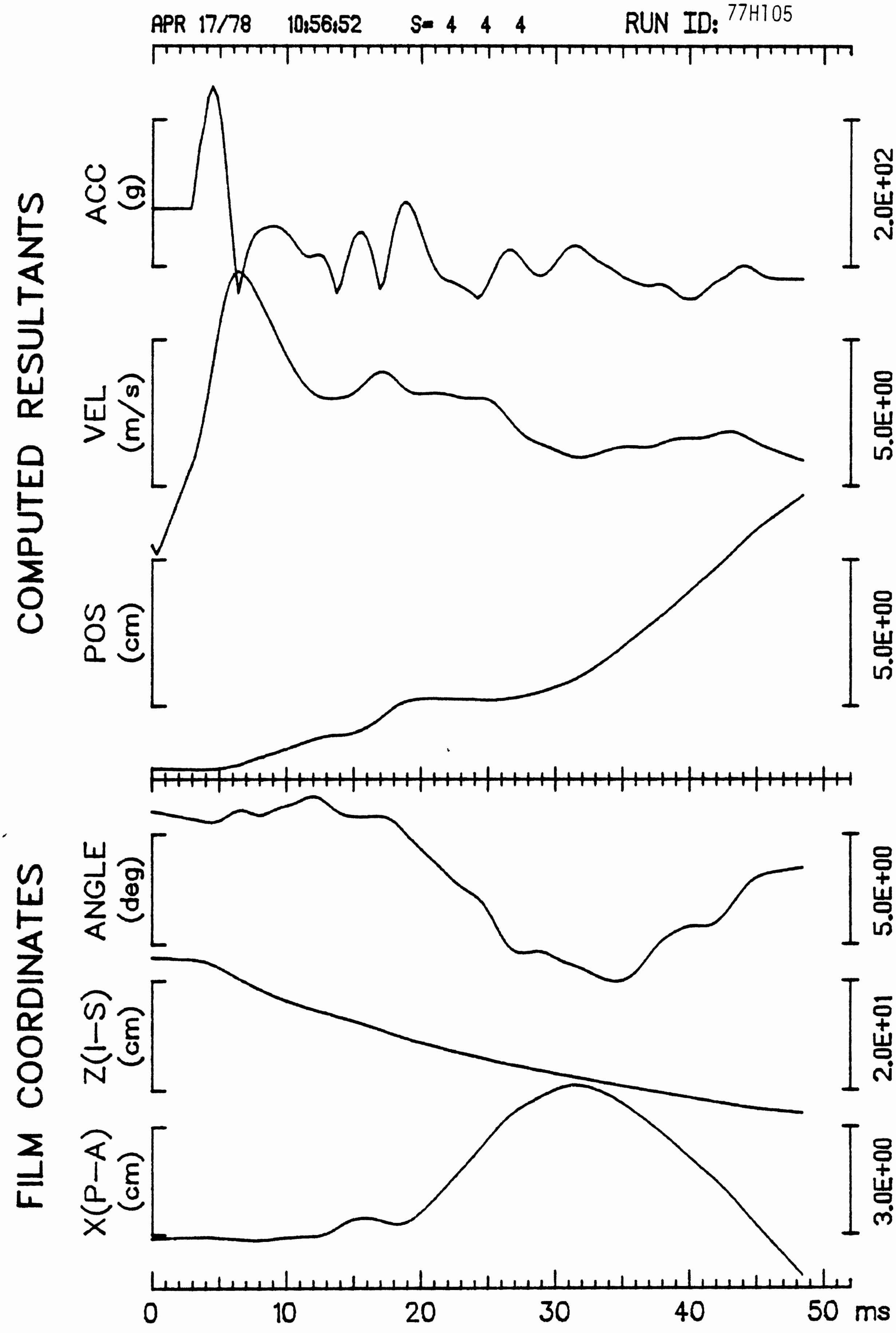

Impactor motion vs. time

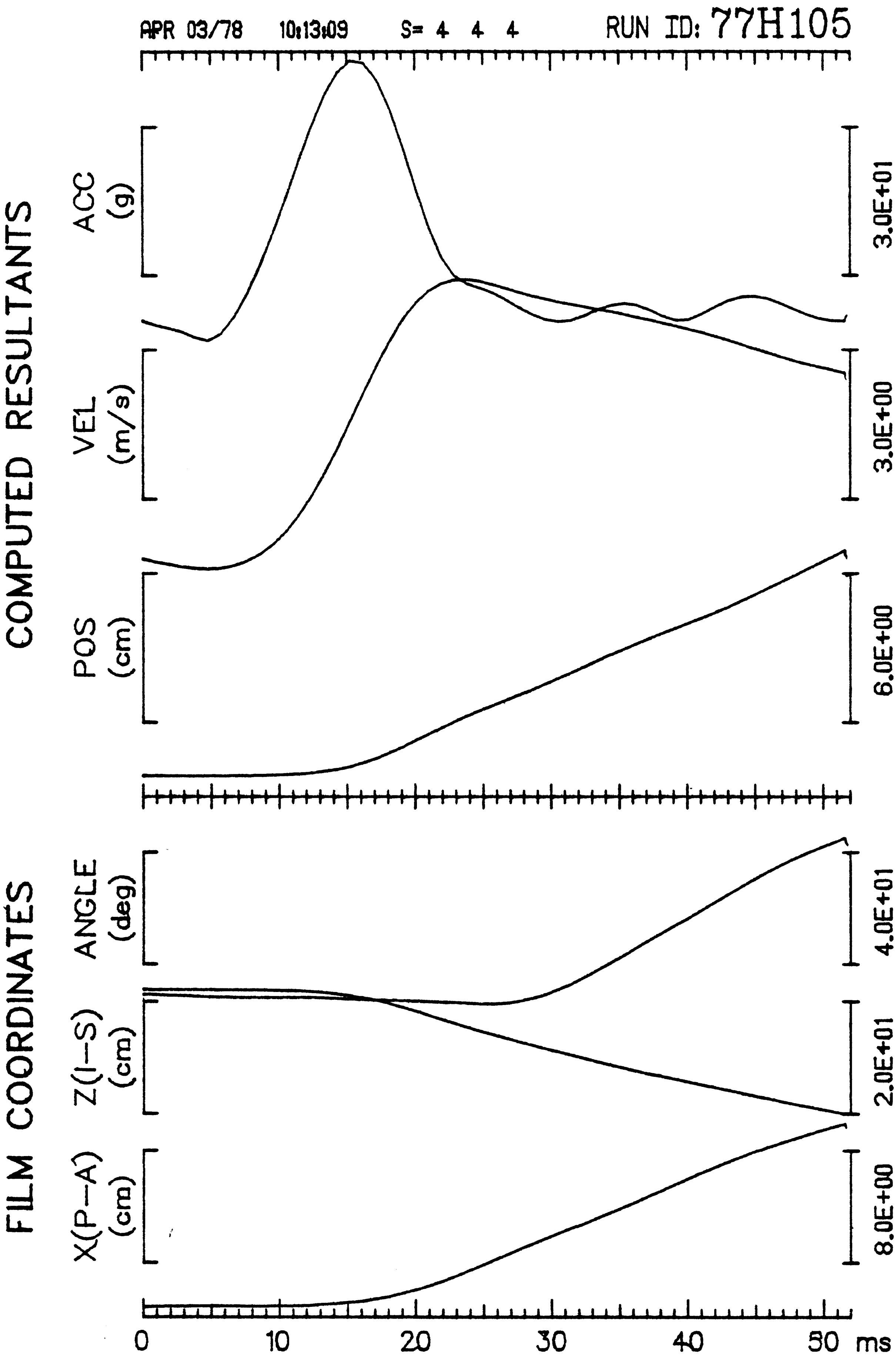

Head Motion vs. Time

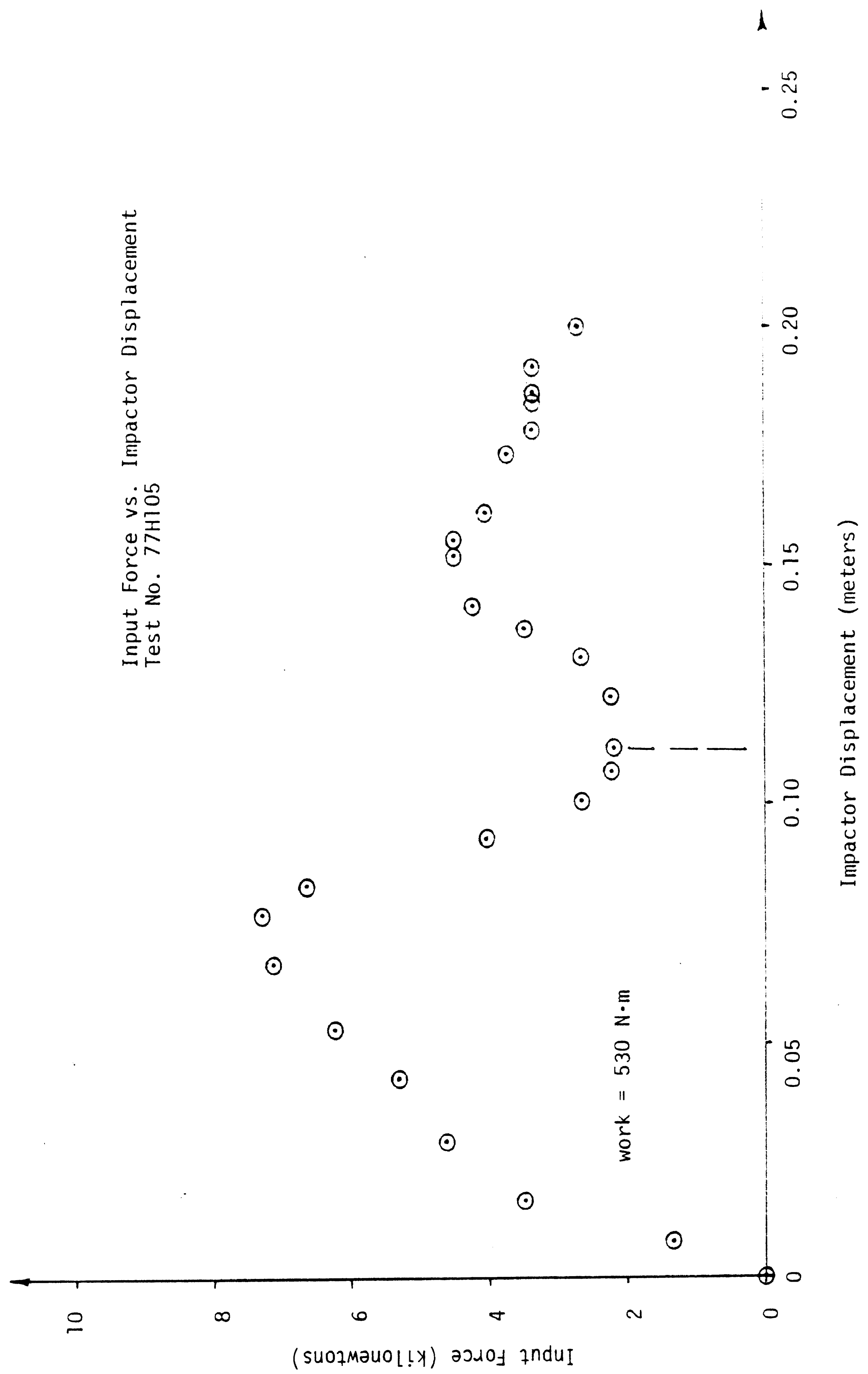
Input Force vs. Impactor Displacement
Test No. 77H105
work = 530 N·m
Input Force (kilonewtons)
0
2
4
6
8
10
Impactor Displacement (meters)
0
0.05
0.10
0.15
0.20
0.25

APPENDIX 9.2.6

TEST DATA FOR

78H106

TEST NO. 78H106

Piston Mass 9.9 kg

Stroke 20.3 cm

Pressure 207 kPa

Padding description 2.54 cm ensolite, 2.54 cm styrofoam

Photographic Coverage 35 mm BW slide, polaroid set-up, 3000 fps color movies

Fixation description Feet rigidly block, crotch block, torso taped down.

% Skull Area Below Impactor Axis 58%

Approximate Cervical Spine Radius of Curvature 15.8 cm

Damage: No fracture of skull or spine.

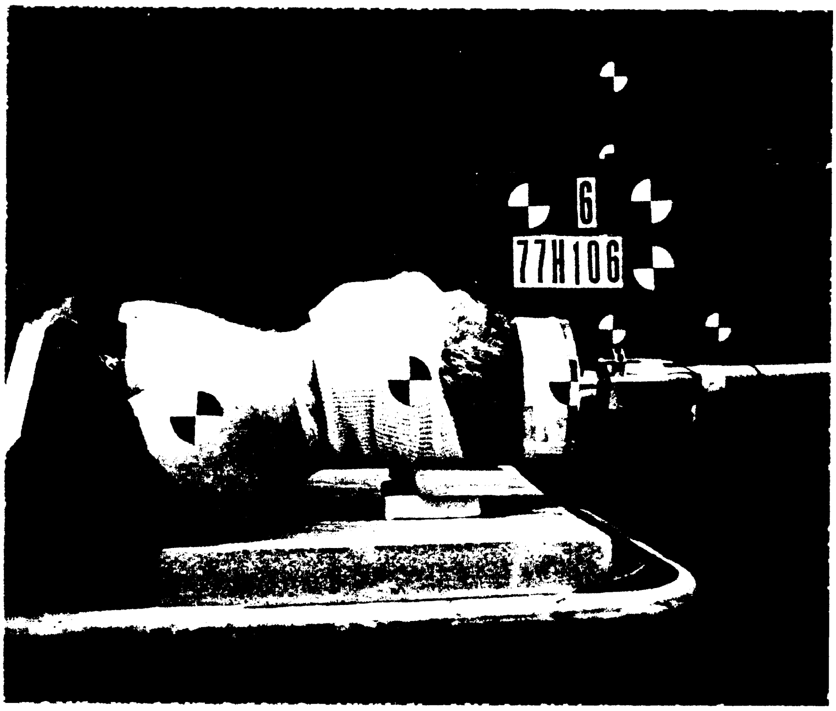

TEST 78H106 Instrumentation Traces

Compensated Force
444.8 N/div
Effectively Filtered
at 1600 Hz

Force
444.8 N/div
Effectively Filtered
at 1600 Hz

Acceleration
25 g's/div
Effectively filtered
at 1600 Hz

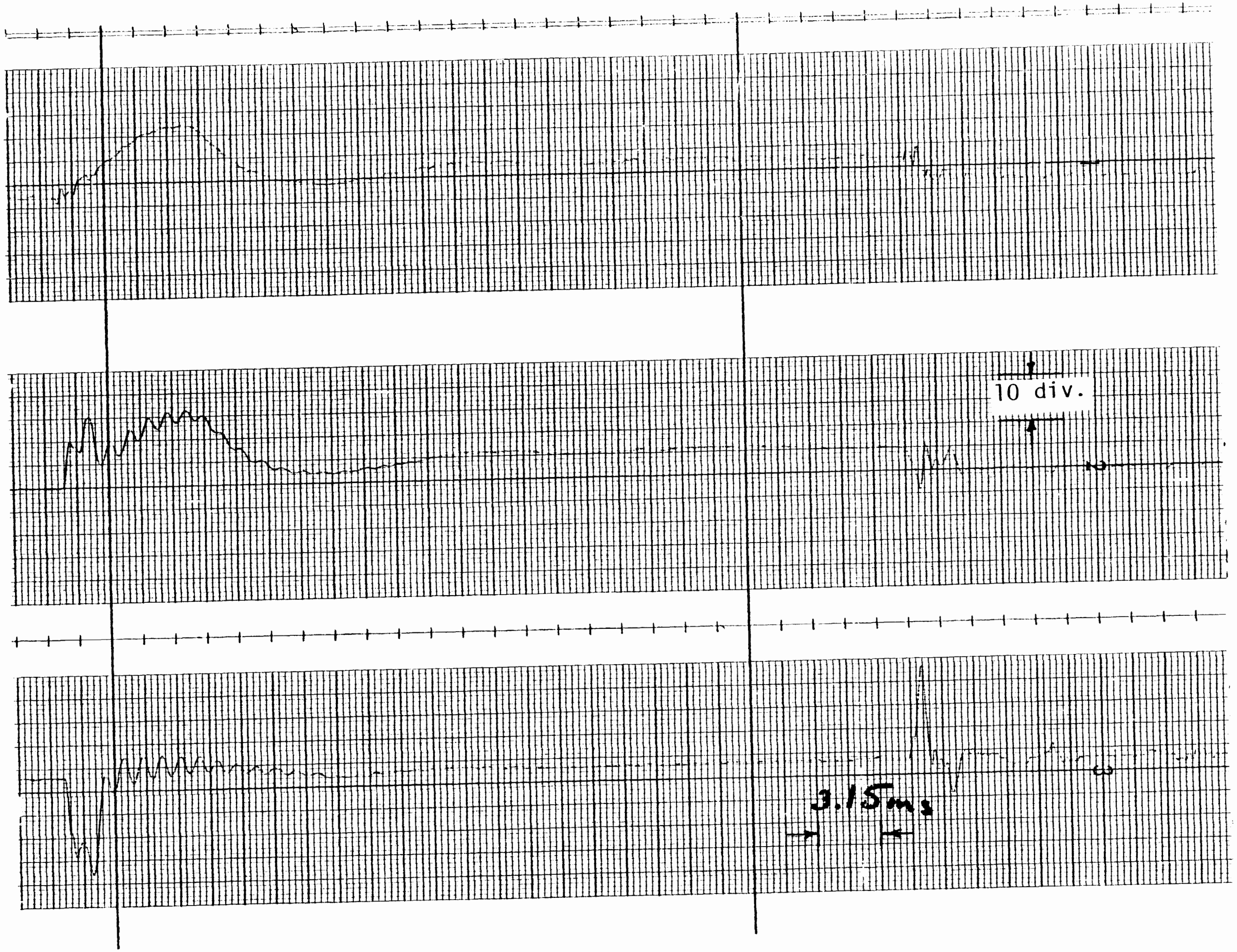

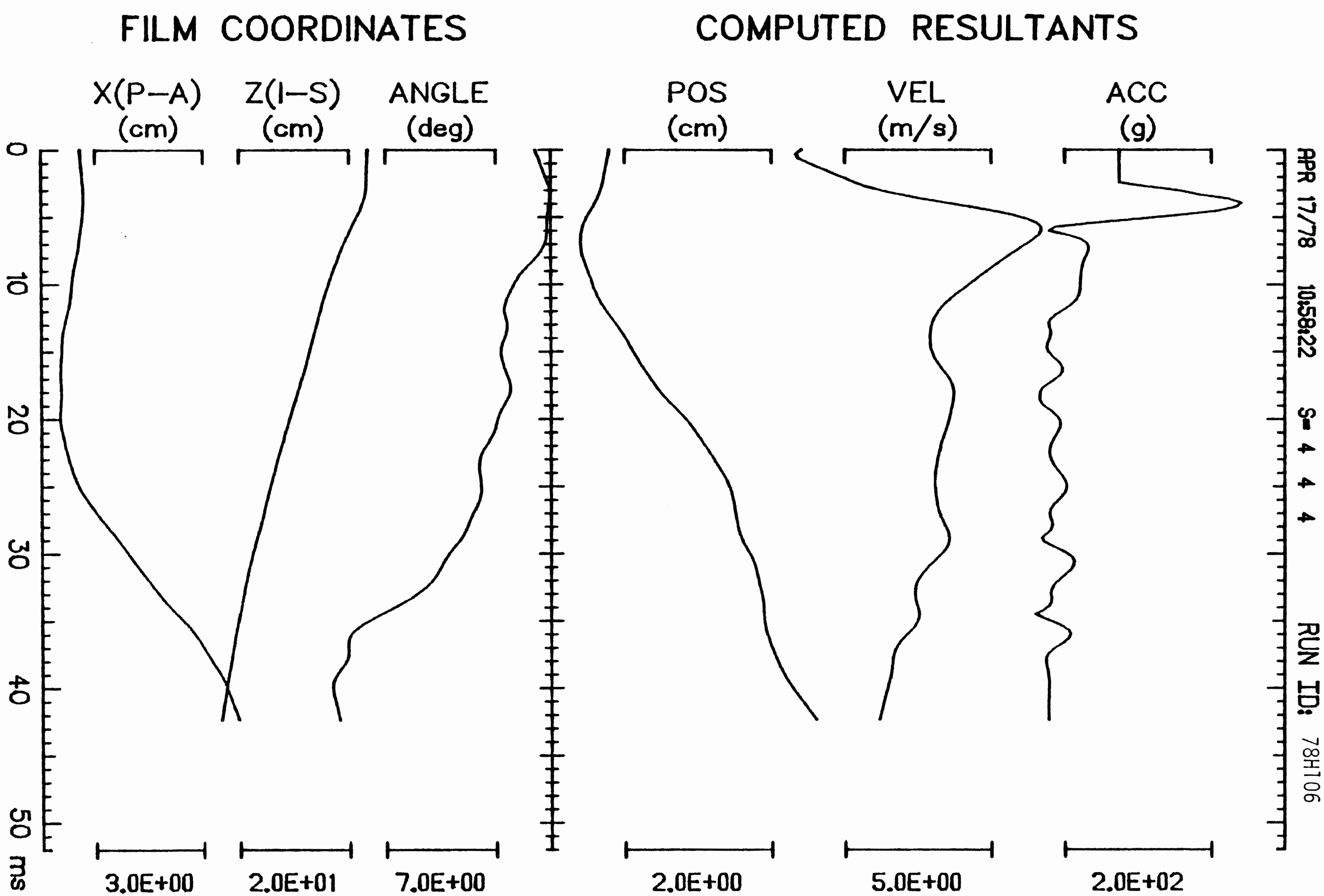

Impactor motion vs. time

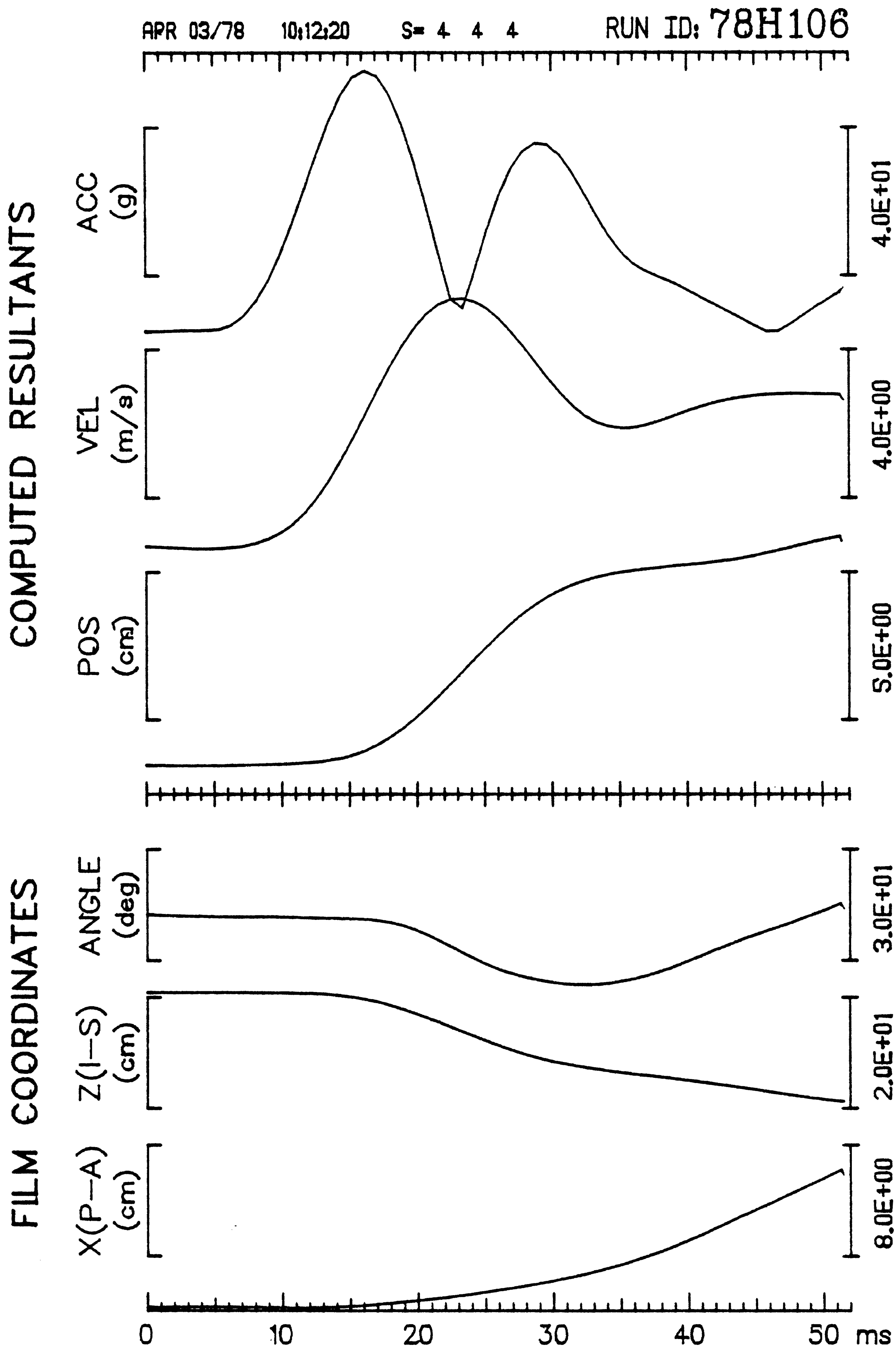

Head Motion vs. Time

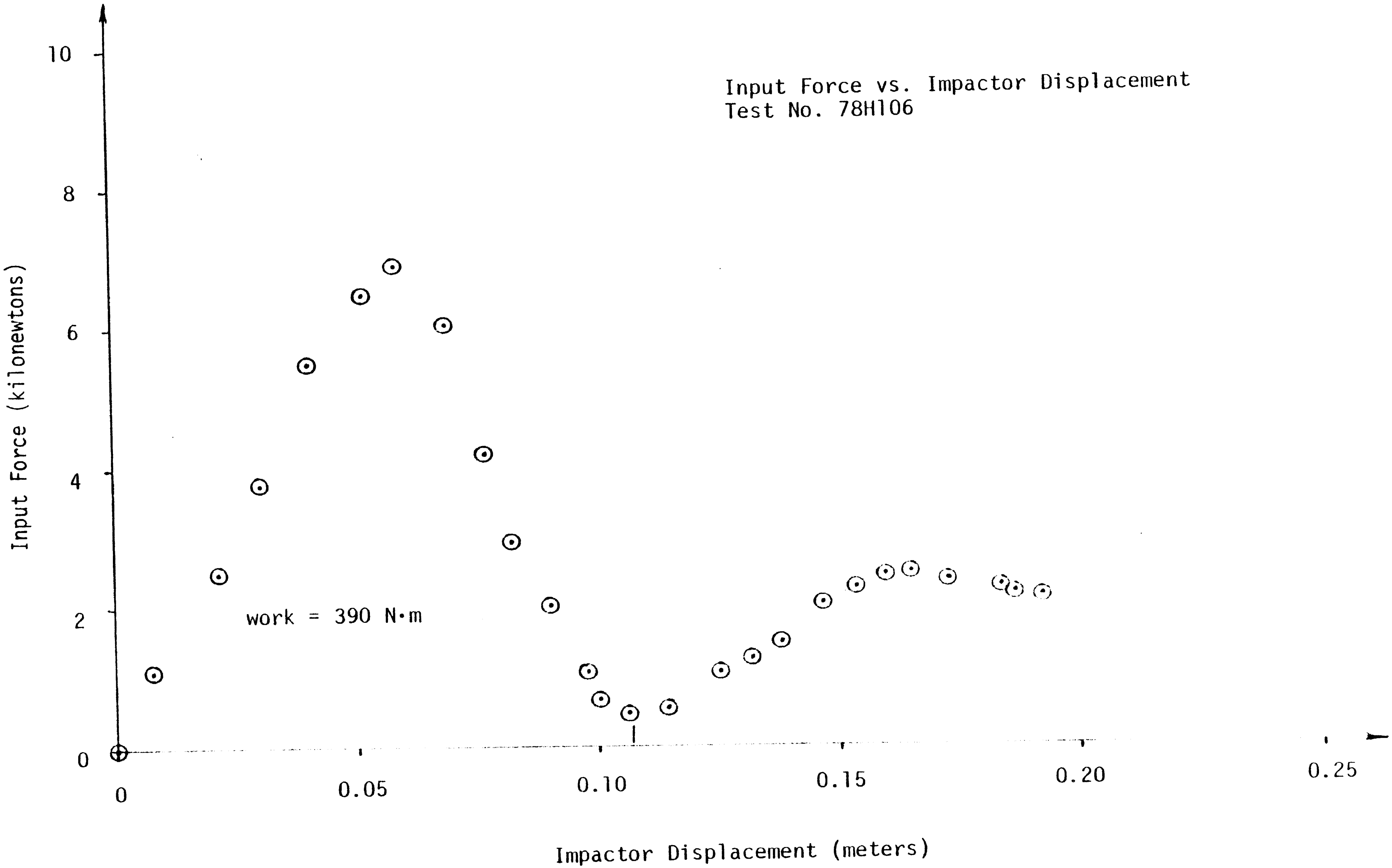
Input Force vs. Impactor Displacement
Test No. 78H106
work = 390 N·m
Input Force (kilonewtons)
Impactor Displacement (meters)
0
2
4
6
8
10
0
0.05
0.10
0.15
0.20
0.25

APPENDIX 9.2.7

TEST DATA FOR

78H107

TEST NO. 78H107

Piston Mass 9.9 kg

Stroke 10.2 cm

Pressure 241 kPa

Padding description 2.54 cm ensolite, 2.54 cm styrofoam

Photographic Coverage 35 mm BW slide, Polaroid set-up, 3000 fps color movies

Fixation description Feet rigidly blocked, crotch block, torso taped

% Skull Area Below Impactor Axis 72%

Approximate Cervical Spine Radius of Curvature 24 cm

Damage: Complete fracture from body of C_3 & C_4 left transverse processes, chip fracture of spinous process of C_5, C_6, C_7, T_2.

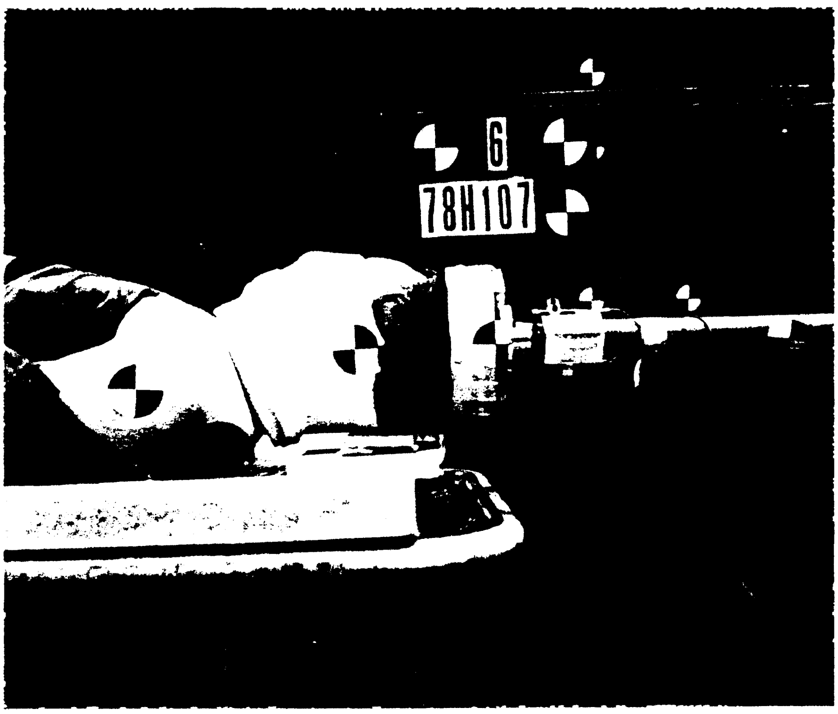

TEST 78H107 Instrumentation Traces

Compensated Force
444.8 N/div
Effectively Filtered
at 1600 Hz

Force
444.8 N/div
Effectively Filtered
at 1600 Hz

Acceleration
35 g's/div
Effectively filtered
at 1600 Hz

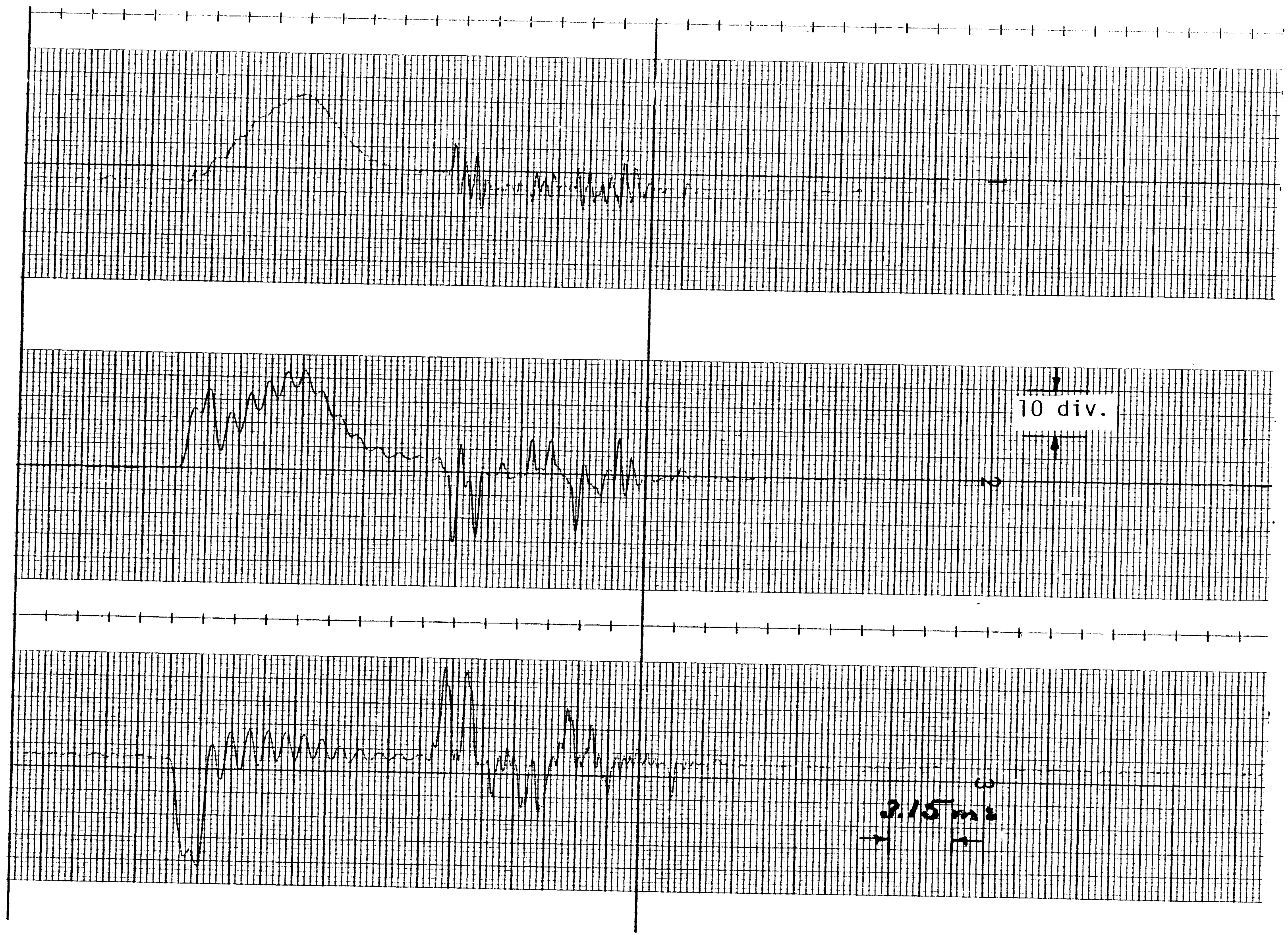

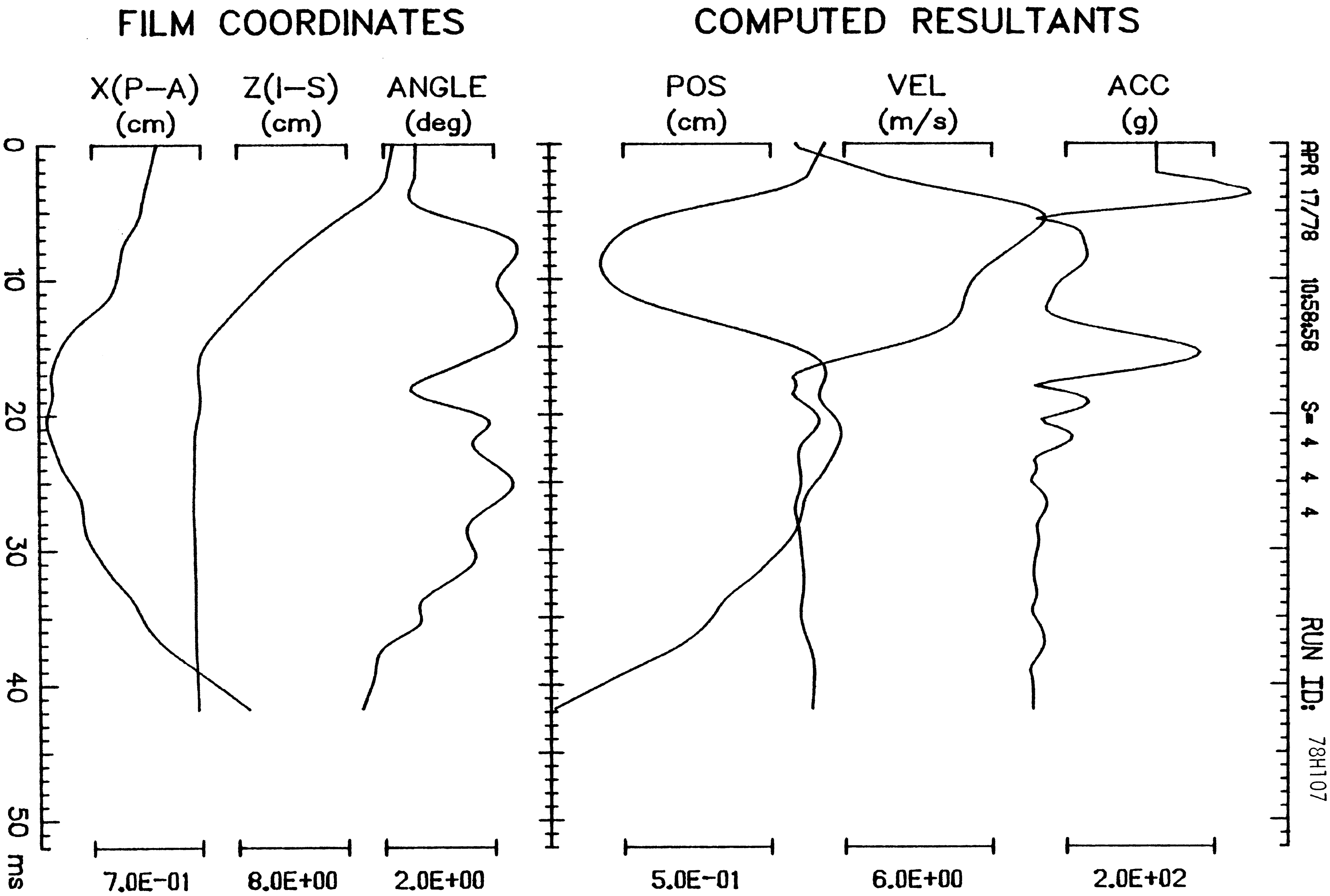

Impactor motion vs. time

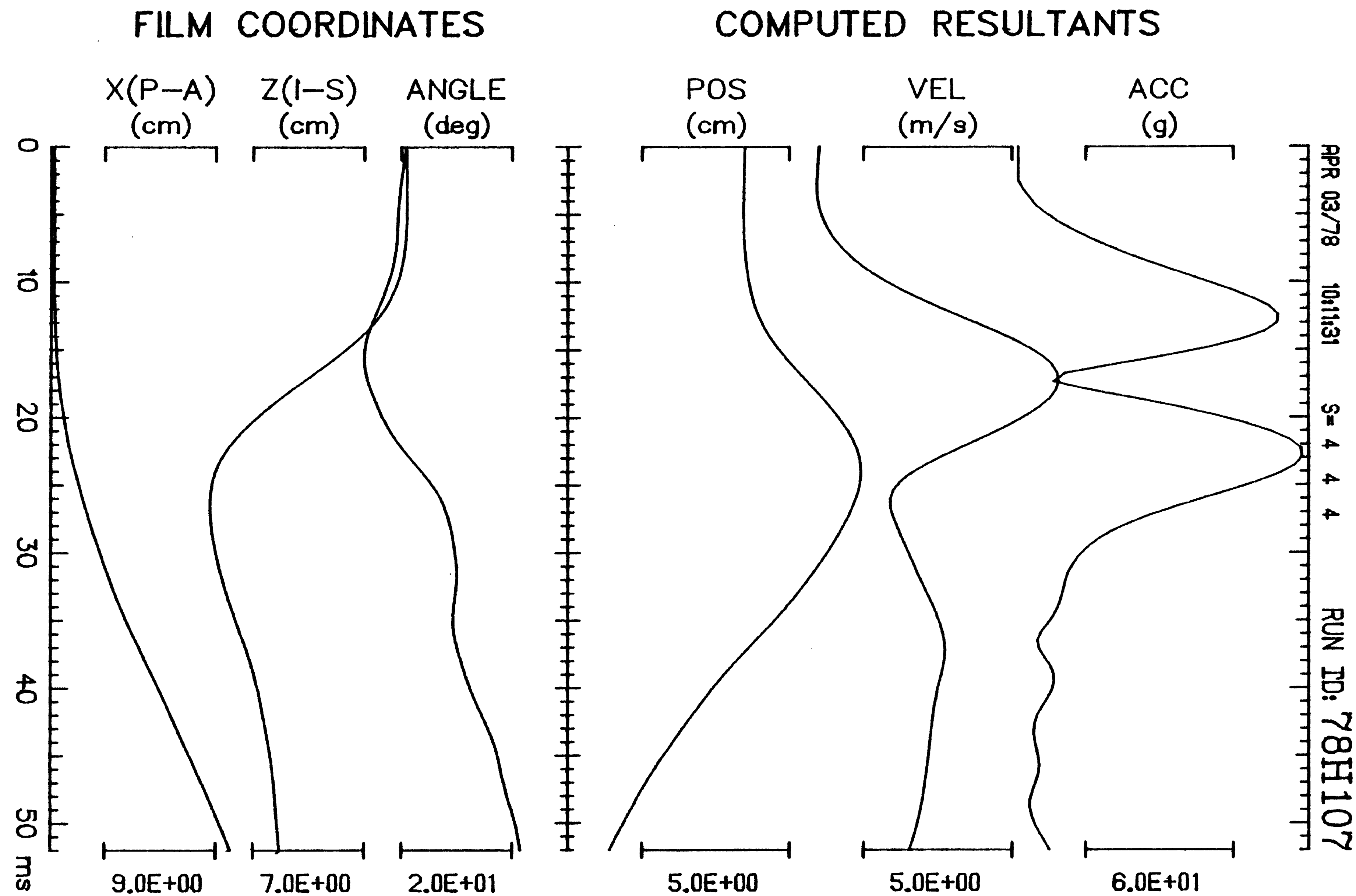

Head Motion vs. Time

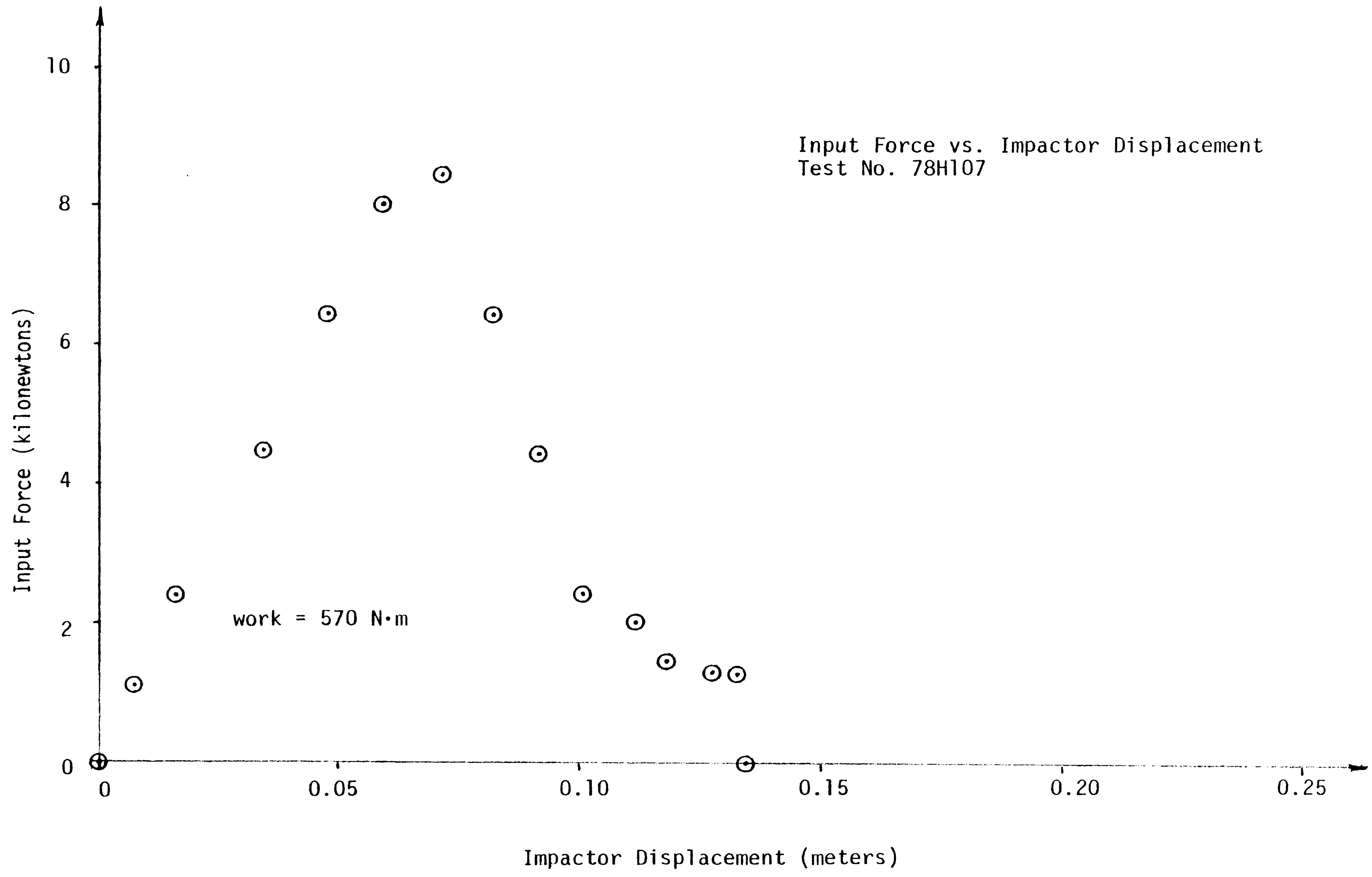
Input Force vs. Impactor Displacement
Test No. 78H107
work = 570 N·m
Input Force (kilonewtons)
0
2
4
6
8
10
0
0.05
0.10
0.15
0.20
0.25
Impactor Displacement (meters)

APPENDIX 9.2.8

TEST DATA FOR

78H108

TEST NO. 78H108

Piston Mass 9.9 kg.

Stroke 10.2 cm

Pressure 207 kPa

Padding description 2.54 cm ensolite, 2.54 cm styrofoam

Photographic Coverage 35 mm BW slide, Polaroid set-up, 3000 fps color movies

Fixation description Feet rigidly blocked, crotch block, torso taped down

% Skull Area Below Impactor Axis 52 %

Approximate Cervical Spine Radius of Curvature 13 cm

Damage: Complete fracture of spinous process of C_1, T_1, T_2 through arches, fracture of tip of spinous process of C_3, C_4, C_7.

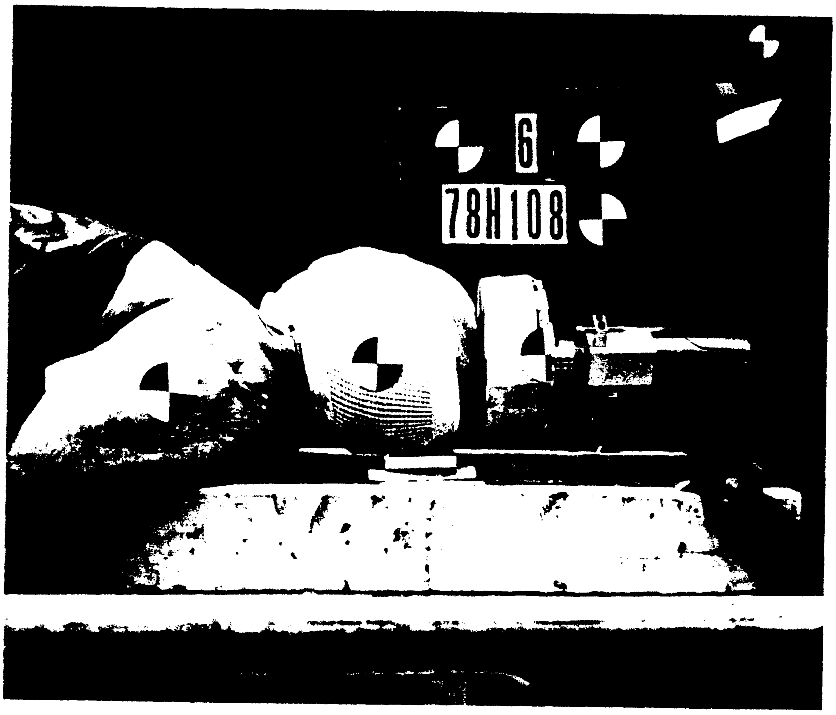

TEST 78H108 Instrumentation Traces

Compensated Force
444.8 N/div
Effectively Filtered
at 1600 Hz

Force
444.8 N/div
Effectively Filtered
at 1600 Hz

Acceleration
35 g's/div
Effectively filtered
at 1600 Hz

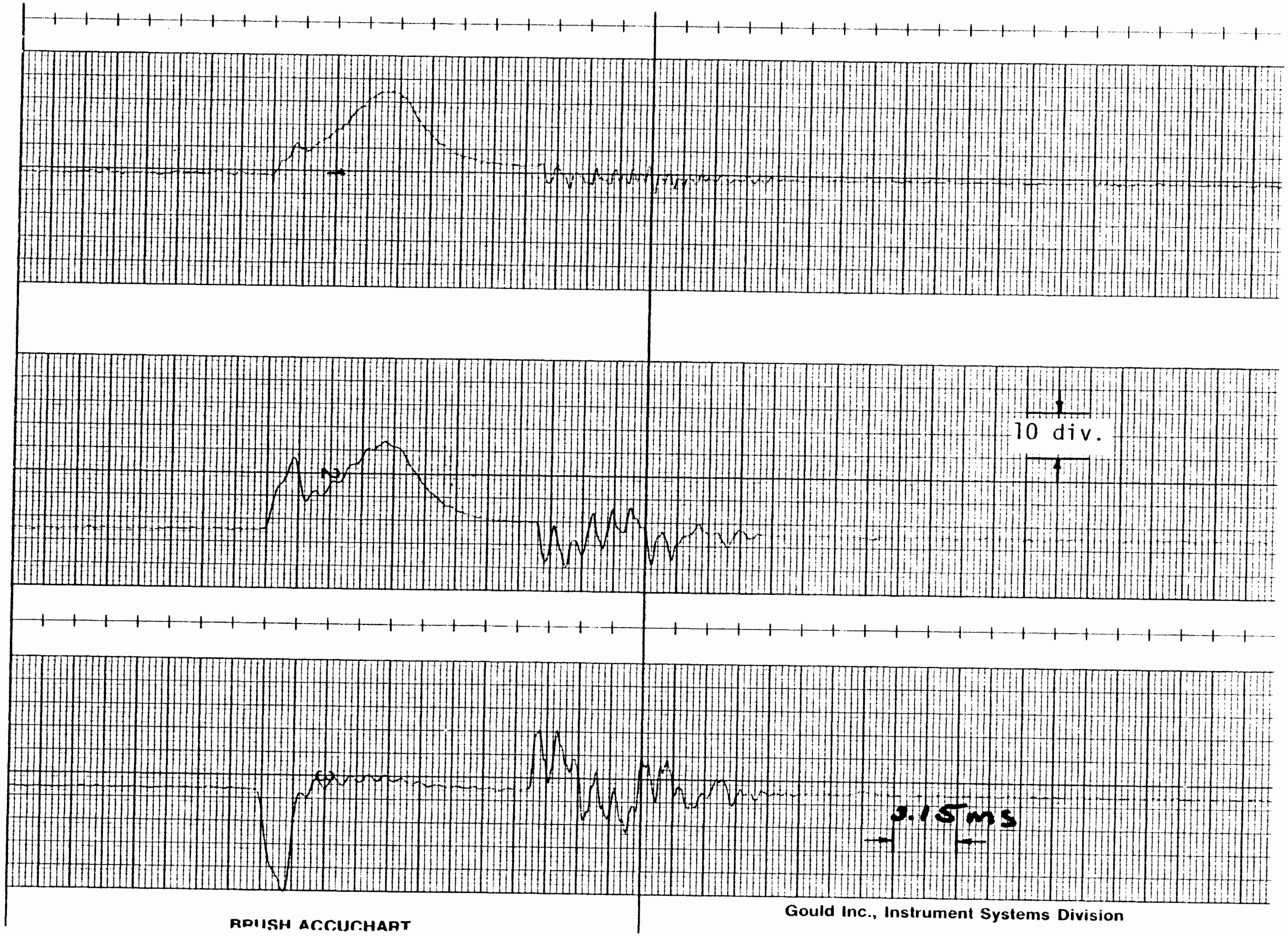

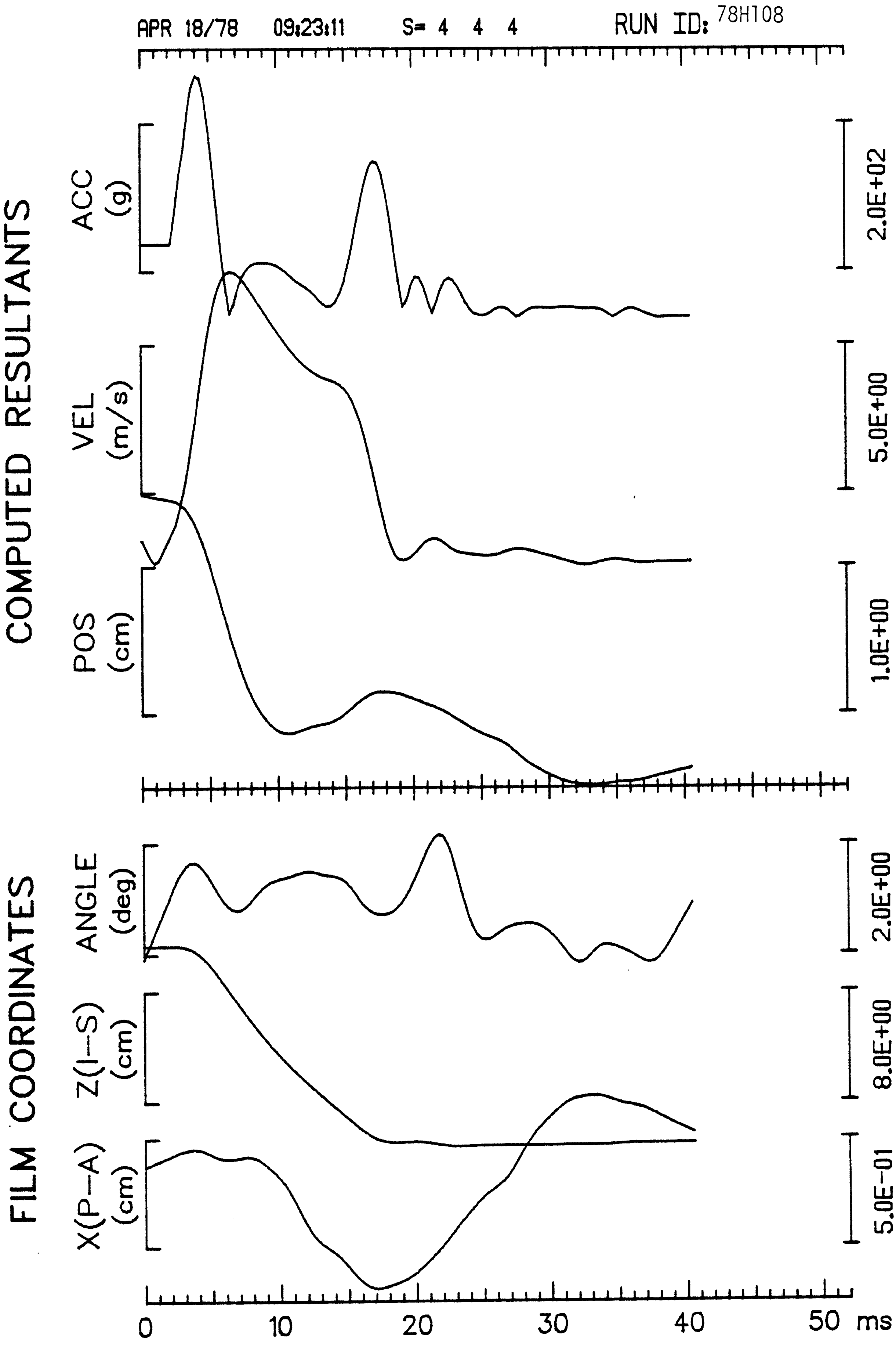

Impactor Motion versus Time

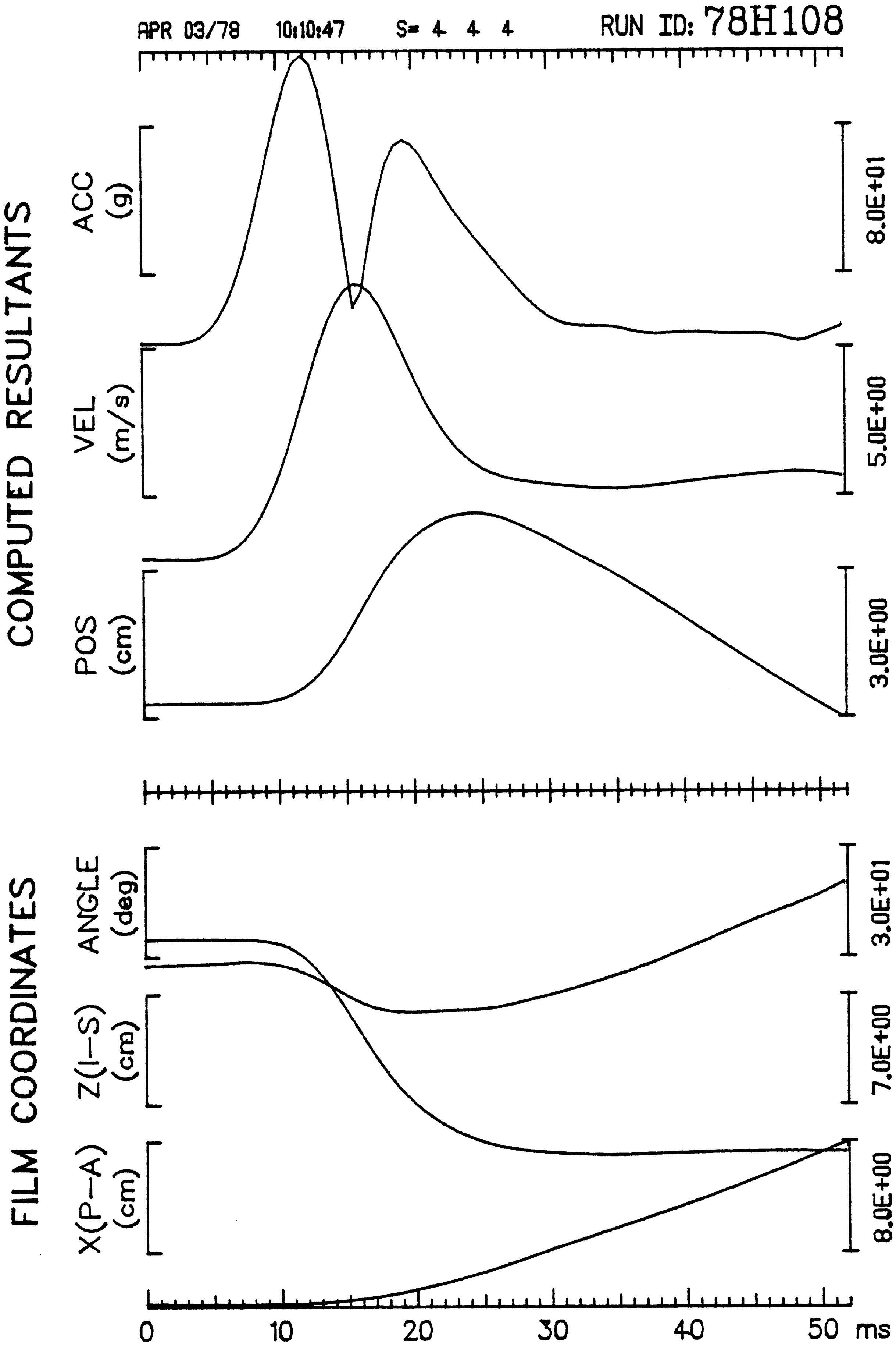

Head Motion vs. Time

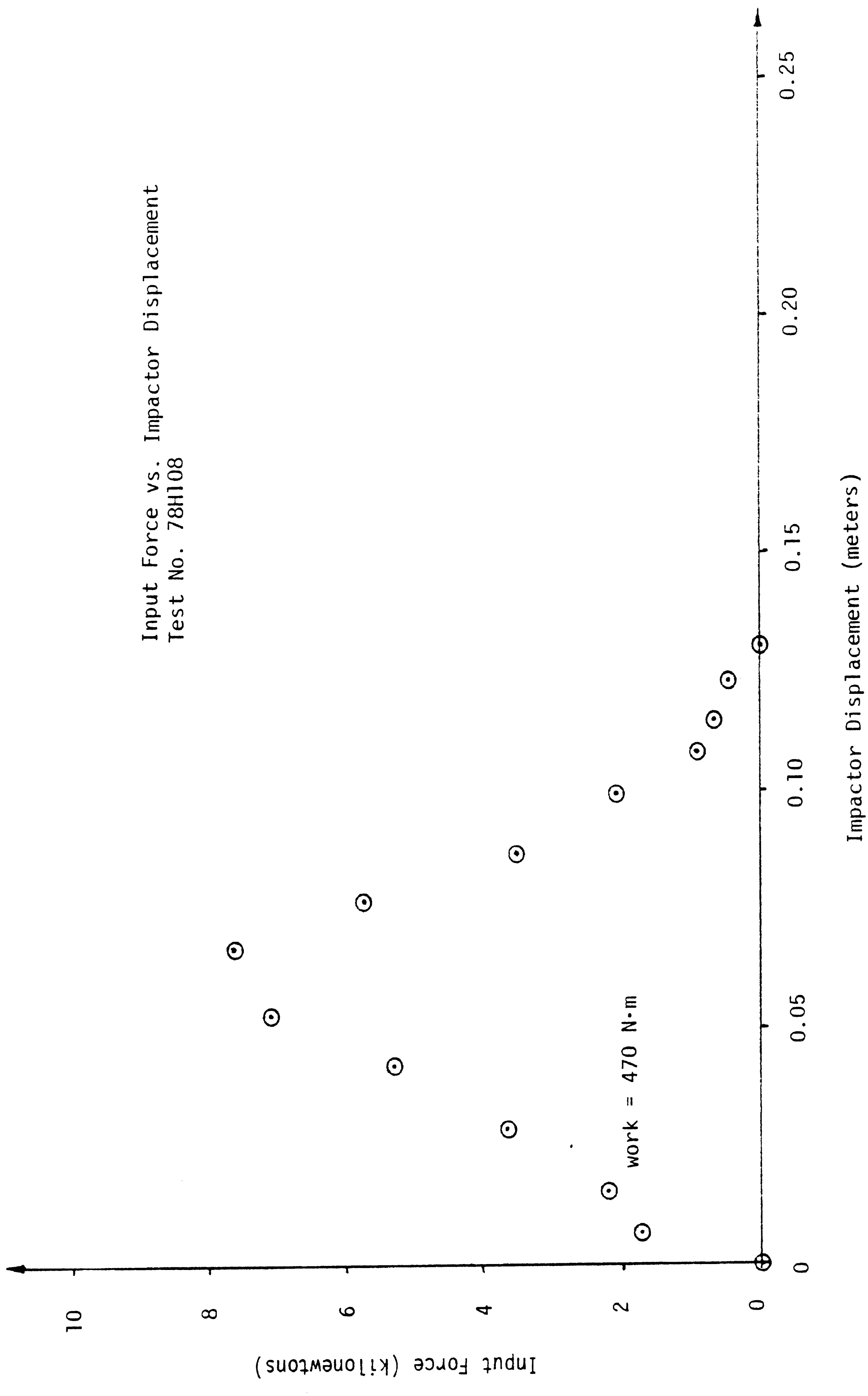
Input Force vs. Impactor Displacement
Test No. 78H108
work = 470 N·m
Input Force (kilonewtons)
0
2
4
6
8
10
Impactor Displacement (meters)
0
0.05
0.10
0.15
0.20
0.25

APPENDIX 9.2.9

TEST DATA FOR

78H109

TEST NO. 78H109

Piston Mass 9.9 kg

Stroke 10.2 cm

Pressure 172 kPa

Padding description 2.54 cm ensolite, 2.54 cm styrofoam

Photographic Coverage 35 mm BW slide, Polaroid set-up, 3000 fps color movies

Fixation description Feet rigidly blocked, crotch block, torso taped down.

% Skull Area Below Impactor Axis NA

Approximate Cervical Spine Radius of Curvature NA

Damage: Spinous processes of C_7, T_1 fractured, Rt. and lt. transverse process of T_1 fractured, rt. transverse process C_7 crushed.

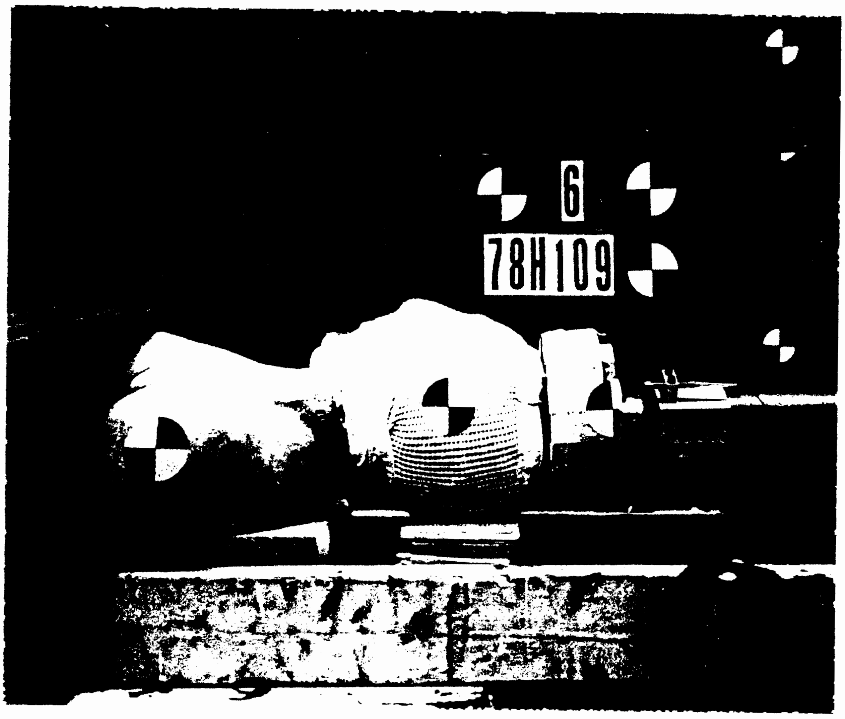

TEST 78H109 Instrumentation Traces

Compensated Force
177.9 N/div
Effectively Filtered
at 1600 Hz

Force
222.4 N/div
Effectively Filtered
at 1600 Hz

Acceleration
16.5 g's/div
Effectively filtered
at 1600 Hz

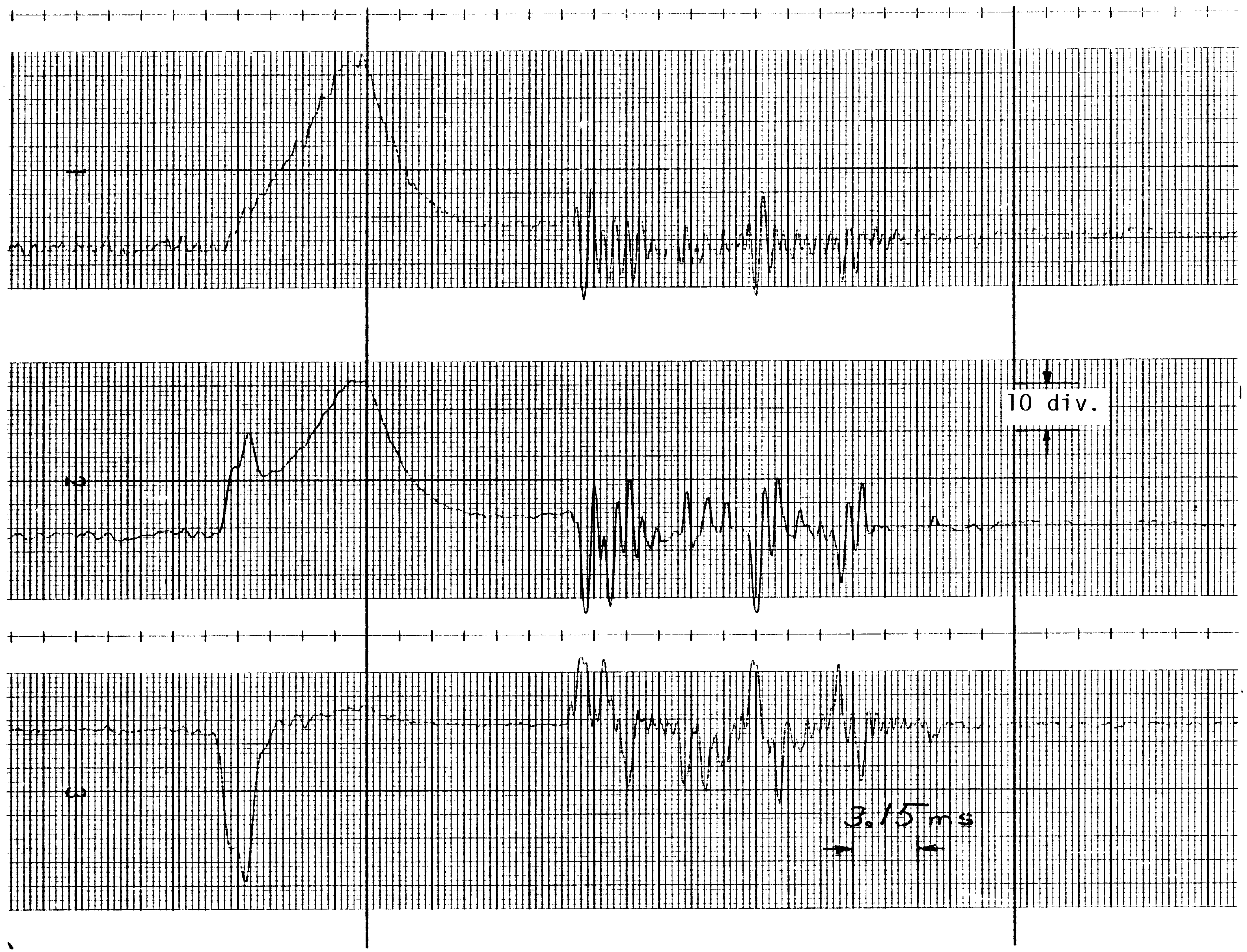

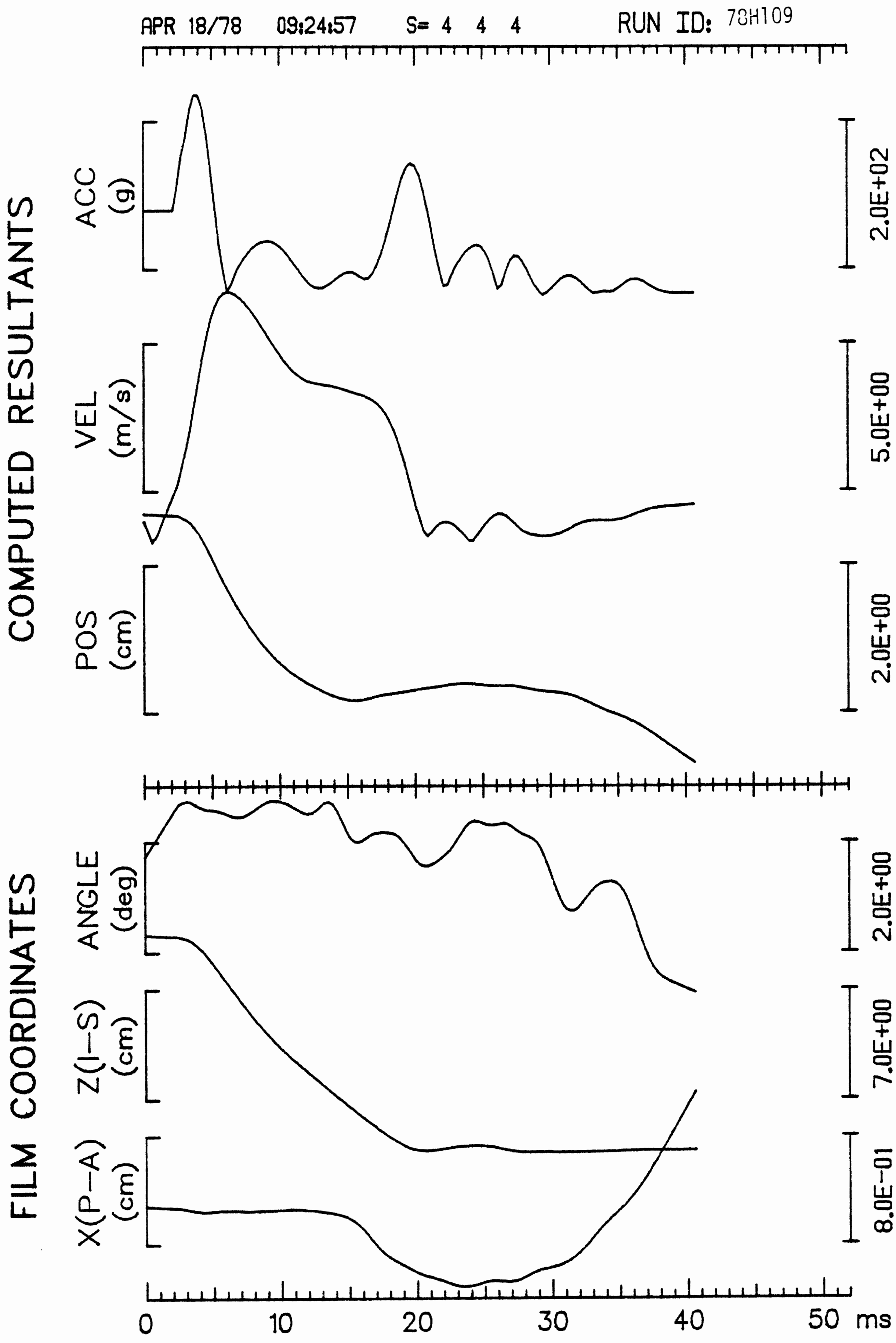

Impactor Motion versus Time

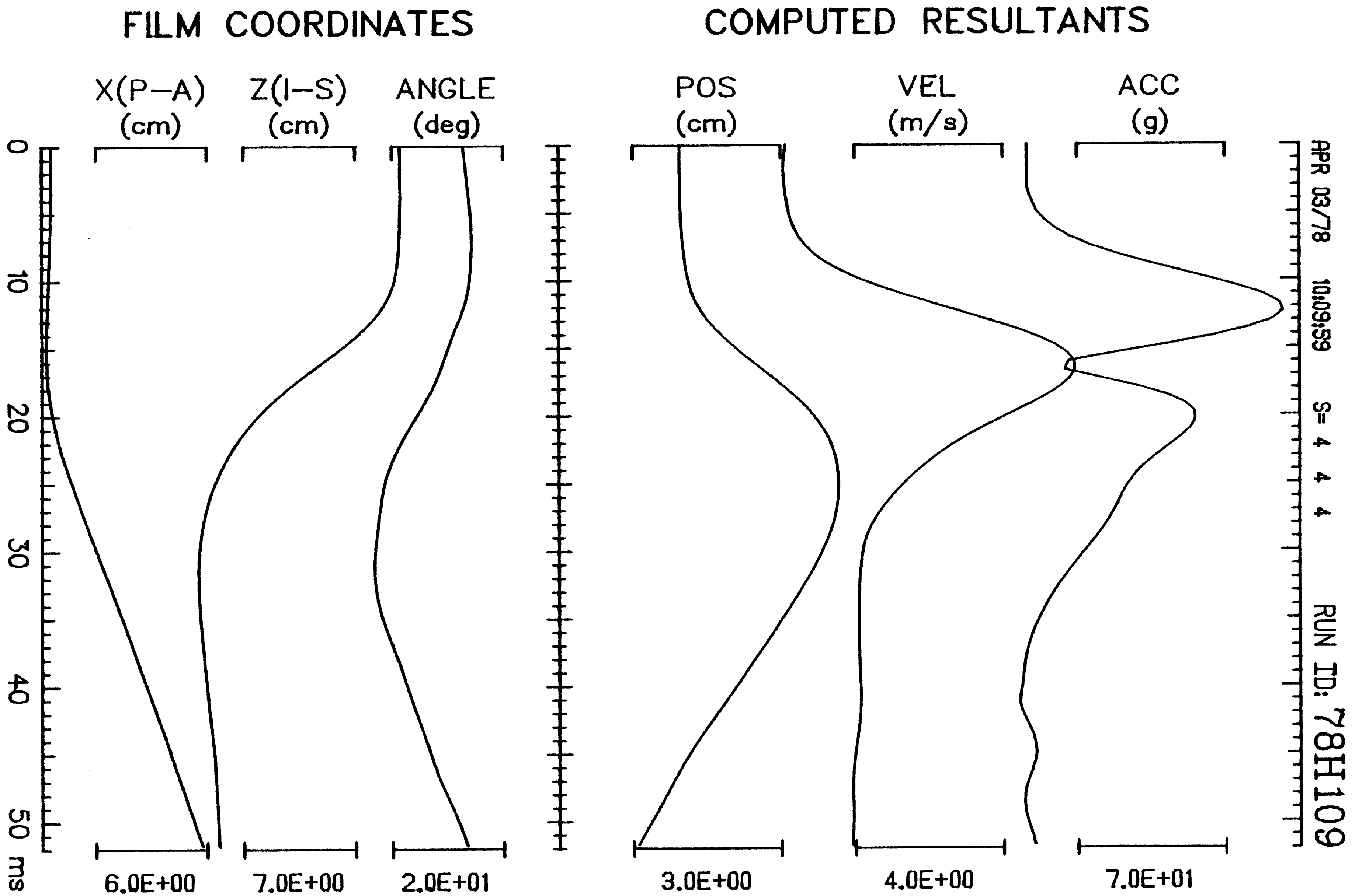

Head Motion vs. Time

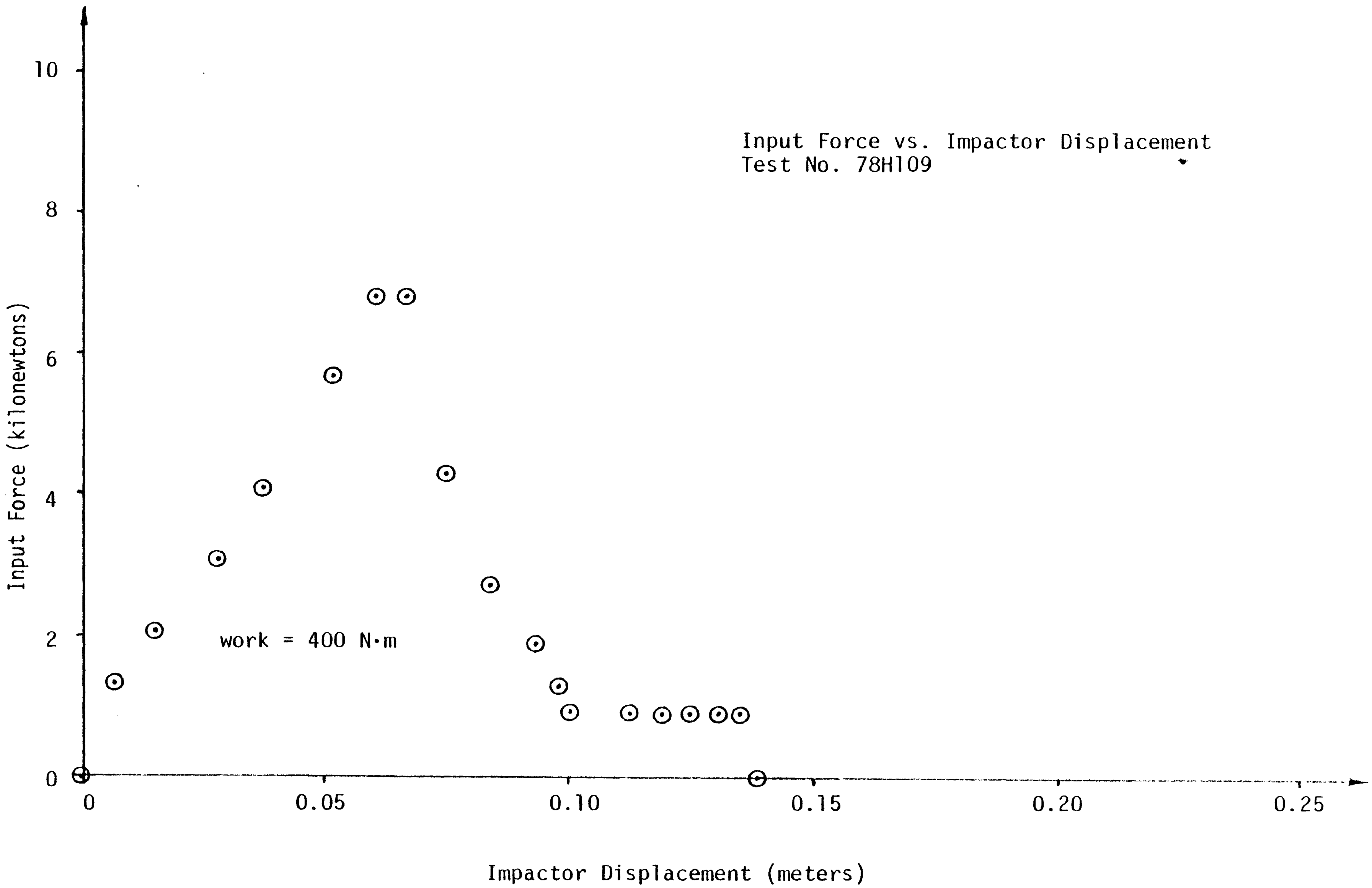
Input Force vs. Impactor Displacement
Test No. 78H109
work = 400 N·m
Input Force (kilonewtons)
Impactor Displacement (meters)
0
2
4
6
8
10
0
0.05
0.10
0.15
0.20
0.25

APPENDIX 9.2.10

TEST DATA FOR

78H110

TEST NO. 78H110

Piston Mass 9.9 kg

Stroke 10.2 cm

Pressure 138 kPa

Padding description 2.54 cm ensolite, 2.54 cm styrofoam

Photographic Coverage 35 mm BW slide, Polaroid set-up, 3000 fps color movies

Fixation description Feet rigidly blocked, crotch blocked, torso taped down.

% Skull Area Below Impactor Axis 76%

Approximate Cervical Spine Radius of Curvature 38 cm

Damage: (Swan neck) spinous processes of C_4, C_5, C_6 fractured, transverse process of C_5 fractured, body of C_5 crushed on right side.

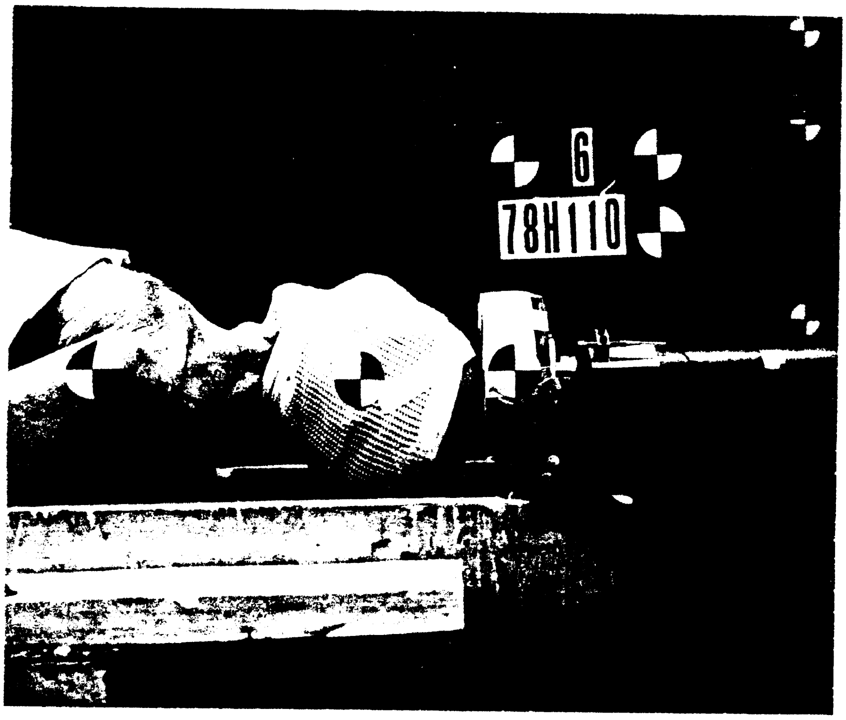

TEST 78H110 Instrumentation Traces

Compensated Force
177.9 N/div
Effectively Filtered
at 1600 Hz

Force
222.4 N/div
Effectively Filtered
at 1600 Hz

Acceleration
16.5 g's/div
Effectively filtered
at 1600 Hz

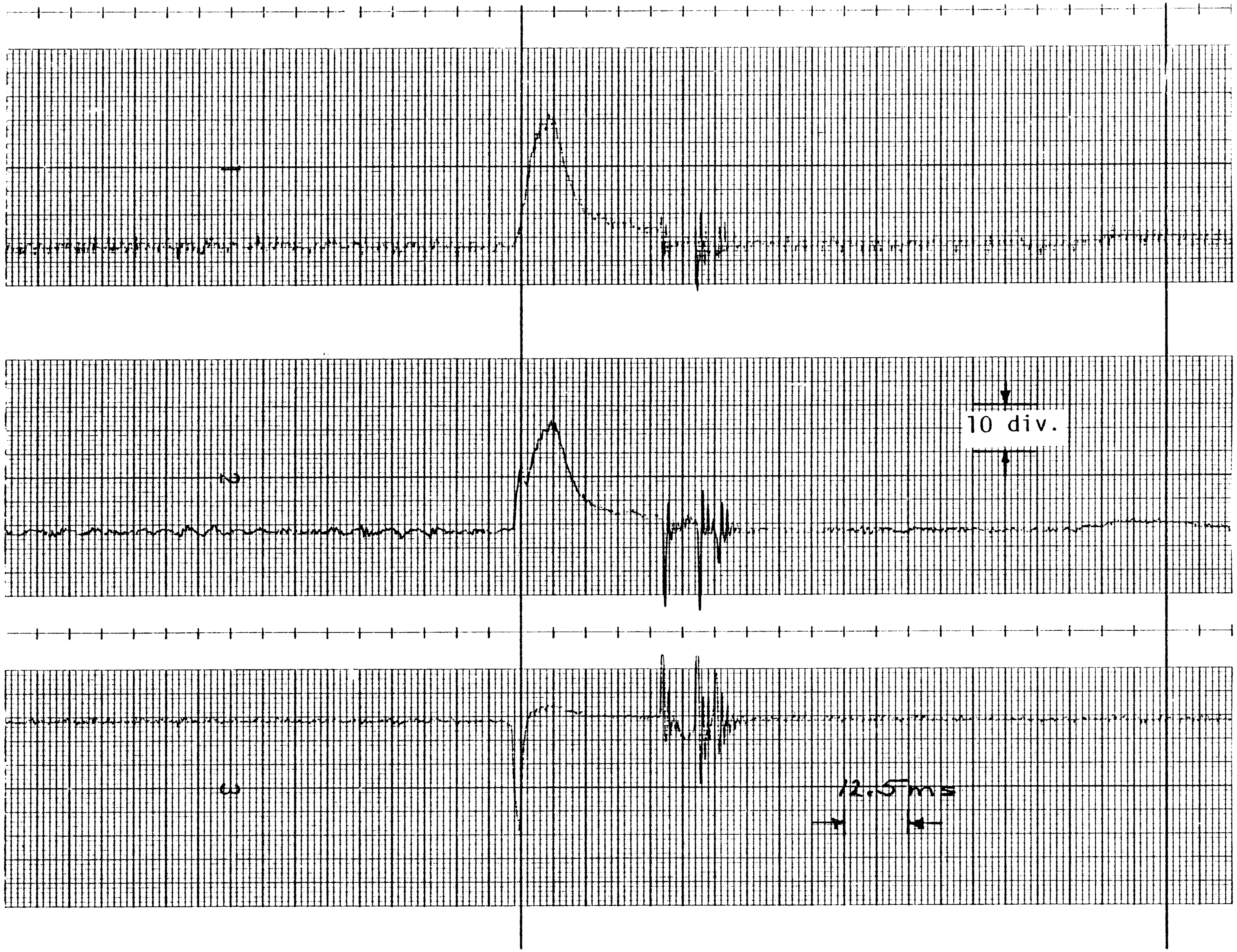

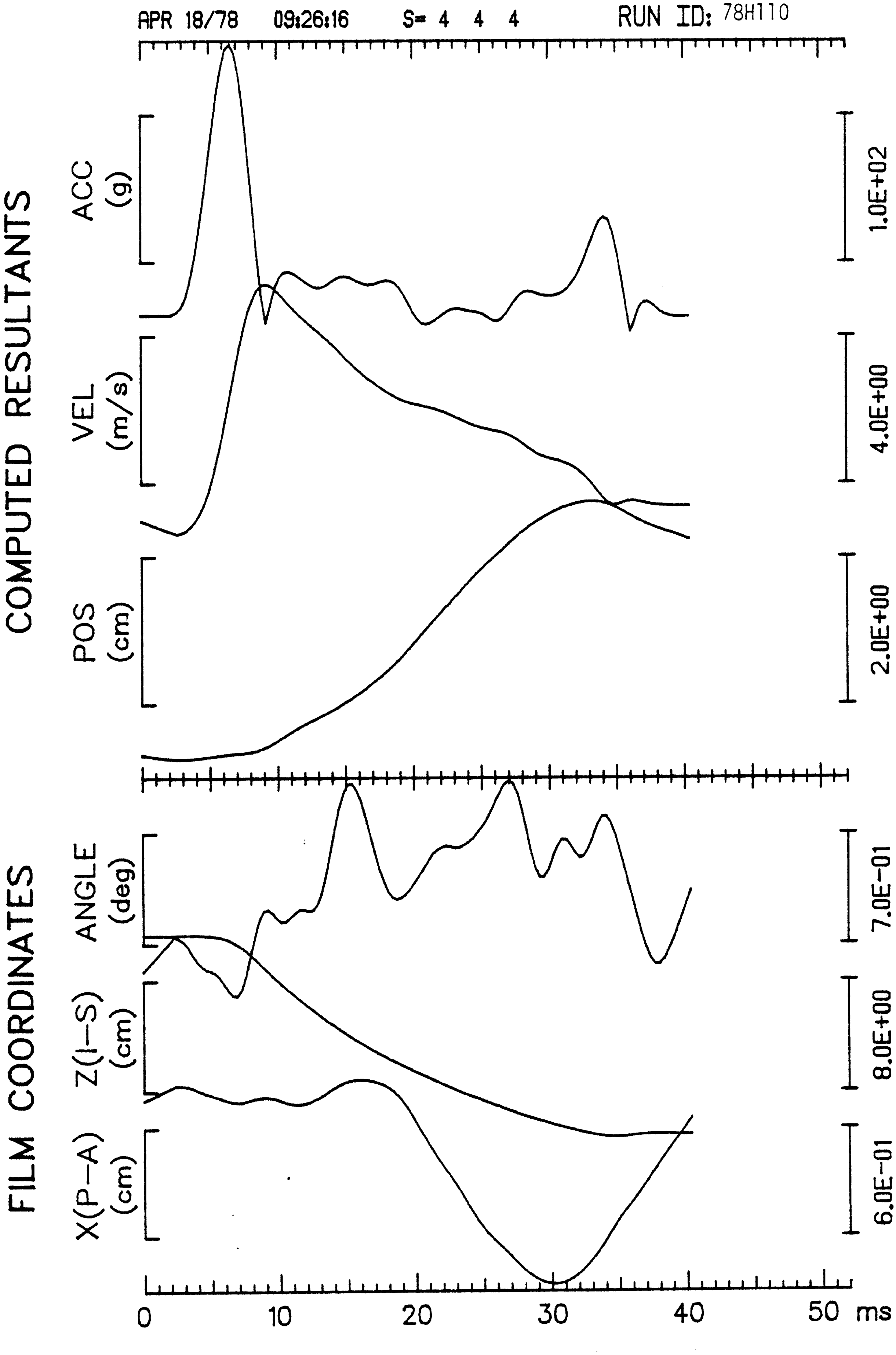

Impactor Motion versus Time

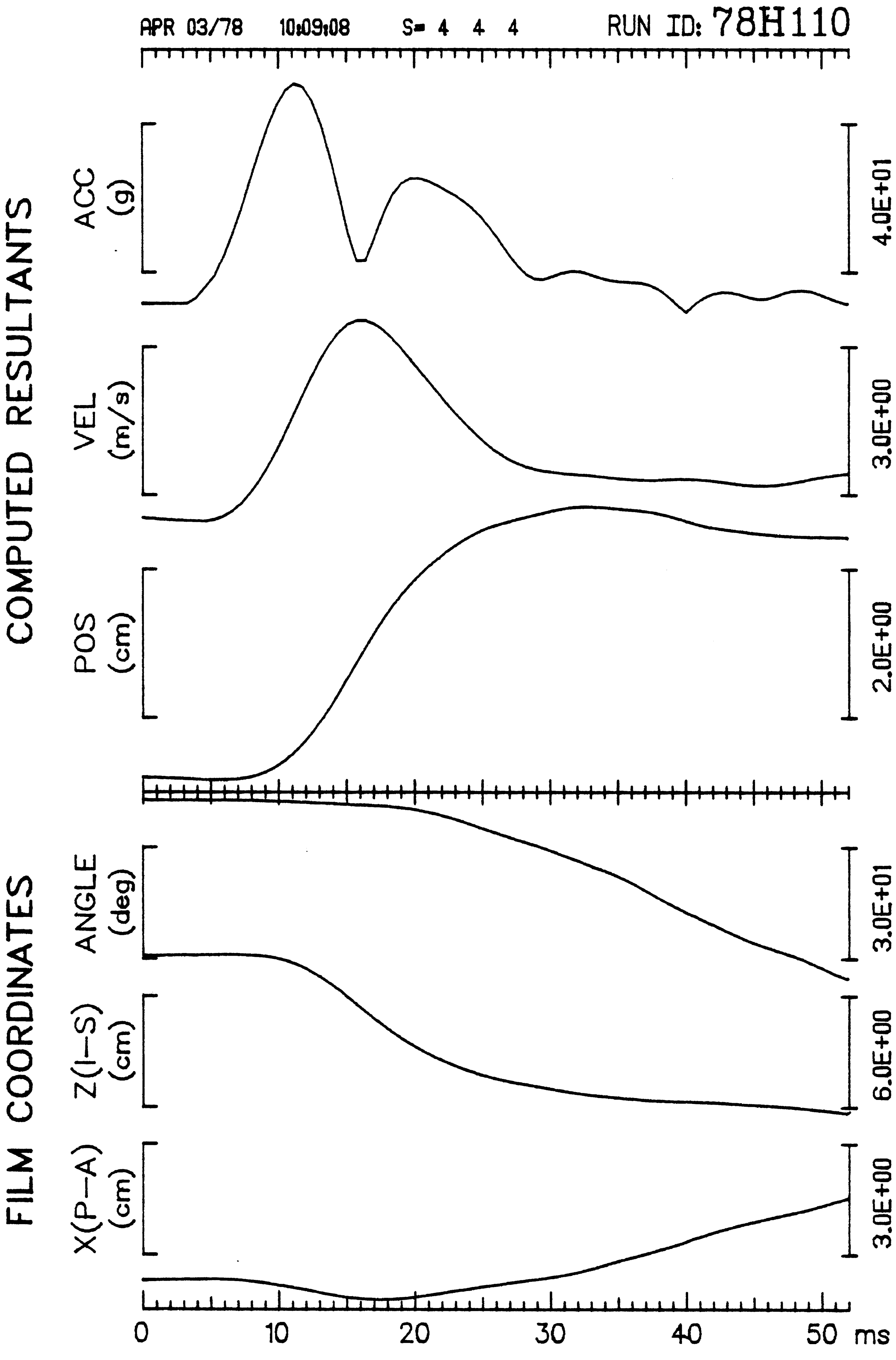

Head Motion vs. Time

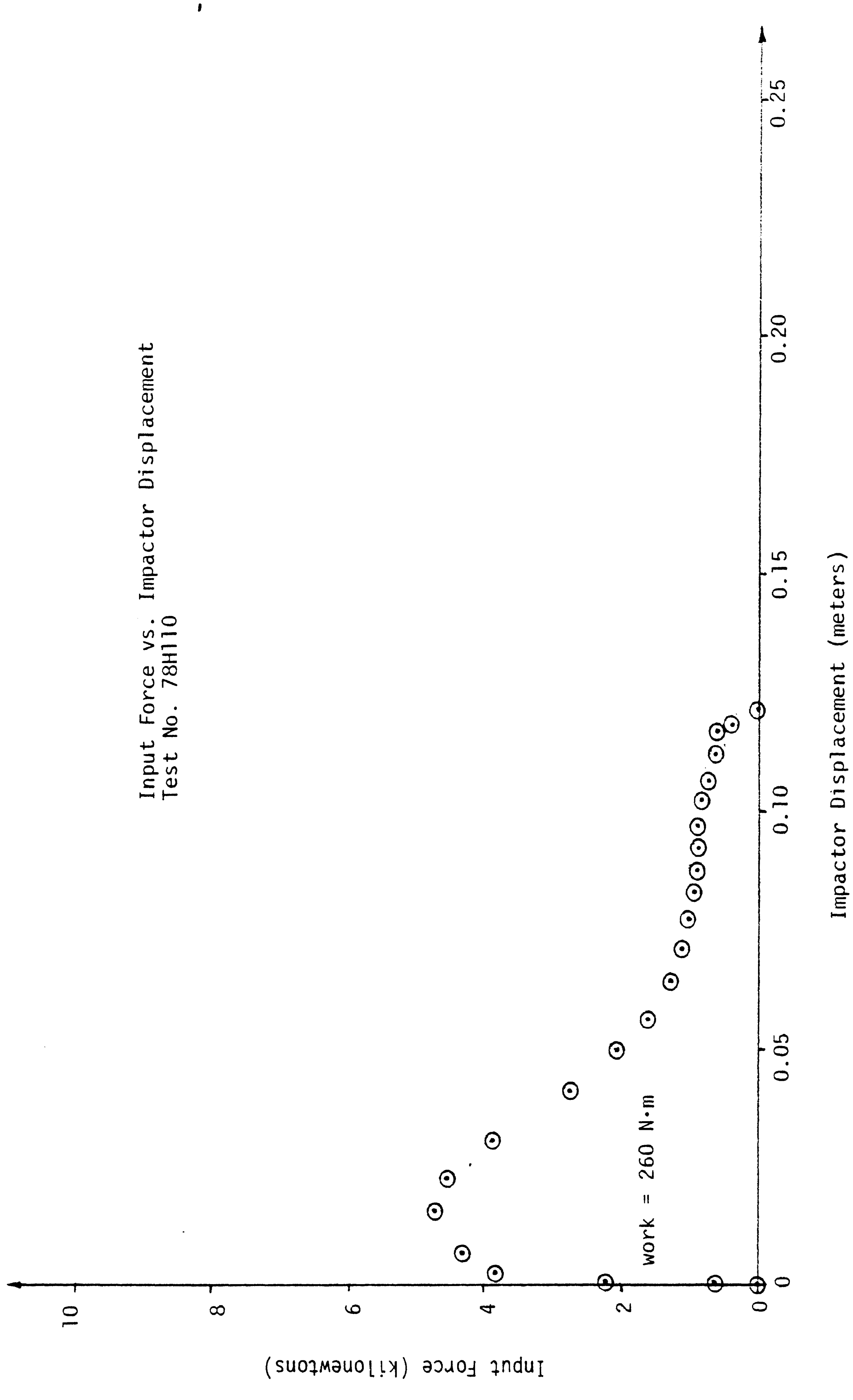

Input Force vs. Impactor Displacement
Test No. 78H110
work = 260 N·m
Input Force (kilonewtons)
0
2
4
6
8
10
Impactor Displacement (meters)
0
0.05
0.10
0.15
0.20
0.25

APPENDIX 9.2.11

TEST DATA FOR

78H111

TEST NO. 78H111

Piston Mass 9.9 kg

Stroke 10.2 cm

Pressure 131 kPa

Padding description 2.54 cm ensolite, 2.54 cm styrofoam

Photographic Coverage 35 mm BW slide, Polaroid set-up, 3000 fps color movies

Fixation description Feet rigidly blocked, crotch block, torso taped down

% Skull Area Below Impactor Axis 75%

Approximate Cervical Spine Radius of Curvature 12 cm

Damage: Fracture of tips of spinous processes of C_3, C_4, C_5.

TEST 78H111 Instrumentation Traces

Compensated Force
444.8 N/div
Effectively Filtered
at 1600 Hz

Force
444.8 N/div
Effectively Filtered
at 1600 Hz

Acceleration
35 g's/div
Effectively filtered
at 1600 Hz

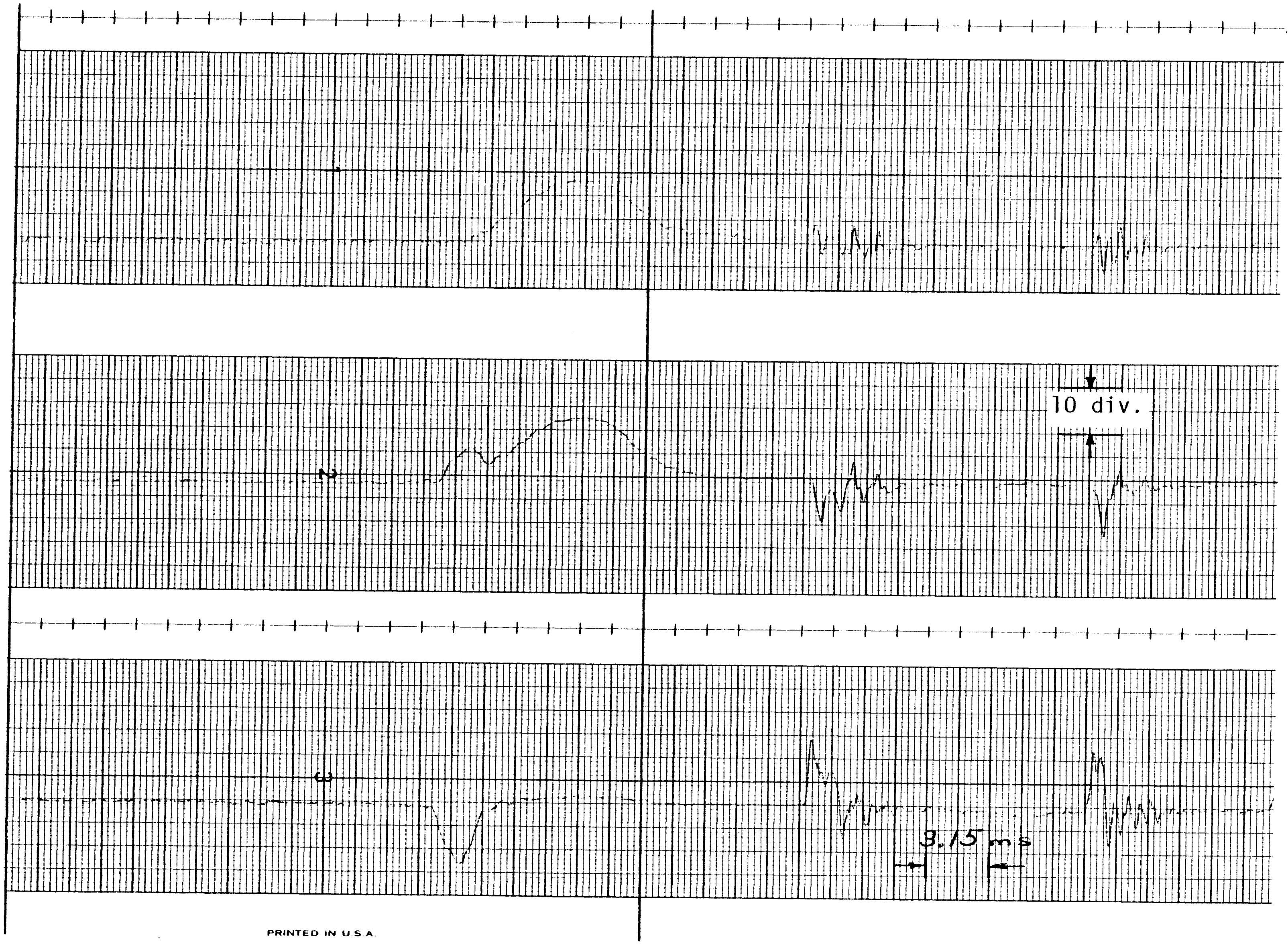

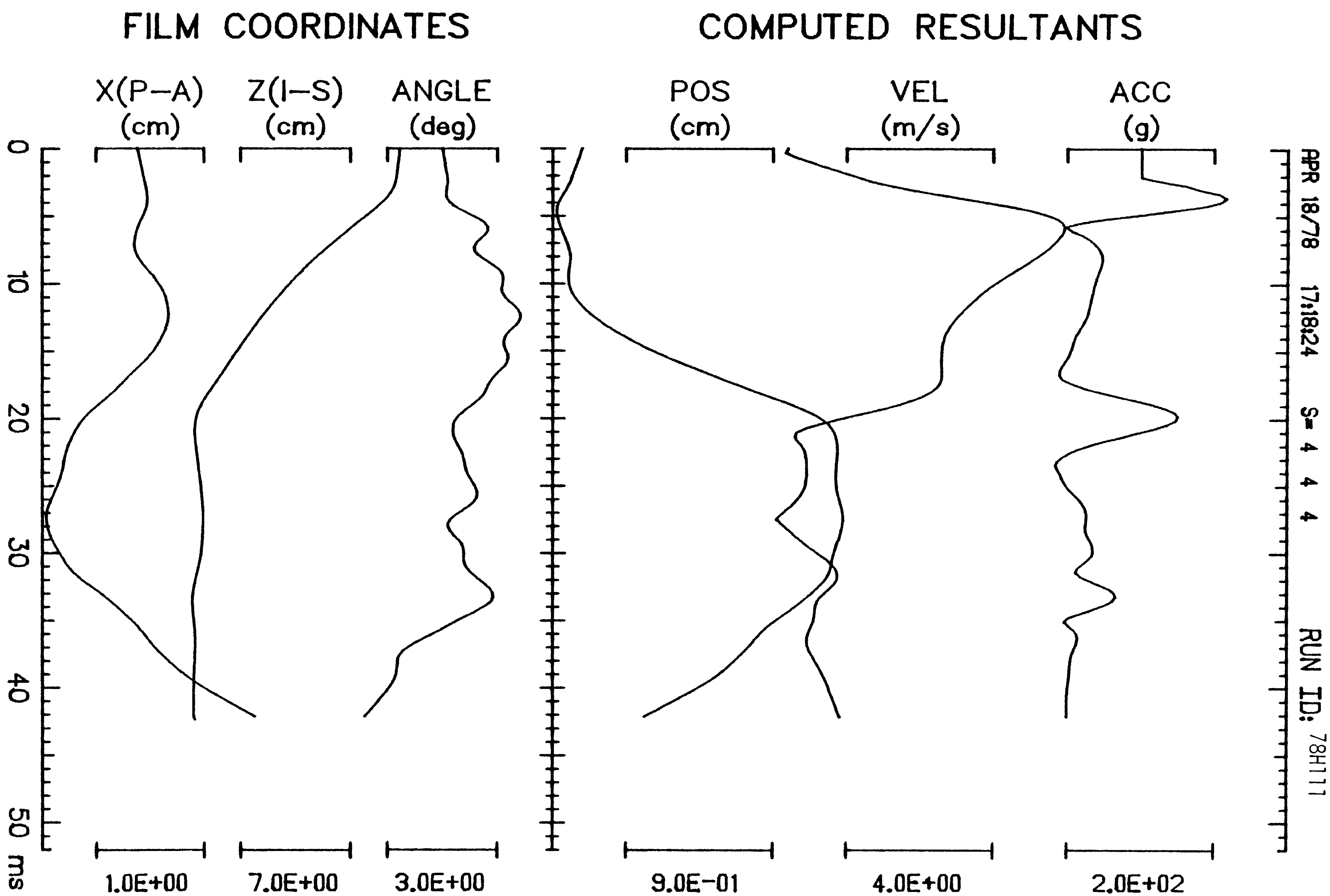

Impactor Motion versus Time

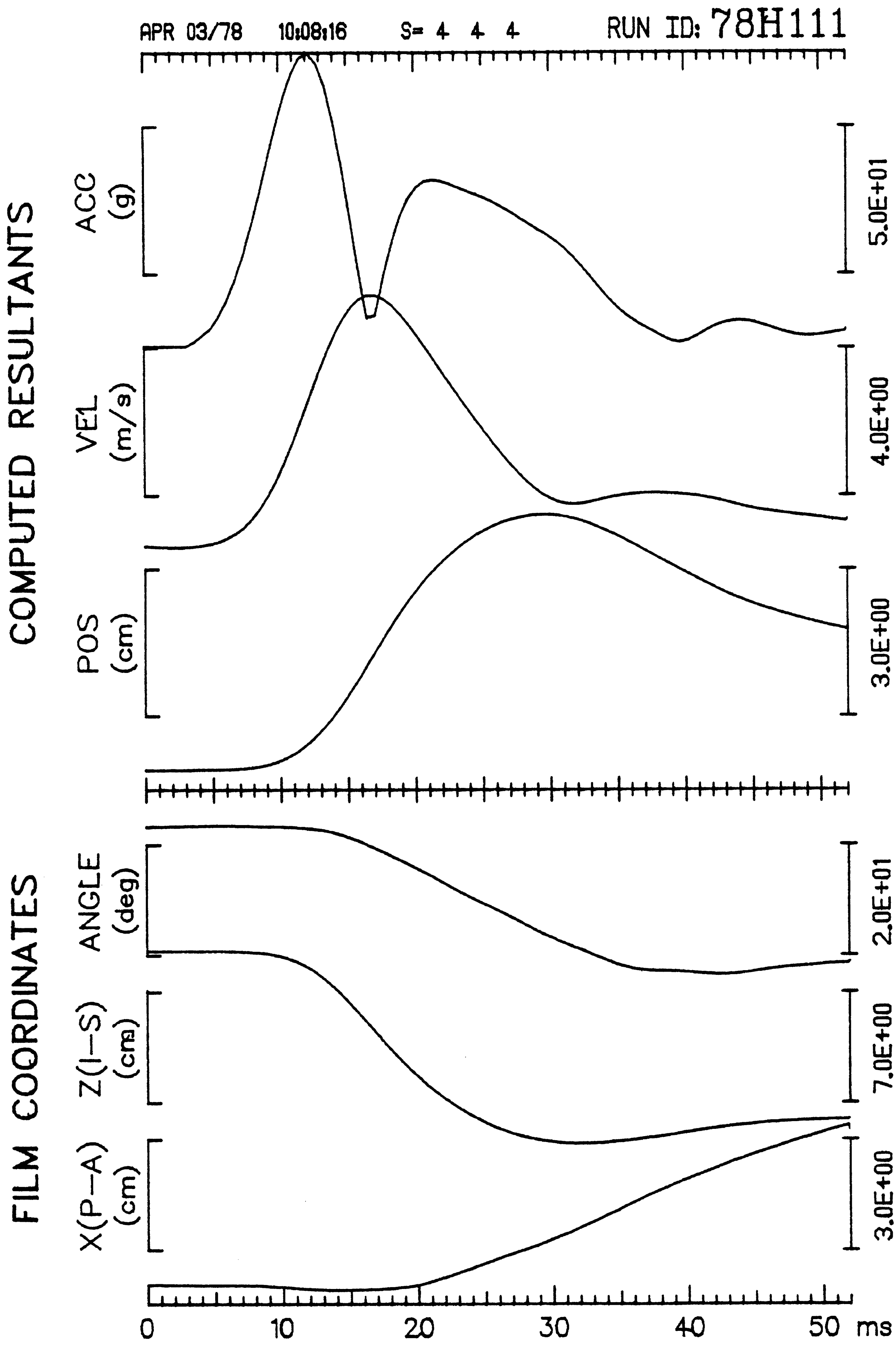

Head Motion vs. Time

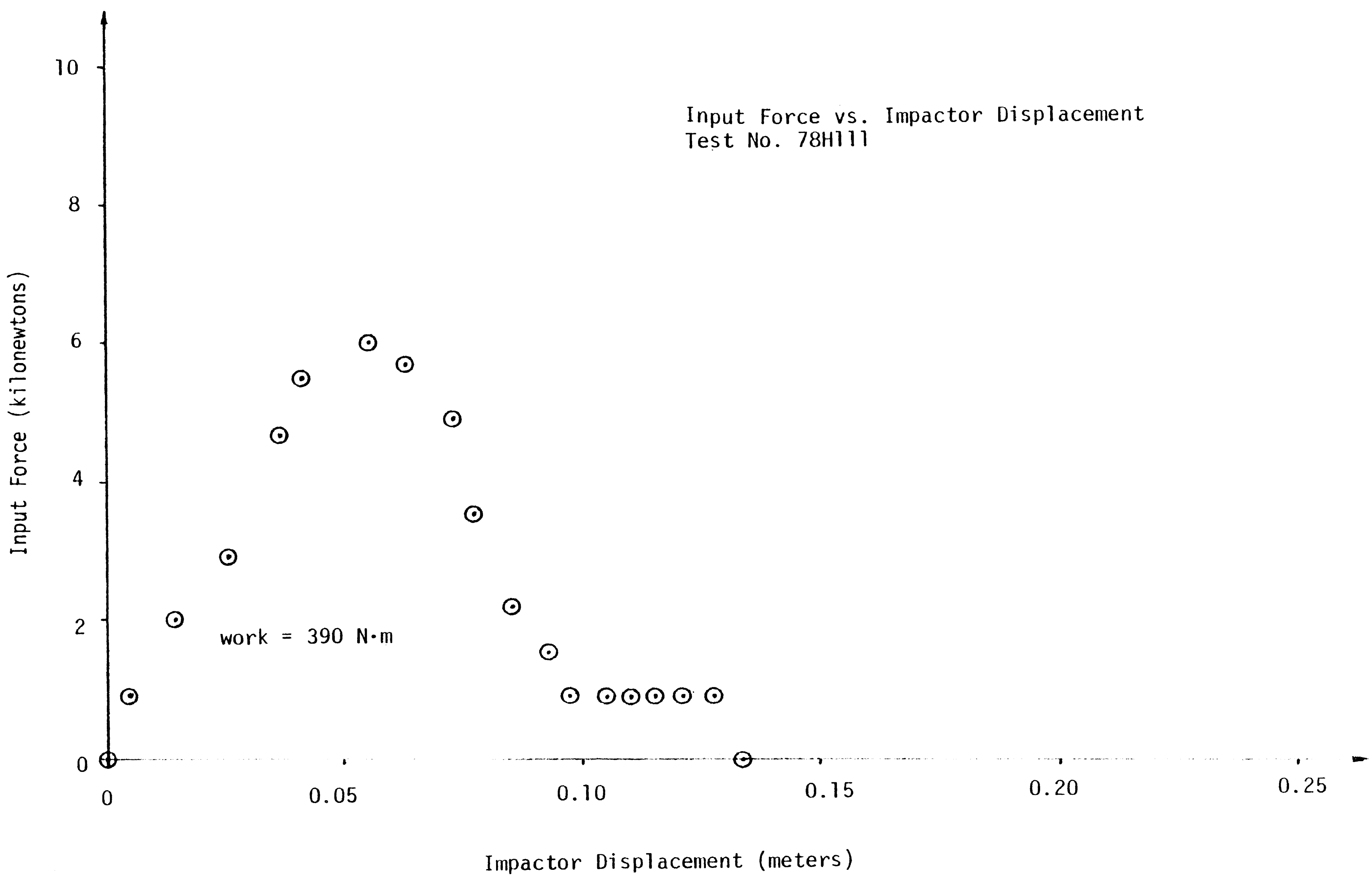
Input Force vs. Impactor Displacement
Test No. 78H111
work = 390 N·m
Input Force (kilonewtons)
0
2
4
6
8
10
Impactor Displacement (meters)
0
0.05
0.10
0.15
0.20
0.25

APPENDIX 9.3

BONE ASH AND TENSILE STRENGTH

DETERMINATION PROCEDURES

9.3.1 Bone Ashing Procedures

Methods of procedure --

1. Wet weight determination -- weigh sample after blotting with absorbent paper.

2. Freeze drying -- freeze dry the sample for at least 36 hours and record the weight.

3. Oven drying -- Oven dry the sample at 75°C for at least 48 hours and until sample reaches a constant weight. This is the dry matter weight.

4. Ash the sample in a muffle at 700°C for more than 72 hours until a constant is reached and that all the residues turn whitish. This is the total ash weight.

5. Calculations:

   a. % wet weight = (mg ash wt./mg wet sample wt) x 100%
   b. % dry weight = (mg ash wt./mg dry sample wt) x 100%

9.3.2 Tensile Testing - Two to four tensile specimens as shown in Figure A were fabricated from each piece of femur. The number of specimens which could be obtained from each femur depended upon the diameter of the initial piece, the degree of osteoporosis, and the ratio of compact to cancellous bone. All specimens were machined while being continuously wetted with a normal saline solution in order to prevent specimen deterioration from either excessive heat or drying. After machining, each specimen was stored in a container of normal saline at -10°C until the time of test.

Prior to testing, all specimens were allowed to equilibrate in a container of normal saline at room temperature for one hour. Testing was performed on an Instron Type C floor model testing machine. The load was monitored with a Lebow 3000 lb capacity tension/compression load cell. An estimate of strain was obtained by measuring crosshead displacement using a Schaevitz 1000 HR LVDT. Load and displacement were recorded on a Honeywell 740 x-y plotter. Load was converted to stress by dividing by the cross-sectional area of the reduced midsection of the specimen. Displacement was converted to strain by dividing by the gage length.

Gripping of the specimens was accomplished by 3/16 inch diameter pins which were passed through holes in the enlarged tab areas of the specimen. Specimen failure occurred in the reduced area in all cases. All testing was done with the specimen wrapped in a moist gauze pad to insure that no drying took place. The testing was performed at cross-head rate of 0.02 in/min.

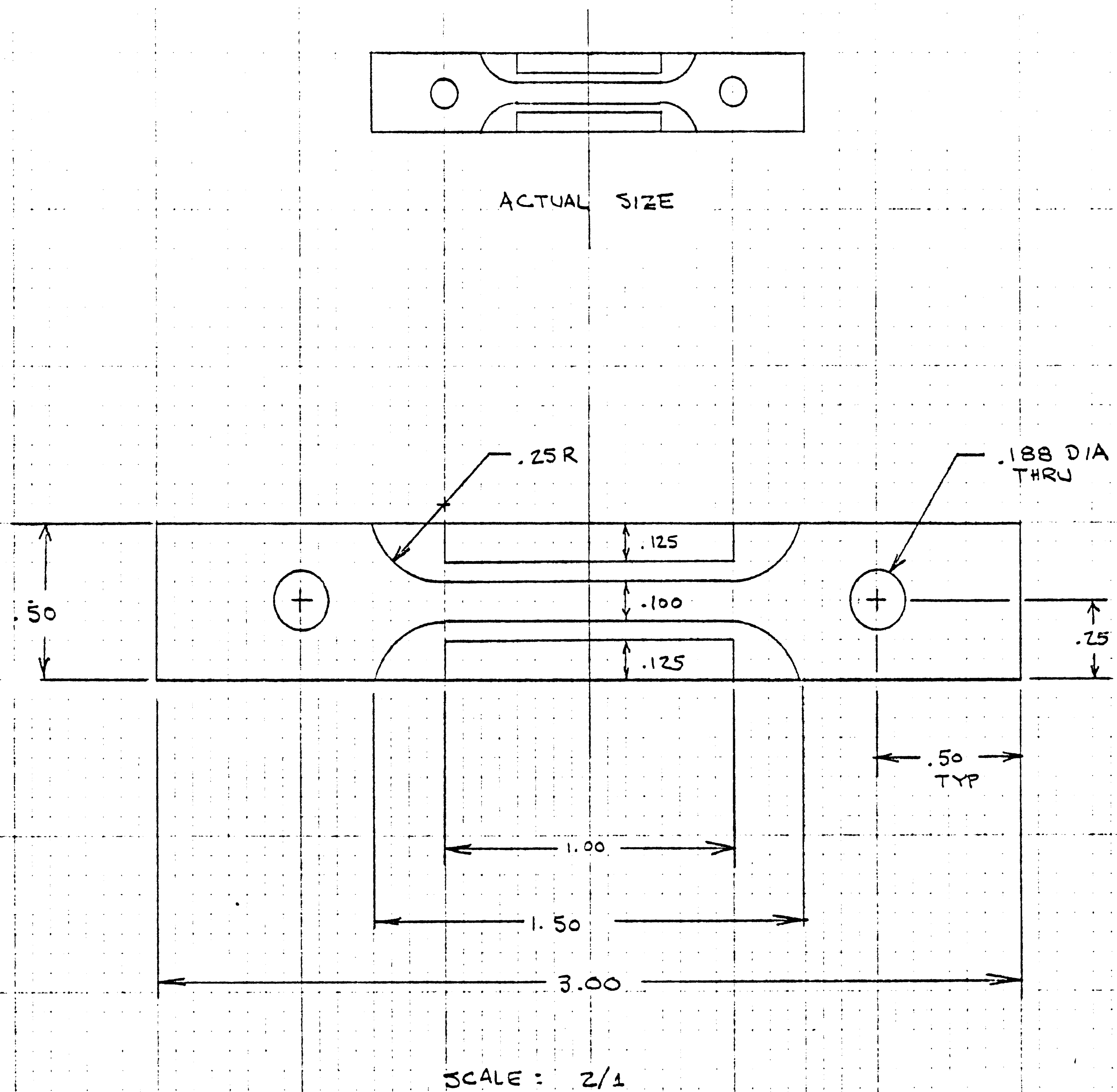

Figure A.

FEMUR SPECIMEN

GKM 12-1-77

APPENDIX 9.4

SLIDE CATALOG

9.4 Slide Catalog

Test 77H101/Cadaver 20817

Slide 1 - Pre-Test AP x-ray

Slide 2 - Pre-Test LR x-ray

Slide 3 - Post-Test AP x-ray

Slide 4 - Post Test LR x-ray

Test 77H102/Cadaver 20827

Slide 5 - Pre-Test AP x-ray

Slide 6 - Pre-Test RL x-ray

Slide 7 - Post-Test AP x-ray

Slide 8 - Post-Test RL x-ray

Test 77H103/Cadaver 20824

Slide 9 - Pre-Test AP x-ray

Slide 10 - Pre-Test RL x-ray

Slide 11 - Post-Test AP x-ray

Slide 12 - Post-Test RL x-ray

Test 77H104/Cadaver 20869

Slide 13 - Post-Test AP x-ray

Slide 14 - Post Test RL x-ray

Slide 15 - Post-Test LR X-ray

Test 77H105/Cadaver 20881

Slide 16 - Pre-Test AP x-ray

Slide 17 - Pre-Test LR x-ray

Slide 18 - Post-Test AP x-ray

Slide 19 - Post Test LR x-ray

Slide 20 - In Test Position x-ray

Test 77H106/Cadaver 20896

Slide 21 - Pre-Test AP x-ray

Slide 22 - Pre-Test LR x-ray

Slide 23 - Post-Test AP x-ray

Slide 24 - Post-Test Oblique x-ray

Slide 25 - In-Test Position x-ray

Test 78H107/Cadaver 20901

Slide 26 - Pre-Test AP x-ray

Slide 27 - Pre-Test LR x-ray

Slide 28 - Post-Test AP x-ray

Slide 29 - Post-Test RL x-ray

Slide 30 - In Test Position x-ray

Test 78H108/Cadaver 20904

Slide 31 - Pre-Test AP x-ray

Slide 32 - Pre-Test LR x-ray

Slide 33 - Post-Test AP x-ray

Slide 34 - Post Test RL x-ray

Slide 35 - In Test Position x-ray

Test 78H109/Cadaver 20922

Slide 36 - Pre-Test AP x-ray

Slide 37 - Pre-Test RL x-ray

Test 78H110/Cadaver 20921

Slide 38 - Pre-Test AP x-ray

Slide 39 - Pre-Test LR x-ray

Slide 40 - Post-Test AP x-ray

Slide 41 - In Test Position x-ray

Test 78H111/Cadaver 20941

Slide 42 - Pre-Test AP x-ray

Slide 43 - Pre-Test LR x-ray

Slide 44 - Post Test AP x-ray

Slide 45 - Post Test RL x-ray

Slide 46 - In Test Position x-ray

Slide 47 - Test 77H101 Test Set-up Photograph

Slide 48 - Test 77H102 Test Set-up Photograph

Slide 49 - Test 77H103 Test Set-up Photograph

Slide 50 - Test 77H106 Test Set-up Photograph

Slide 51 - Test 78H107 Test Set-up Photograph

Slide 52 - Test 78H108 Test Set-up Photograph

Slide 53 - Test 78H109 Test Set-up Photograph

Slide 54 - Test 78H111 Test Set-Up Photograph